INVESTIGATION OF THE EFFECT OF GPCR OLIGOMERIZATION ON THE GNAI1 PROTEIN HOMODIMERIZATION IN LIVE CELLS USING FRET

A THESIS SUBMITTED TO
THE GRADUATE SCHOOL OF NATURAL AND APPLIED SCIENCES
OF
MIDDLE EAST TECHNICAL UNIVERSITY

BY

ENISE NALLI

IN PARTIAL FULFILLMENT OF THE REQUIREMENTS
FOR
THE DEGREE OF MASTER OF SCIENCE
IN
BIOTECHNOLOGY

JANUARY 2022

Approval of the thesis:

INVESTIGATION OF THE EFFECT OF GPCR OLIGOMERIZATION ON THE GNAI1 PROTEIN HOMODIMERIZATION IN LIVE CELLS USING FRET

submitted by **Enise Nalli** in partial fulfillment of the requirements for the degree of **Master of Science** i**n Biotechnology, Middle East Technical University** by,

Prof. Dr. Halil Kalıpçılar
Dean, Graduate School of **Natural and Applied Sciences** _____

Prof. Dr. Güzin Candan Gürakan Gültekin
Head of the Department, **Biotechnology** _____

Assoc. Prof. Dr. Çağdaş Devrim Son
Supervisor, **Biotechnology, METU** _____

Dr. Fatma Küçük Baloğlu
Co-Supervisor, **Biology , Giresun University** _____

Examining Committee Members:

Assoc. Prof. Dr. Tülin Yanık
Biological Sciences, METU _____

Assoc. Prof. Dr. Çağdaş Devrim Son
Biotechnology, METU _____

Assoc. Prof. Dr. Alpan Bek
Physics, METU _____

Assist. Prof. Dr. Ahmet Acar
Biological Sciences, METU _____

Assoc. Prof. Dr. Gamze Bora
Medical Biology Department, Hacettepe University _____

Date: 26.01.2022

I hereby declare that all information in this document has been obtained and presented in accordance with academic rules and ethical conduct. I also declare that, as required by these rules and conduct, I have fully cited and referenced all material and results that are not original to this work.

Name, Last Name : Enise Nalli

Signature :

ABSTRACT

INVESTIGATION OF THE EFFECT OF GPCR OLIGOMERIZATION ON THE GNAI1 PROTEIN HOMODIMERIZATION IN LIVE CELLS USING FRET

Nalli, Enise
Master of Science, Biotechnology
Supervisor: Assoc. Prof. Dr. Çağdas Devrim Son
Co-Supervisor: Dr. Fatma Küçük Baloğlu

January 2022, 94 pages

G-Protein Coupled Receptors (GPCR) are membrane proteins that pass the cell membrane seven times. In classical GPCR signaling pathways, one GPCR-one heterotrimeric G-protein interaction model is enough to transmit the signal to effector proteins. Studies since 2000 showed that one GPCR dimer-one heterotrimeric G-protein interaction model is more likely, and GPCRs having homo-/hetero- dimers interact with a single Gα-protein. Recently, studies on GPCRs indicated that more than two receptors interact to form active receptor oligomers during signal transduction. Navarro *et al.* showed that within a heterotetrameric receptor complex, formed by the dimerization of the dimers, the G proteins interacting with the dimers were brought into close proximity (Navarro *et al*., 2018).

Furthermore, studies with Ras proteins, which are members of the G-protein family, have shown that these proteins form dimers playing important roles in various signaling pathways. More recently, a member of our Lab., Özge Atay, has shown the physical interaction of Gαi1 proteins on the cell membrane. However, it is still not

clear whether the Gαi1 protein homodimerization is a result of the formation of receptor tetramers or if the Gαi1 homodimers form independently of the receptors. Receptor independent G-protein dimerization might play a role in stabilizing the receptor tetramers. In order to answer this question, Förster Resonance Energy Transfer (FRET) method was used to quantitatively investigate the effect of GPCR oligomerization on the Gαi1 homodimerization under two conditions: (1) blocking GPCR-Gαi1 interaction with Gαi1-specific minigenes and (2) receptor oligomerization by agonist (Quinpirole) treatment.

Keywords: Gαi1 protein, Homodimer formation, Receptor oligomerization, Receptor dependency, FRET

ÖZ

GPKR OLIGOMERİZASYONUNUN GNAI1 PROTEİN HOMODİMER OLUŞUMUNUN ÜZERİNDEKİ ETKİSİNİN FRET YÖNTEMİ İLE CANLİ HÜCRELERDE ARASTIRILMASI

Nalli, Enise
Yüksek Lisans, Biyoteknoloji
Tez Yöneticisi: Assoc. Prof. Dr. Çağdas Devrim Son
Ortak Tez Yöneticisi: Dr. Fatma Küçük Baloğlu

Ocak 2022, 94 sayfa

G-Protein Kenetli Reseptörler (GPKR), hücre zarını yedi kez geçen zar proteinleridir. Klasik GPCR sinyal yolaklarında, bir GPKR-bir heterotrimerik G-protein etkileşim modeli, sinyali efektör proteinlere iletmek için yeterlidir. 2000'li yıllarda başlanan araştırmalar, bir GPKR dimer-bir heterotrimerik G-protein etkileşim modelinin daha olası olduğunu ve homo-/heterodimerleşen GPKR'lerin tek bir Gα-proteini ile etkileşime girdiğini göstermiştir. Son zamanlarda, GPKR çalışmaları, sinyal iletimi sırasında aktif reseptör oligomerleri oluşturmak için ikiden fazla reseptörün entegre olduğunu göstermiştir. Navarro *et al.* GPKR dimerlerinin dimerizasyonuyla oluşturulan bir heterotetrametrik reseptör kompleksi içinde, bağlı G proteinlerinin etkileşim mesafesinde yakın hale getirildiğini gösterilmiştir (Navarro ve diğerleri, 2018).

Ayrıca, G-protein ailesinin üyesi olan Ras proteinleri ile yapılan çalışmalar, bu proteinlerin dimer oluşturduğunu göstermiştir ve bu dimerlerin farklı sinyal yolaklarında önemli roller oynadığı saptanmıştır. Yakın zamanda, laboratuvarımızın bir üyesi olan Özge Atay, Gαi1 proteinlerinin hücre zarında fiziksel etkileşimini

göstermiştir. Fakat, Gαi1 protein homodimerlerinin GPKR tetramerlerinin oluşumunun bir sonucu olup olmadığı henüz açık değildir. Bu bilgiler ışığında, GPCR oligomerizasyonunun Gαi1 homodimerizasyonu üzerindeki etkisi iki kondisyon içinde kantitatif olarak Förster Rezonans Enerji Transferi (FRET) yöntemi ile araştırılmıştır: (1) GPCR-Gαi1 etkileşiminin Gαi1'e özgü minigenlerle bloke edilmiş ve (2) Quinpirole uygulaması ile reseptör oligomerizasyonu tetiklenmiştir.

Anahtar Kelimeler: Gαi1 protein, Homodimer formasyonu, Receptor oligomerizasyonu, Receptor bagımlılığı, FRET

To my beloved family for their patience, ever-lasting support, and unconditional love.

ACKNOWLEDGMENTS

Throughout this work I have received a great deal of support and assistance. The completion of this study could not have been possible without the help of so many invaluable people.

First and foremost, I would like to express my deep and sincere gratitude to my supervisor, Çagdaş Devrim Son, who welcomed me as a MSc student in his laboratory. As a Turkish Belgian, I treasure that he made me feel comfortable from the very first moment. Besides that, he introduced me in the world of protein protein interactions (PPIs) and fluorescence microscopy. He guided me on all the PPI detection methods, and helped me interpret all the data. I am grateful to him for including me in this TUBITAK supported project, guiding and encouraging me in the beginning of my academic life. I will always joyfully remember the morning coffee conversations in which 'motivation and dedication' in scientific research was the key subject.

A great debt of gratitude is also owed to my co-advisor, Fatma Kucuk Baloglu, for guiding me along the way and providing me with endless suggestions for this thesis. She taught me so much about scientific research and the importance of organization in laboraty environment and genuinely helped me grow into a woman in science. I will always remember her encouragements and motivational speeches even during the most stressy moments of this thesis work. I will also treasure the cheerful tea breaks and endless conversations not only about science but also about general aspects in daily life.

I would like to thank my thesis examining committee; Assoc. Prof. Tülin Yanık, Assist. Prof. Ahmet Acar, Assoc. Prof. Dr. Alpan Bek and, Assoc. Prof. Gamze Bora.

I would like to thank all the past and present members of the Son Lab and the partner lab in the Ankara University Stem Cell Institute for their assistance and support

throughout these years. All the protocols and procedures, needed to conduct the experiments, were taught by Özge Atay. Additionally, I would like to acknowledge Hüseyin Evci for the construction of the positive and negative FRET controls which I used in this study. Another former lab member I also want to thank is Sara Mingu whose supported and help with the experiments. I would also like to thank Tolgahan Suat Sezen, Irem Aydin, Yağnur Işık and Burcu Şekerzade for the numerous times I asked for your help. Especially, my special thanks to my friend and project partner, Seyda Tuğçe Balkan, for the many hilarious moments in and outside the lab, for your invaluable point-of-views during the interpretation of my data and, most importantly for your priceless friendship. I genuinely wish that our ways in the scientific field will cross again. Special thanks to the Scientific and Technological Research Council of Turkey for the partial funding of this work under the grant number TUBİTAK 117Z868.

In the Biology Department, I would like to extend my gratitude to Dr. Murat Erdem. I would like thank Murat Erdem for his friendship, guidance and for teaching me so much about molecular cloning procedures. I would also like to thank Ayça Hatıl who like-wise helped with molecular cloning techniques. I would like to recognize the invaluable assistance that you both provided during my study.

Finally, I wish to thank my friends, my family and my husband whose assistance, support and motivation was a milestone in the completion of this work. My friends, especially Feyza Matisli and Seyda Tugce Balkan, for providing me the pep-talks I always need to hear. I am thankful for the presence of my childhood friend, Feyza Matisli, in my life eventhough we are miles apart from eachother the connection of love is still there. My family, especially my mom, dad, brothers and sisters for giving the opportunity to pursue me dreams and for the unconditional love and support throughout my entire life. My dear husband, Muhammed Fatih Sezer, for providing me the right amount of love, support and motivation throughout this study. You are the reason I strongly believe in the power of moments, since we were at the right place at the right moment.

TABLE OF CONTENTS

LIST OF TABLES

TABLES

LIST OF FIGURES

FIGURES

LIST OF ABBREVIATIONS

ABBREVIATIONS	
A1AR	Adenosine A1 receptor
A2AR	Adenosine A2 receptor
AC	Adenylyl Cyclase
AGS	Activators of G-proteins
ASBT	Acceptor spectral bleed-through
ATP	Adenosine triphosphate
bp	base pair
cAMP	cyclic AMP
CREB	cAMP Response Element-binding Protein
DNA	Deoxyribonucleic Acid
D1R	Dopamine 1 receptor
D2R	Dopamine 2 receptor
D3R	Dopamine 3 receptor
DMEM	Dulbecco's Modified Eagle Medium
DSBT	Donor Spectral Bleed-Through
EDTA	Ethylenediamine tetraaccetic acid
EGFP	Enhanced Green Fluorescent Protein
ERK	Extracellular Signal-Regulated Kinase
FBS	Fetal Bovine Serum
FP	Fluorescent Protein
FRET	Fröster Resonance Energy Transfer
$GABA_{B1}$	Gamma-aminobutyric acid type B receptor subunit 1
$GABA_{B2}$	Gamma-aminobutyric acid type B receptor subunit 2
GAP	GTPase-activating protein
GDP	Guanosine diphosphate

GDS	GDP-dissociation stimulator
GEF	Guanine nucleotide exchange factor
GNAI1	G protein Subunit Alpha I1
GPCR	G protein-coupled receptor
GTP	Guanosine triphosphate
kb	kilo base pair
LB	Luria Bertani
MAPK	Mitogen-activated protein kinase
mCherry	monomeric Cherry
N2a	Neuro-2a
NDPK	Nucleoside-diphosphate kinase
PBS	Phosphate Buffered Saline
PCR	Polymerase Chain Reaction
PI3K	Phosphoinositide 3-kinase
PKA	Protein Kinase A
PPI	Protein-Prptein Interaction
RGS	Regulator of G protein signalling
SOC	Super Optimal Broth
TAE	Tris-Acetate-EDTA-Buffer

CHAPTER 1

INTRODUCTION

1.1 GTP-binding proteins

GTP-binding proteins are regulatory proteins that act as molecular on/off switches inside the cell. As the name states, these proteins possess a structurally preserved GTP-binding domain. They control a wide range of biological processes, including receptor signaling, intracellular signal transduction pathways, and protein synthesis (Y et al., 2001).

G-proteins cycle between an inactive GDP-bound confirmation (the “Off-state”) and an active GTP-bound confirmation (the “On-state). In their On-state, G-proteins interact with effector proteins and induce downstream signaling pathways. Their activity is regulated by Guanine nucleotide exchange factors (GEFs) and GTPase-activating proteins (GAPs). While GEFs turn on signaling by catalyzing the GDP /GTP exchange, GAPs terminate signaling events by facilitating GTP hydrolysis. (Siderovski & Willard, 2005) (Bos et al., 2007)

GTP-binding proteins classified into two classes of; small G-proteins and heterotrimeric G-proteins. Small G-proteins, also known as the Ras protein family, are monomeric proteins (20-25 kDa) where active GTP-bound form is restricted by their low intrinsic GTPase activity and the GAPs. Heterotrimeric G proteins contain three different subunits (α, β, and γ), and similar to small G-proteins, the α subunit contains a GTP-binding domain (Figure 1.1). (Takai et al., 2021)

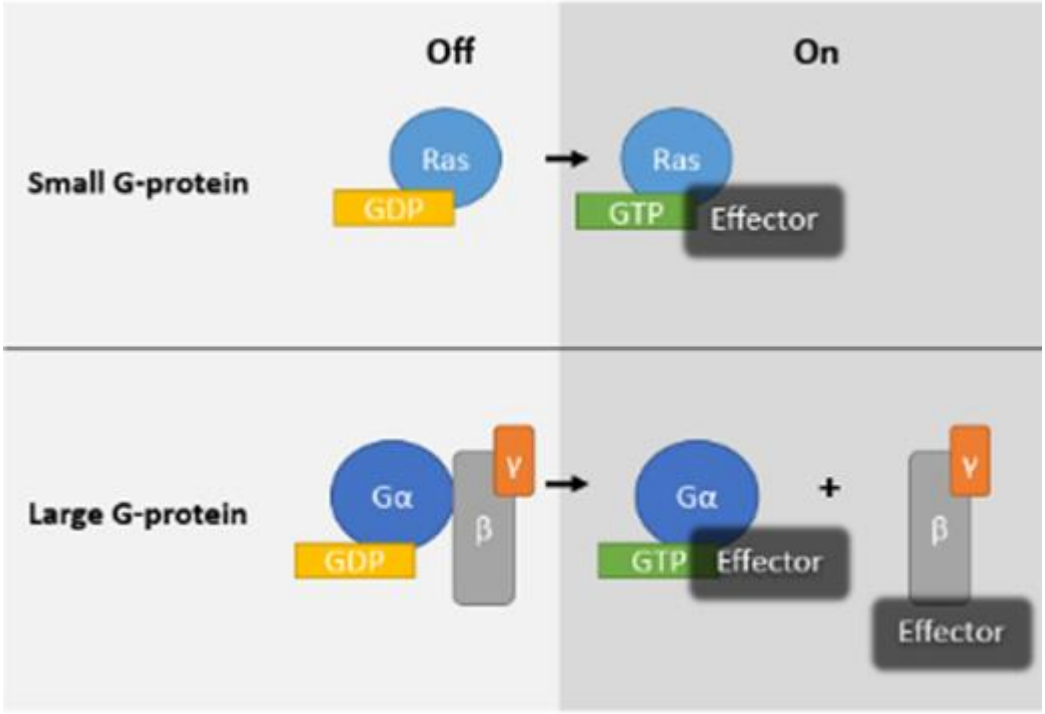

Figure 1.1 Simplified Illustration of "On" and "Off" states of GTP-binding proteins. While small G proteins and the alpha subunit (Gα) of heterotrimeric G proteins both contain a GTPase domain (G-domain), Gα contains an additional helical domain (H-domain) and forms a complex with the Gβ and Gγ subunits. (Taken from https://umaine.edu/kelleylab/home/research-interests/g-protein-signaling/)

1.1.1 Small GTP-binding proteins

Small GTPases have been accepted as cellular molecular switches which are defined by their intrinsic biochemical activity of binding GTP (active state) and hydrolyzing it to GDP (inactive state). These proteins need to be strictly regulated.The exchange of GDP to GTP is mediated by GEFs (mostly cytosolic proteins), while the hydrolysis of GTP to GDP is co-regulated by GAPs (Schmidt & Hall, 2002).

The story of small GTPases started with the discovery of Ras oncogenes of the sarcoma viruses (H-Ras, K-Ras, and N-Ras), the founding members of this superfamily, around 1980. This was followed by the discoveries of related proteins now forming the RAS-like superfamily of small GTPases (Y et al., 2001). Most small G proteins are only present in eukaryotes (from yeast to humans). At present, this

superfamily has over 153 members and is divided into five different families (Ras, Rho, Rab, Arf, and Ran) and respective subfamilies based on sequence, structural and functional similarities (Figure 1.2) (Qu et al., 2019)(Song et al., 2019).

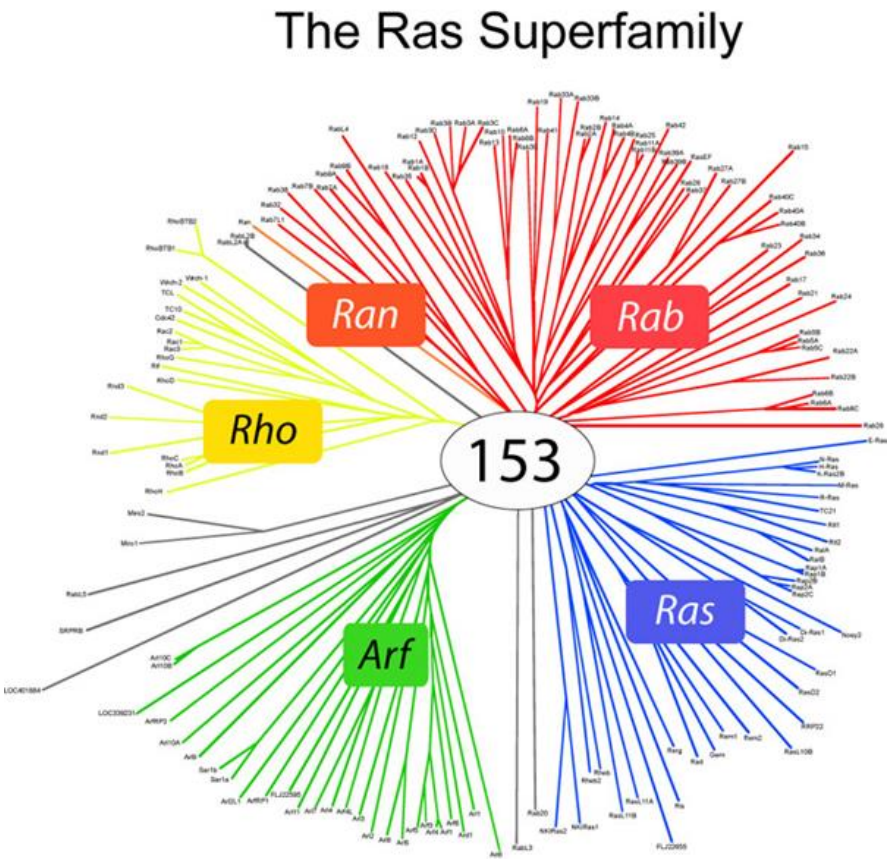

Figure 1.2 Phylogenetic tree of proteins in the Ras Superfamily. (Taken from https://www.med.unc.edu/pharm/der-fig-1-the-ras-superfamily/)

The functions of many small G proteins have recently been elucidated: members of the Ras family, which are the most universal components of signaling pathways, mainly regulate gene expression; Rho family members can mostly regulate both gene expression and cytoskeletal reorganization; members of the Rab and Sar1/Arf families predominantly involved in intracellular vesicle transport; and the Ran family members, which are the most abundant small GTPase in the cell, regulate nuclear transport and the cell cycle. (Paduch et al., 2001) (Wennerberg et al., 2005)

Among all Ras-like superfamily proteins, the basic biochemical activity of GTP binding and hydrolysis is directly reflected in their structure at the G-domain (20 kDa). The crystal structure of small GTPases reveals that this domain consists of five α helices (A1-A5), six β strands (B1-B6), and five highly conserved polypeptide loops (G1-G5), also called "G motifs" (Figure 1.3-A) (Qu et al., 2019). According to the bound guanine nucleotide (GDP or GTP), small GTPases are in the inactive confirmation (GDP-bound off-state) or active confirmation (GTP-bound on-state). The nucleotide-regulated conformational changes are mainly constricted to two loop regions: switch I (also called G2 motif) and switch II, which contains the G3 motif and part of A2 helix (Figure 1.3-B) (Ali Khan Pathan et al., 2016).

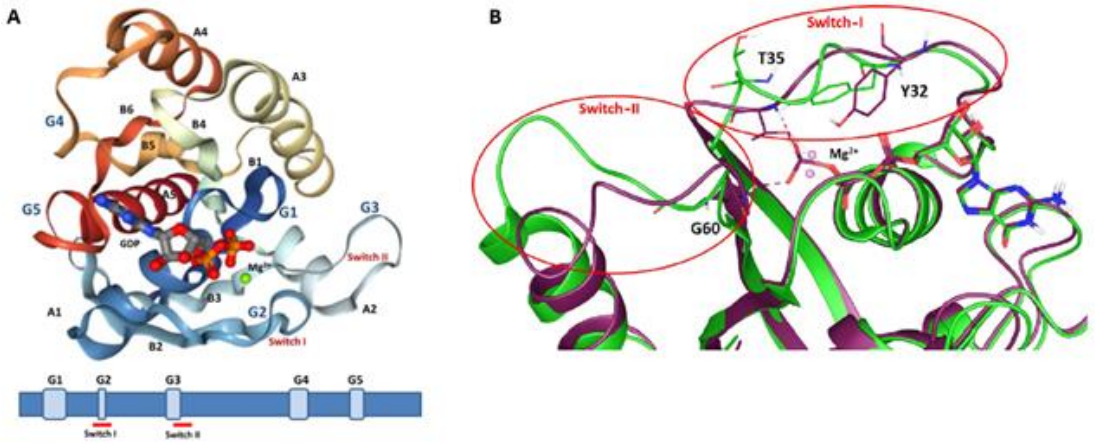

Figure 1.3 A - The crystal structures of Ras GDP Mg2+ complex (upper) and the position relationship among various parts is shown below (Taken from (Qu et al., 2019)). B - Superposition of GDP (green) and GTP (purple)-bound conformation of K-Ras protein (Taken from (Ali Khan Pathan et al., 2016)

The G1 motif (also known as P-loop) is a purine nucleotide binding signal; besides the conformational reorientation of G2 motif upon GTP or GDP binding, G2 motif also plays an important role in effector binding. On the othe hand, G3 motif is involved in binding of nucleotide-related Mg^{2+} ion; where as, G4 motif residues interact with G1 motif residues providing stability and form hydrogen bonds with the guanine ring which ensures the specificity to GTP over ATP; G5 motif is

indirectly associated with guanine nucleotide and are, compared to the other G motif, less well conserved among the superfamily members (Colicelli, 2004).

1.1.2 Heterotrimeric G-proteins

Akin to small GTPases, heterotrimeric guanine-nucleotide binding proteins (G proteins) function as signal-transducing on/off switches with their biological activity being dependent to the bound guanine nucleotide. Heterotrimeric G proteins are made up of α-, β- and γ-subunits, and in their inactive GDP-bound state they exist in the Gαβγ form. The β and γ subunits are tightly associated and are seen as one functional unit (Syrovatkina et al., 2016). In mammalian cells, the α, β and γ subunits are encoded by 16, 5, and 12 genes, respectively (Table 1.1).

Table 1.1 Classification of Gα-, β- and γ- subtypes and their effectors.

Table 1 The family of mammalian heterotrimeric G-protein subunits: function and regulation

Family	*Subtype*	*Effectors*	*Expression*	*Disease relevance*	*Pharmacological modulation*
$G_s\alpha$	$G_{s(S)}\alpha$ $G_{s(L)}\alpha$ $G_{s(XL)}\alpha$ $G_{olf}\alpha$	Adenylyl cyclases↑($G_{s,s(XL),olf}\alpha$) Maxi K channel↑($G_s\alpha$) Src tyrosine kinases (c-Src, Hck) ↑ ($G_s\alpha$) GTPase of tubulin ↑($G_s\alpha$)	$G_s\alpha$: ubiquitous $G_{olf}\alpha$: olfactory neurons, certain CNS ganglia; digestive and urogenital tract	$G_{s(XL)}\alpha$: brachydactyly, trauma-related bleeding tendency, neurological problems $G_s\alpha$: McCune–Albright syndrome, cholera, pseudohypoparathyroidism type Ia/b, testotoxicosis, adenomas of pituitary and thyroid	$G_s\alpha$: CTX $G_{olf}\alpha$: CTX
$G_{i/o}\alpha$	$G_{o1}\alpha$ $G_{o2}\alpha$ $G_{i1-i3}\alpha$ $G_z\alpha$ $G_{t1/2}\alpha$ $G_{gust}\alpha$	Adenylyl cyclase ↓ ($G_{i,o,z}\alpha$) Rap1GAPII-dependent ERK/MAPkinase activation ↑ ($G_i\alpha$) Ca^{2+} channels ↓ ($G_{i,o,z}\alpha$) K^+ channels ↑ ($G_{i,o,z}\alpha$) GTPase of tubulin ↑ ($G_i\alpha$) Src tyrosine kinases (c-Src, Hck) ↑ ($G_i\alpha$) Rap1GAP ↑ ($G_z\alpha$) GRIN1-mediated activation of Cdc42 ↑ ($G_{i,o,z}\alpha$) cGMP-PDE ↑ ($G_t\alpha$) $G_{gust}\alpha$: ?	$G_{o1-2}\alpha$: neurons, neuroendocrine cells, astroglia, heart $G_{i1-i3}\alpha$: neurons and many others $G_z\alpha$: platelets, neurons, adrenal chromaffin cells, neurosecretory cells $G_{t1}\alpha$: rod outer segments, taste buds $G_{t2}\alpha$: cone outer segments $G_{gust}\alpha$: sweet and/or bitter taste buds, chemoreceptor cells in the airways	$G_i\alpha$: whooping cough, adrenal and ovarian adenomas $G_t\alpha$: congenital cone dysfunction, night blindness	$G_{o(1/2)}\alpha$: PTX $G_{i1-i3}\alpha$: PTX $G_z\alpha$: ? $G_{t1/2}\alpha$: PTX, CTX $G_{gust}\alpha$: PTX
$G_{q/11}\alpha$	$G_q\alpha$ $G_{11}\alpha$ $G_{14}\alpha$ $G_{15}\alpha$ $G_{16}\alpha$	Phospholipase Cβ isoforms ↑ p63-RhoGEF ↑ ($G_{q/11}\alpha$) Bruton's tyrosine kinase ↑ ($G_q\alpha$) K^+ channels ↑ ($G_q\alpha$)	$G_{q/11}\alpha$: ubiquitous $G_{15/16}\alpha$: hematopoietic cells	$G_{q/11}\alpha$: dermal hyperpigmentation and melanocytosis?	$G_{q/11}\alpha$: YM-254890 $G_{14}\alpha$: ? $G_{15}\alpha$: ? $G_{16}\alpha$: ?
$G_{12/13}\alpha$	$G\alpha_{12}$ $G\alpha_{13}$	Phospholipase D ↑ Phospholipase Cε ↑ NHE-1 ↑ iNOS ↑ E-cadherin-mediated cell adhesion: ↑ p115RhoGEF ↑ PDZ-RhoGEF ↑ Leukaemia-associated RhoGEF (LARG) ↑ Radixin ↑ Protein phosphatase 5 (PP5) ↑ AKAP110-mediated activation of PKA ↑ HSP90 ↑	Ubiquitous	Recent SNPs identified but no disease correlation yet	$G_{12}\alpha$: ? $G_{13}\alpha$: ?
$G\beta/\gamma$	β_{1-5} γ_{1-12}	PLCβs ↑ Adenylyl cyclase I ↓ Adenylyl cyclases II, IV, VII ↑ PI-3 kinases ↑ K^+ channels (GIRK1,2,4) ↑ Ca^{2+} (N-, P/Q-, R-type) channels ↓ P-Rex1 (guanine nucleotide exchange factor for the small GTPase Rac) ↑ c-Jun N-terminal kinase (JNK) ↑ Src kinases ↑ Tubulin GTPase activity ↑ G-protein-coupled receptor kinase recruitment to membrane ↑ Protein kinase D ↑ Bruton's tyrosine kinase ↑ p114-RhoGEF ↑	$\beta_1\gamma_1$: retinal rod cells $\beta_3\gamma_8$: retinal cone cells β_5: neurons and neuroendocrine organs $\beta_{5(L)}$: retina Most cell types express multiple β and γ subtypes	$G\beta_3$: atherosclerosis, hypertension, metabolic syndrome	$G\beta\gamma$: ?

CTX = cholera toxin; PTX = pertussis toxin; ↑ = enhances function; ↓ = reduces function; YM-254890 = a cyclic depsipeptide isolated from *Chromobacterium* sp QS3666.

Mammalian heterotrimeric G proteins generally classified into four families based on their α subunit, which also defines the basic properties of the respective G protein: (1) 'Gi/o' family mainly inhibits adenylyl cyclase, (2) 'Gs' family stimulates adenylyl cyclase, (3) 'G12/13' family predominantly regulate RhoGEF (Siehler, 2009), (4) while, 'Gq/11' family activates phospholipase C ß (Kamato et al., 2015). As shown in Figure 1.4, each family consists of various members that share sequence similarities and functional properties; the largest and most diverse family, the Gi/o family, includes Gαi1, Gαi2, Gαi3, Gαo (highly expressed in neurons), Gαt (expressed in specific cells in the eye), Gαg (expressed in taste receptor cells), and Gαz (expressed in neuronal tissues and platelets); the Gs family consists of two members, Gαs and Gαolf (primarily expressed in olfactory sensory neurons); the $G_{12/13}$ family contains $G\alpha_{12}$ and $G\alpha_{13}$; in humans, the Gq family includes $G\alpha_{q}$, $G\alpha_{11}$, $G\alpha_{14}$ (mainly expressed in kidney, lung, and liver), and $G\alpha_{16}$ (typically expressed in hematopoietic cells) (Downes & Gautam, 1999) (Wettschureck & Offermanns, 2005) (Syrovatkina et al., 2016)

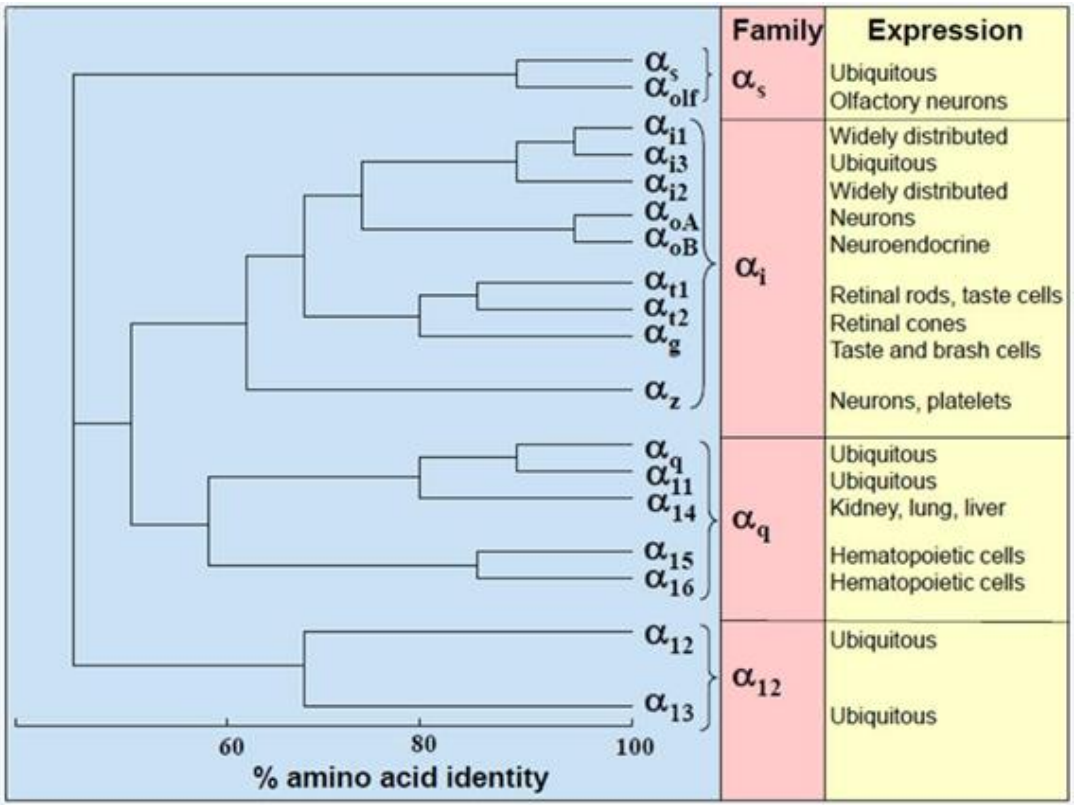

Figure 1.4 Phylogenetic relationship of human and mouse Gα subunits and their expression (Taken from Syrovatkina *et al*., (2016)).

Upon binding to a GEF, usually ligand-bound active GPCRs, the α subunits of G proteins release GDP and bind GTP. As a result, the dissociation of the Gα and βγ subunits occur. Afterward, by recruiting distinct effectors, many downstream signaling pathways get activated (Figure 1.5). G proteins can deactivate themselves because of their intrinsic GTPase activity. However, GTP hydrolysis is mainly promoted by binding of a GAP leading to the inactive GDP-bound confirmation state. (Cabrera-Vera et al., 2003) (Tilman et al., 2015)

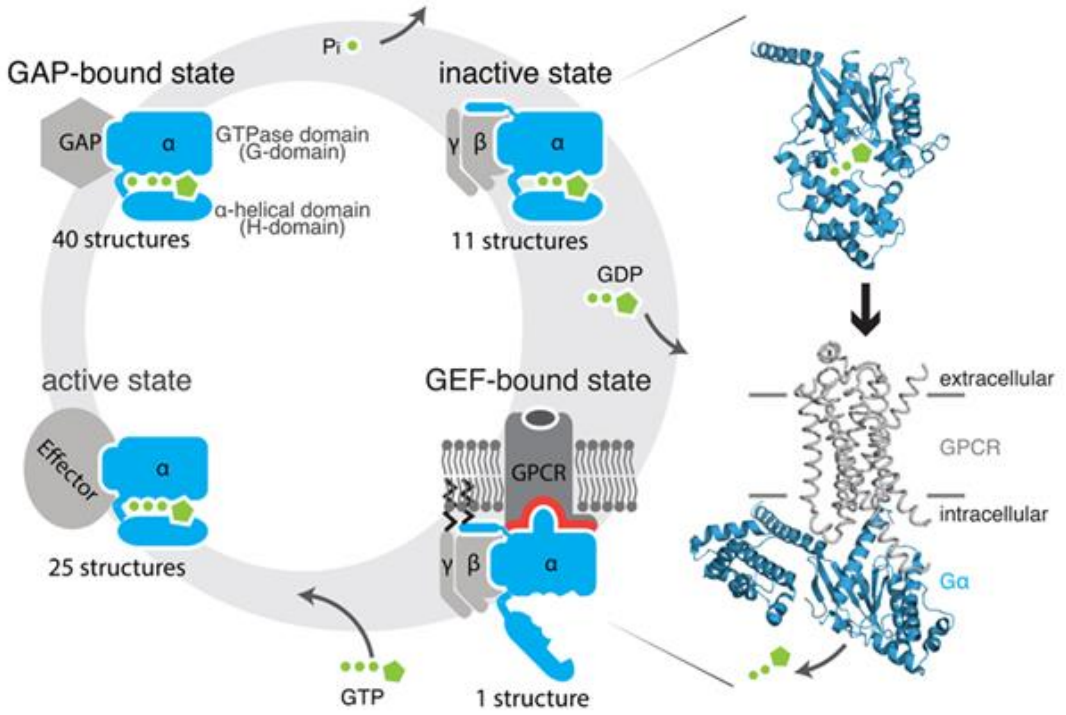

Figure 1.5 Activation and deactivation of heterotrimeric G protein. (Taken from Tilman Flock *et al*. (2016))

The Gα subunit consists of two domains: GTP-binding domain (also called as G-domain or Ras-like domain) is involved in binding and hydrolyzing GTP (red box in figure 1.6-A) and a unique α-helical domain (blue box in figure 1.6-A). While the G domain; containing six-stranded β-sheet (β1 – β6), five helices (α1 – α5), and five G motifs (G1-G5); is structurally similar to Ras proteins (figure 1.6-B), the unique helical domain has an entirely α-helical secondary structure that is composed of a six α-helix bundle (αA – αG). The interface between the Ras-like domain and the helical domain forms the nucleotide-binding pocket (Lambright et al., 1994).

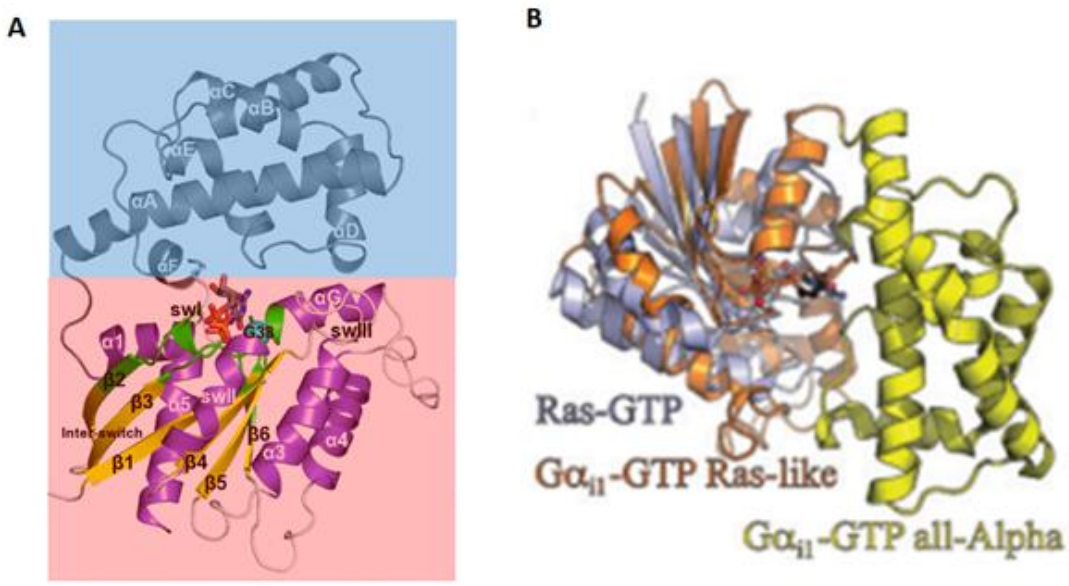

Figure 1.6 A - Tertiary protein folding structure of Gα subunit holds a Ras-like domain (red box) and an α-helical domain (blue box). (Taken from Mariani *et al*., (2013)) B - Structural similarities between GTP-bound Ras and Gαi1 subunit (Taken from Gerwert *et al*., (2017)).

Lipid modifications play a crucial regulatory role for membrane localization of heterotrimeric G proteins. Besides the fact that all Gα proteins post-translationally undergo palmitoylation at the N-terminus, members of the Gαi family are also co-translationally modified with fatty acid myristate at the N-terminus (Sikarwar *et al.*, 2019). One or both modifications are required to regulate membrane localization and protein-protein interactions, such as interaction with the Gβγ heterodimer, effectors, and regulators of G protein signaling (RGS) (C. A. Chen & Manning, 2001)(Oldham & Hamm, 2008).

1.2 G-protein signalling

Cellular signaling is accomplished by a multitude of proteins, peptides, lipids, ions, and small molecules (CR et al., 2005). Abnormal G protein signaling leads to pathogenesis; for example, loss-of-function or gain-of-function mutations within the G protein α subunit genes play a role in several diseases, including endocrine tumors

(Lyons et al., 1990). Therefore, the “on/off” state of these molecular switches is tightly regulated by cytosolic proteins, GEFs, and GAPs, respectively.

Classically, G protein signaling is initiated by agonist bound G protein-coupled receptors (GPCRs) at the plasma membrane (C & SGB, 2019). In the last decades, studies indicate that several intracellular accessory proteins, called the activators of G protein signaling (AGS), can regulate the “on” state of G proteins in a GPCR-independent fashion (Takesono et al., 1999) (Blumer et al., 2005). As a summary, Figure 1.7 shows G protein signaling enabling binding partners (Blumer et al., 2005).

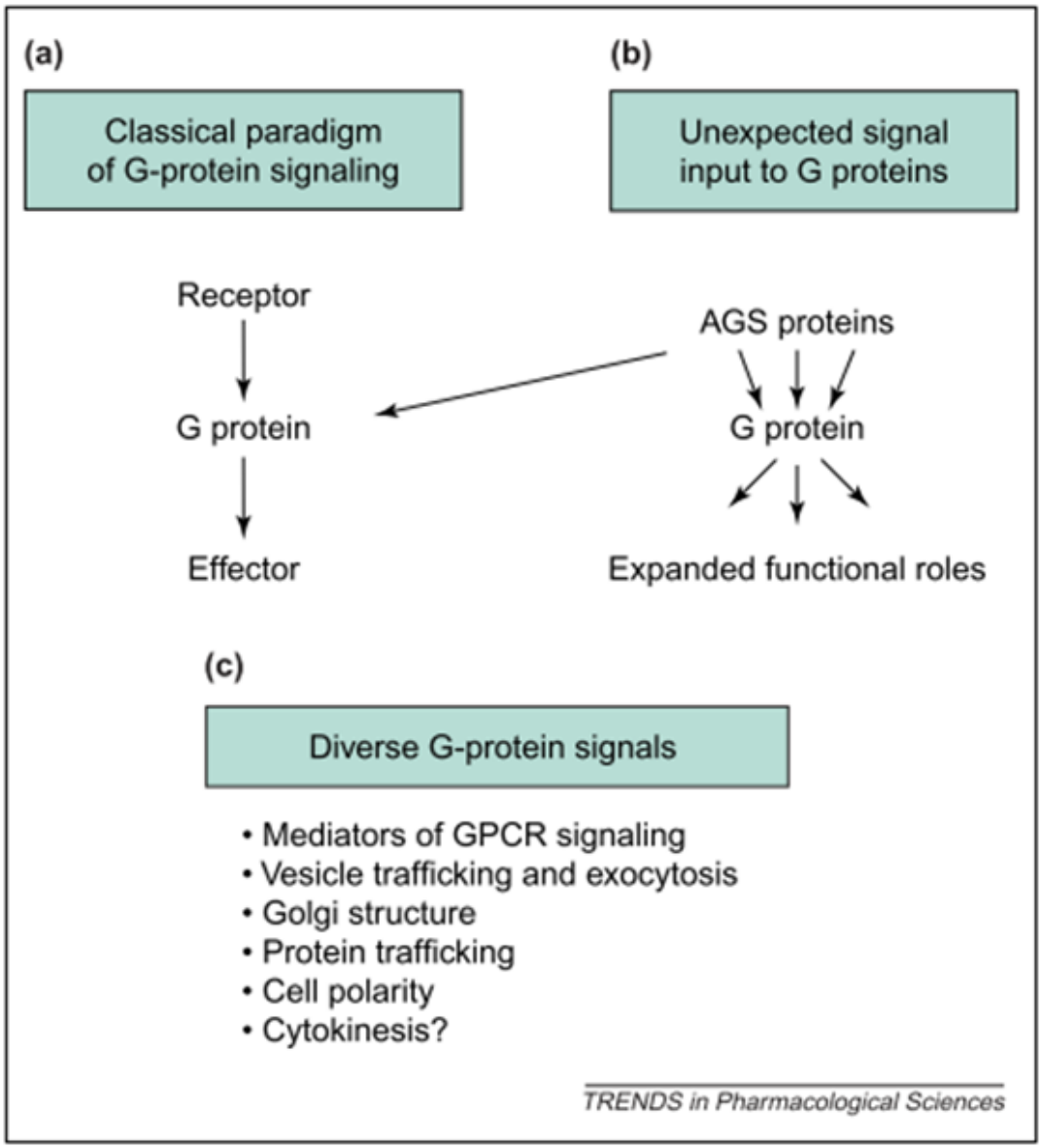

Figure 1.7 Diversification of G-protein signaling. (Taken from Blumer *et al*., (2005))

1.2.1 GPCR-mediated G protein signaling

Many extracellular signals, such as peptide hormones, sensory stimuli, odors, light, neurotransmitters, chemokines, growth factors, have an intracellular output by activating transmembrane receptors. In humans, the superfamily of GPCRs, also known as seven-pass-transmembrane-domain (7TM) receptors, are the largest class

of plasma membrane-bound receptors (>826 human GPCRs) (Yang et al., 2021). From their presence at the cell membrane GPCRs are known to overbridge a broad array of external stimuli. Due to their regulation of a large variety of human physiological and pathological processes, including homeostasis, GPCRs have been an important target of about 35 % of the approved and currently marketed drugs (RT & JS, 2007) (Hauser et al., 2017).

1.2.1.1 GPCR structure and Classical GPCR activation

Based on their sequence and structural similarity, human GPCRs can be divided into five major families: Glutamate-like, Rhodopsin-like (largest family), Adhesion, Frizzled/Taste2, and Secretin-like (Figure 1.8).

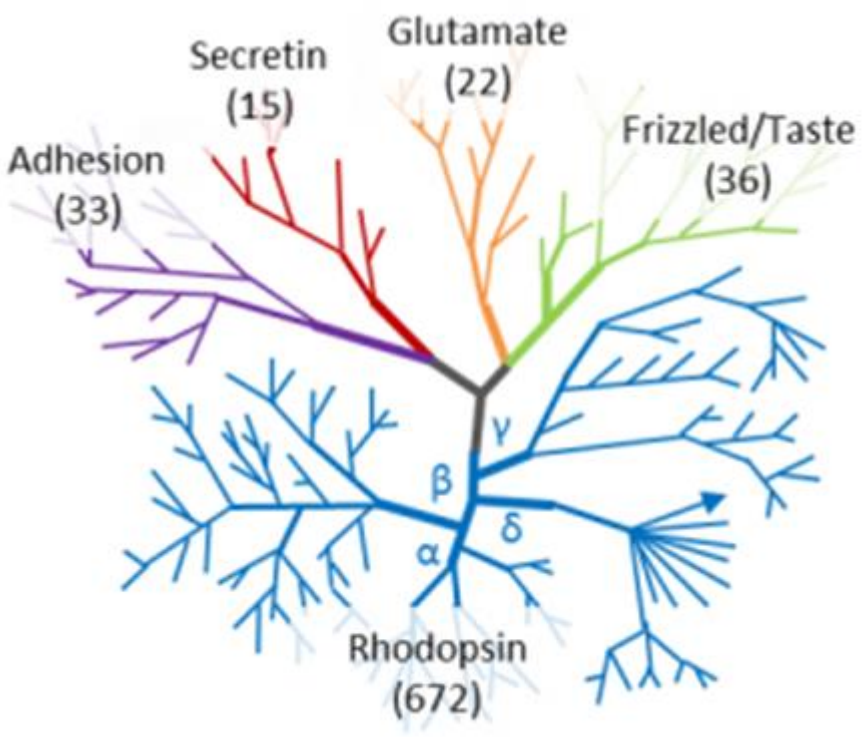

Figure 1.8 Classification scheme of GPCRs. (Taken from https://www.adhesiongpcr.org/adhesion-gpcrs/)

All members of the GPCRs superfamily share a common seven transmembrane (7TM)-spanning α-helical segments (TM1-TM7), which are linked by three intracellular (ICL1-ICL3) and three extracellular loops (ECL1-ECL3) (Figure 1.9). The extracellular part (EC) is responsible for ligand-binding. It has a higher structural diversity ranging from short unstructured sequences to large globular-like domains among the GPCR families (Lagerström & Schiöth, 2008). Conversely, the intracellular part (IC) is involved in intracellular signaling by binding to downstream effectors such as G proteins and is more conserved between GPCRs. However, the intracellular loops could also play a role in G-protein selectivity (Wong, 2003).

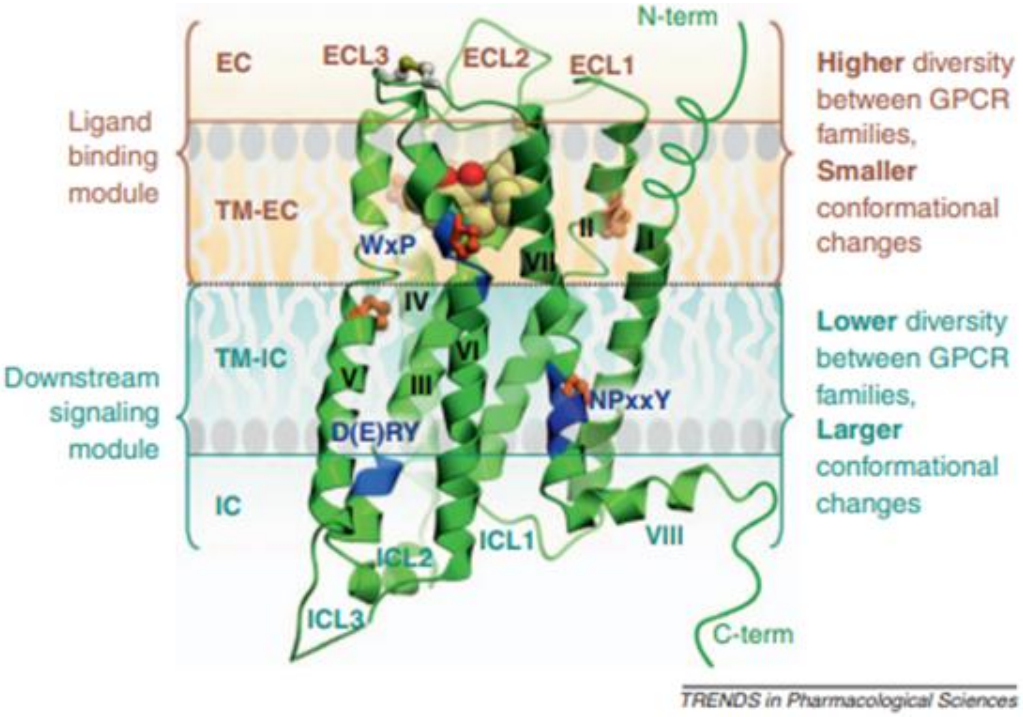

Figure 1.9 General structure of GPCRs. Major structural characteristics are given on an example of the D3R crystal structure. (Taken from Katritch *et al*., (2012))

Traditionally, GPCRs are accepted as monomeric units that function solely on their own. According to the classical GPCR pathway, 'one GPCR-one heterotrimeric G-protein' interaction model is sufficient to elicit physiological responses (Ng et al., 2013). Classical GPCR activation occurs via the binding of a ligand at the

extracellular site of the receptor. Specifically, a single ligand is enough to activate a single receptor and, in this way, bind and activate a single G protein (Figure 1.10 A-C).

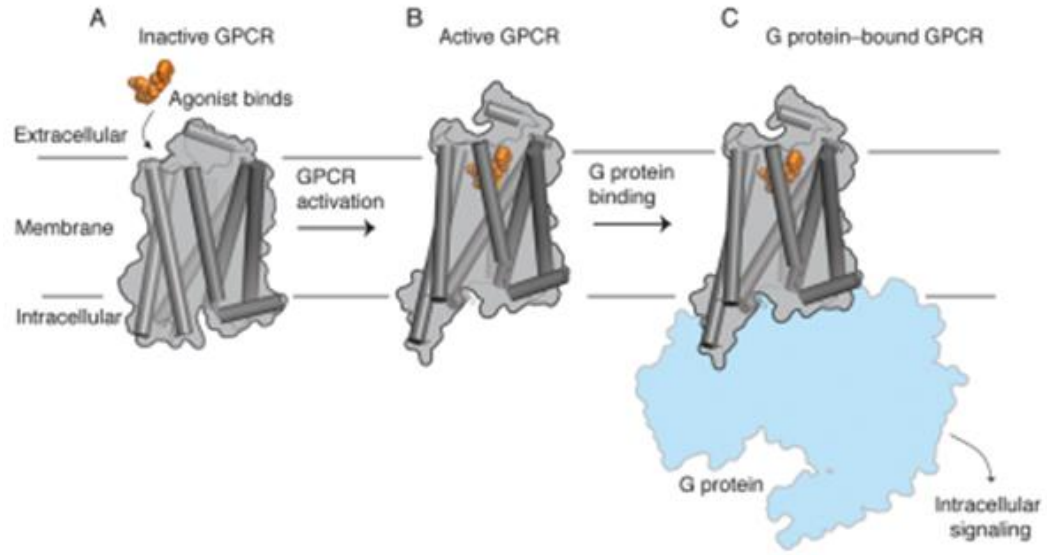

Figure 1.10 **Classical GPCR-mediated signaling model.** A – ligand-binding to an inactive GPCR, B – ligand-bound GPCR, which will act as a GEF, undergoes structural rearrangements to its active state, C – an active GPCR binds a G protein (Taken from (Latorraca *et al*., (2017))

Upon ligand-binding, conformational changes occur predominantly in the transmembrane region of the GPCR (Figure 1.11). Studies have shown that the structural rearrangements occurring at transmembrane helices 5-7 play a critical role in downstream signaling by creating an intracellular pocket along with the intracellular loops at which their primary coupling partner, Gαβγ protein, can bind (Latorraca et al., 2016).

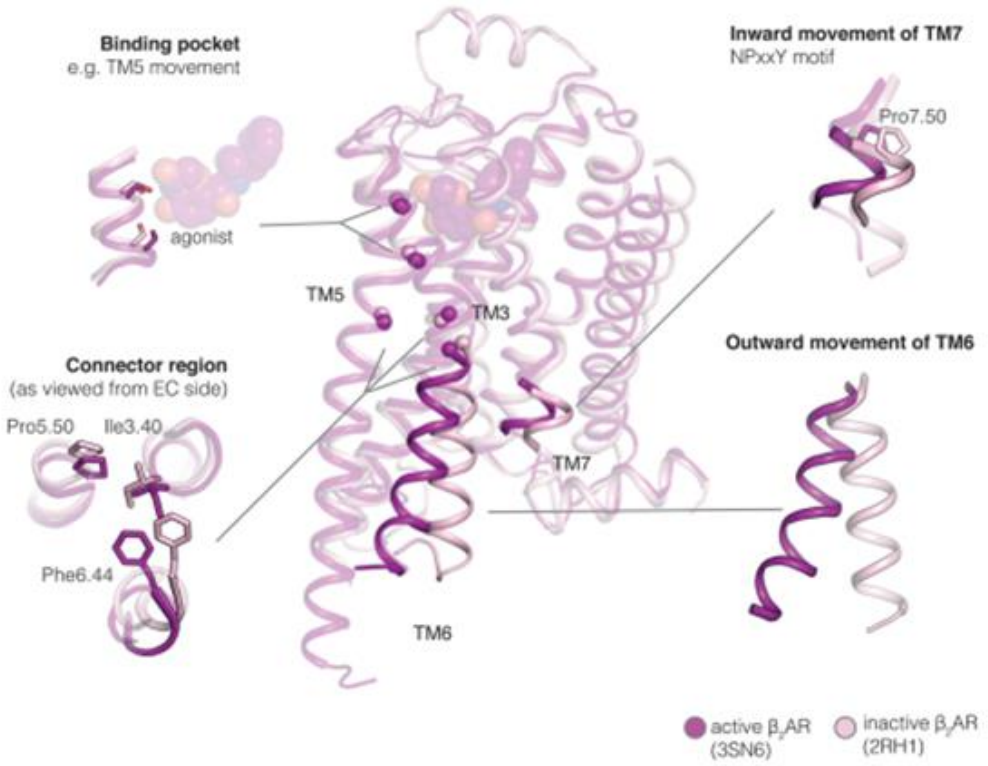

Figure 1.11 **Confirmational rearrangements during the activation of GPCR signaling.** Inactive (light pink) and active (dark purple) conformations of the β2AR show differences in helix position: TM6 rotates and swings nearly 14 Å away from the center of the helical bundle, accompanied by rotations and slight inward movements of TM5 and TM7. (Taken from (Latorraca *et al*., (2017))

The GPCR-G protein coupling promotes (1) GDP to GTP exchange from the α subunit, (2) dissociation of the GTP-bound α-subunit and βγ-dimer from the GPCR. As a result, the Gα- and Gβγ subunits stimulate different effector molecules, thereby activating or inhibiting the production of a wide range of second messengers. The signals mediated by the four G protein α subunits are shown in Figure 1.12. Depending on the coupled Gα protein (Gαi/o, Gαs, Gαq/11 and Gα12/13) GPCRs can regulate key biological functions, such as cell motility, cell metabolism, cell proliferation, metastasis (Figure 1.12) (Radhika & Dhanasekaran, 2001).

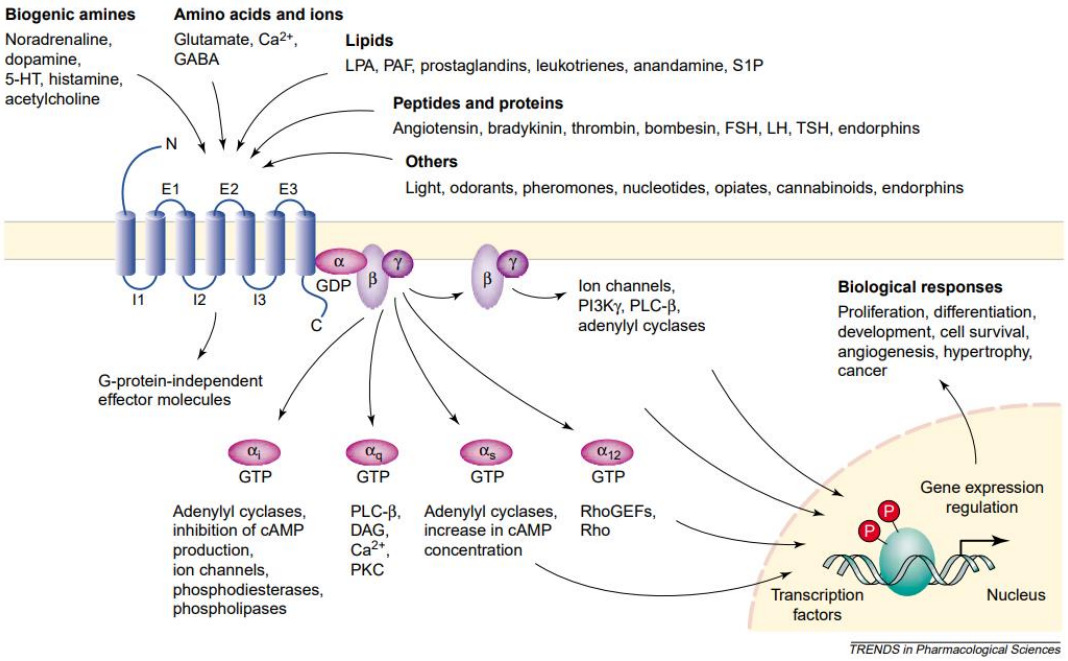

Figure 1.12 **G-Protein-coupled receptor (GPCR)-mediated signaling pathways.** (Taken from (Marinissen and Gutkind, (2001))

1.2.1.2 Gαi protein signaling pathway

Upon agonist-binding, GPCRs undergo a conformational change, which results in catalysis of GDP-GTP exchange on the Gα subunit by coupling to the membrane-localized GPCR. The rate-limiting step of the cycle is the GDP release. On the other hand, the binding of GTP induces conformational changes in three switch regions of the Gα subunit and eventually leading to the dissociation of Gβγ dimer and GTP-activated Gα monomer (Gα-GTP). Ultimately, both act upon their distinct downstream effectors and thereby initiate unique intracellular responses. The signal termination, after the signal propagation, occurs by hydrolysis of the GTP on the Gα-GTP to GDP, becoming inactive Gα-GDP and eventually causing its re-association with the Gβγ dimer (inactive heterotrimeric complex) (Johnston & Siderovski, 2007).

The classical signaling mechanism for Gαi protein subunit is the inhibition of the cAMP dependent pathway through inhibition of adenylate cyclase (AC), the

membrane-associated enzyme that catalyzes the production of cyclic AMP (cAMP), which in turn results in the activation of protein kinase A (PKA) and eventually leading to the activation of cAMP-responsive element-binding protein (CREB). However, activated Gαi proteins can have a variety of responses by affecting the activation of multiple effectors besides AC, such as activating the mitogen-activated protein kinase (MAPK) and phosphatidylinositol 3-kinase (PI3K) pathways (Figure 1.13) (Dessauer et al., 2002) (Leurs et al., 2005).

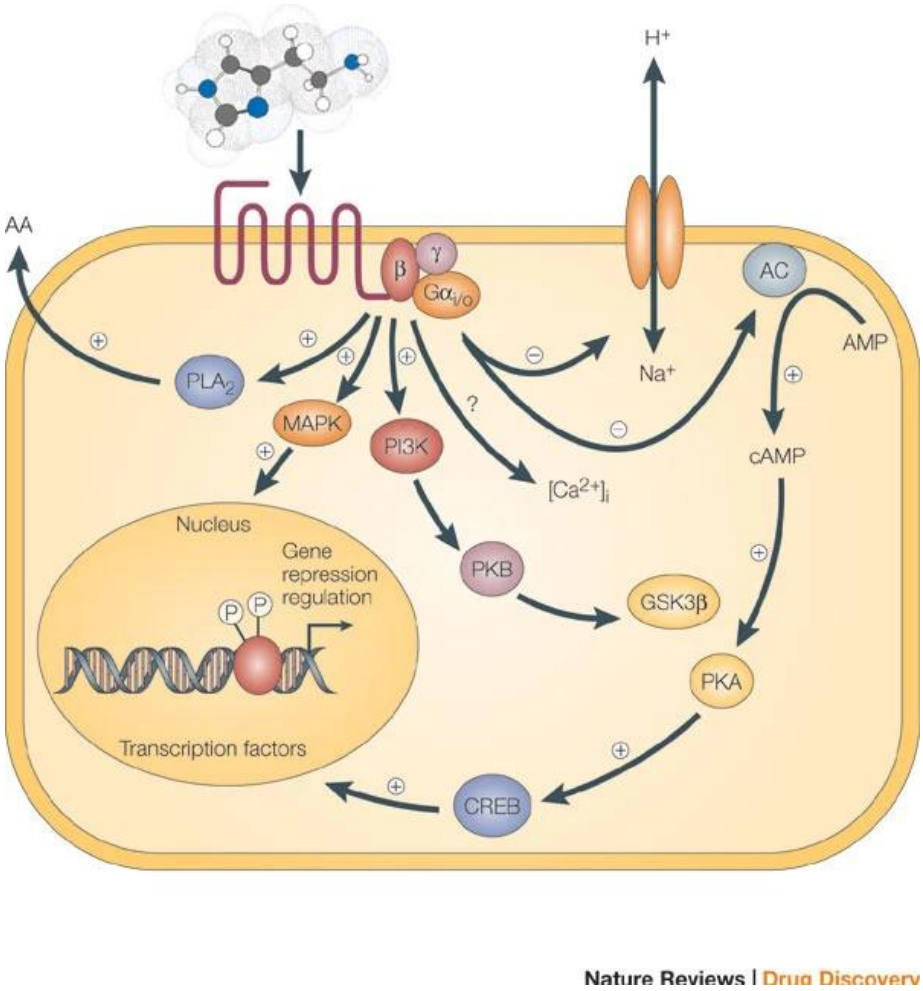

Figure 1.13 Gαi signaling pathways (taken from (Leurs et al., 2005))

1.2.2 GPCR-independent G-protein signaling

Heterotrimeric G-protein signaling pathways are classically activated by the seven-membrane receptors (GPCRs). This signaling system is a generally accepted aspect of how the cell links extracellular stimuli to produce a variety of biological responses (Blumer et al., 2007). However, during characterization studies of the heterotrimeric G-proteins activation-deactivation cycle, several studies suggested that receptor-independent G-protein activation was possible. In 1999 a new class of proteins were discovered and named as Activators of G proteins (AGS) (Cismowski, 2006).

1.2.2.1 Activators of G proteins (AGS)

The AGS proteins were first discovered through a yeast-based functional screening assays for mammalian cDNAs that activated G protein signaling in the absence of a G protein–coupled receptor (GPCR) (Takesono et al., 1999). Currently, AGSs define a wide range of regulatory proteins which (1) influence signal transduction from GPCR to G-protein, (2) guanine nucleotide binding and hydrolysis, and (3) G protein subunit interactions (JB & SM, 2014). Based upon their interaction and regulation of G-protein subunits, AGS proteins are categorized into three major groups (Figure 1.14): (group I) entities that act as GPCRs in terms of functioning as GEF for G-protein activation, (group II) Guanine nucleotide dissociation inhibitors that can activate heterotrimeric G-protein signalling by showing an effect on G-protein subunit interactions independently of nucleotide exchange, and (group III) entities that bind to solely bind to Gβγ. While the group I members can bind to all G protein subclasses, Group II protein members preferentially bind to $G_i/G_{s/o}$ proteins (Blumer et al., 2005; JB & SM, 2014).

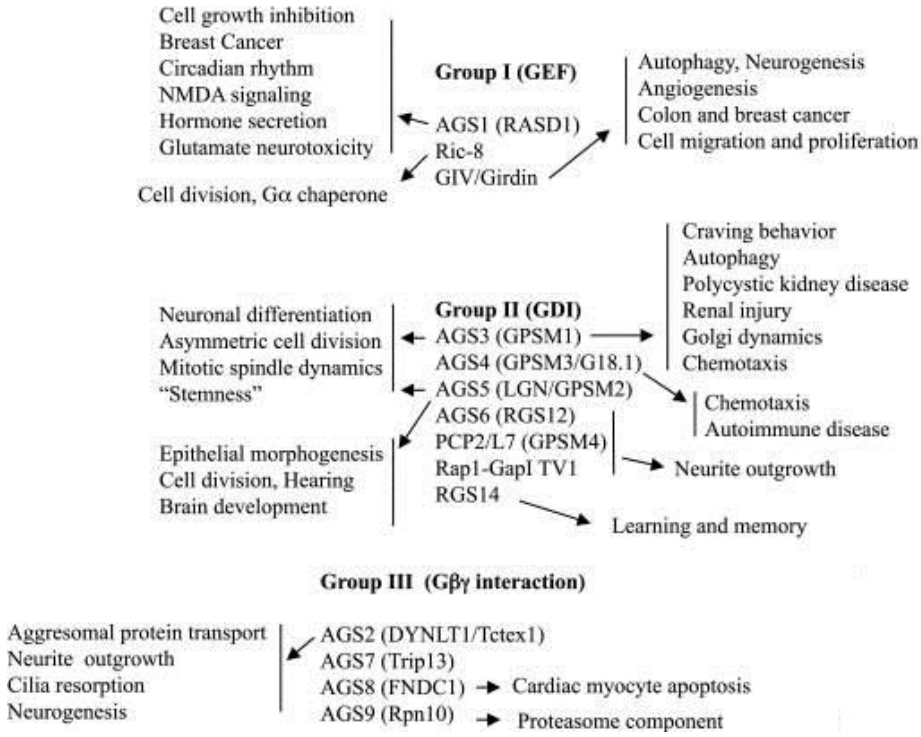

Figure 1.14 Diversity of AGS proteins. (adapted from Blumer *et al*., (2014))

1.2.2.2 Gαi protein signaling via Ric-8

Ric-8, also known as synembryn, was identified in a yeast two-hybrid screen to search for proteins interacting with mammalian heterotrimeric Ga subunits (Papasergi et al., 2015). In vertebrates two ortohologs have been described: (1) Ric-8A which acts within the signaling pathway of the Gαi/o, Gαq/11, and Gα12/13 subclasses and (2) Ric-8B which primarily acts on the Gαs/olf subfamily (Gabay et al., 2011; Tall et al., 2003). *In vitro* studies have shown that Ric-8A (60kDA) binds to GDP-bound Giα1, Gαq, and Gαo and catalyzes the GDP-GTP exchange on the Gα subunit resulting in a constitutive active state. In addition, several studies have reported that Ric-8A act in a GPCR-independent regulation of asymmetric cell division through Gαi that is essential for embryonic development (Tõnissoo et al., 2010)(McClelland et al., 2020). In figure 1.15, the non-canonical activation of Gα subunits through Ric-8 is shown. Ric-8 acts as an GEF when interacting with the G-domain (Ras-like domain) of the Gα subunit, promoting the

exchange of GDP to GTP and eventually activating the signalling pathway in a receptor-independent way. Papasergi and colleagues suggest that the binding of Ric-8 to the GDP-bound Gα subunit may result in reduced affinity for GDP due to partial unfolding. At the open-confirmation, the GTP can then bind to the Gα subunit which result in the forming of the active confirmation and eventually dissociating the Ric-8 (Figure 1.15).

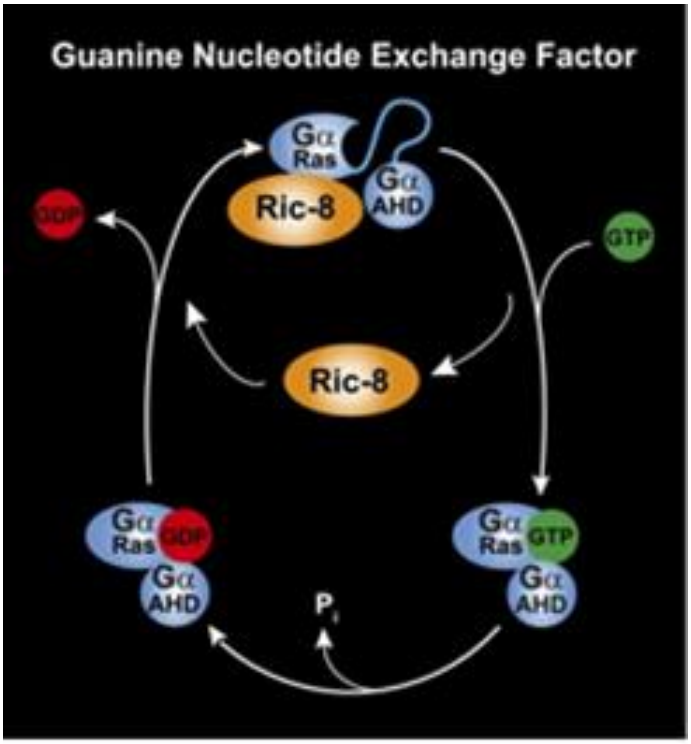

Figure 1.15 Regulation of G-protein activation by non-receptor GEF, RIC-8 (AGSI). (Taken from Papasergi et al., 2015))

1.3 Homo- and Heterodimerization of GPCRs and Gα proteins

During the last two decades, GPCR dimerization/oligomerization has been intensively investigated by using pharmacological, biochemical, and biophysical approaches (Derouiche & Massotte, 2019). These studies have shown that 'one GPCR dimer-one G protein' coupling model is more likely under physiological conditions. GPCRs that show dimerization activation can be classified into three

major categories (Figure 1.16): (1) GPCRs that can mediate signaling only in dimerized conditions (homo- or heterodimerization), for example, $GABA_{B1}$ and $GABA_{B2}$ receptors dimerization required for their function in native tissues. Since ligands can only bind to $GABA_{B1}$ but it has no ability to conduct subsequent signaling, whereas $GABA_{B2}$ has no ligand-binding pocket but is able to transduce signaling (Rondard et al., 2008) (Wang et al., 2018) (2) dimeric GPCRs that couple to different G proteins compared with monomeric GPCRs, for example dopmaine D1 receptor (D1R) normally signals through Gαs, while dopamine D2 receptor (D2R) transduces signals through Gαi. However, D1R-D2R heteromer couples and signals through Gαq (Wang et al., 2018). (3) dimeric GPCRs that induce a G protein/β arrestin switch (Wang et al., 2018).

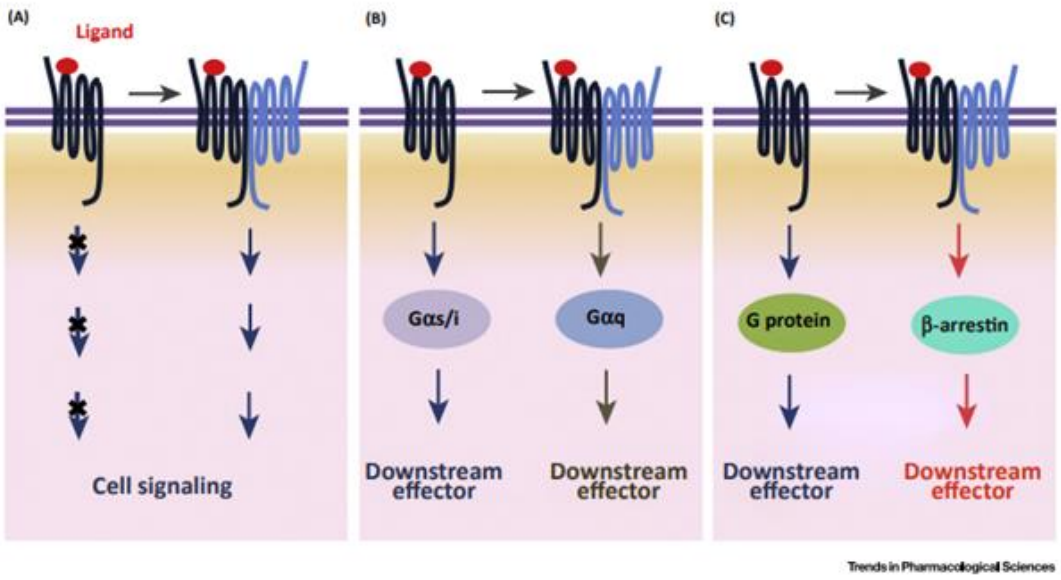

Figure 1.16 Different GPCR dimerization activation modes. (Taken from Wang *et al.*, (2018))

Besides those major categories, allosteric receptor-receptor interactions have also been reported. Various allosteric alternations can be induced, such as changes in ligand-binding affinity and/or signaling efficacy. While ***agonistic allosterism*** depicts the situation of allosteric enhancement of ligand binding to receptor heterodimer, ***antagonistic allosterism*** explains the situation at which ligand binding to one of the receptors in the heterodimer decreases the agonist binding affinity of the partner

receptor. The best example of the latter case is the allosteric antagonistic interaction between adenosine A2 receptors (A2AR) and D2R, both highly expressed in the striatum and function in motor coordination of the striatal pathway, by which A2AR agonists decrease the D2R-agonist binding affinity and is shown in Figure 1.17 (Ferré et al., 2016). These two receptors have opposite effects on the adenylyl cyclase (AC) mediated signaling pathway. While A2AR coupled to Gαs (stimulatory proteins), D2 receptors coupled to Gαi (inhibitory proteins).

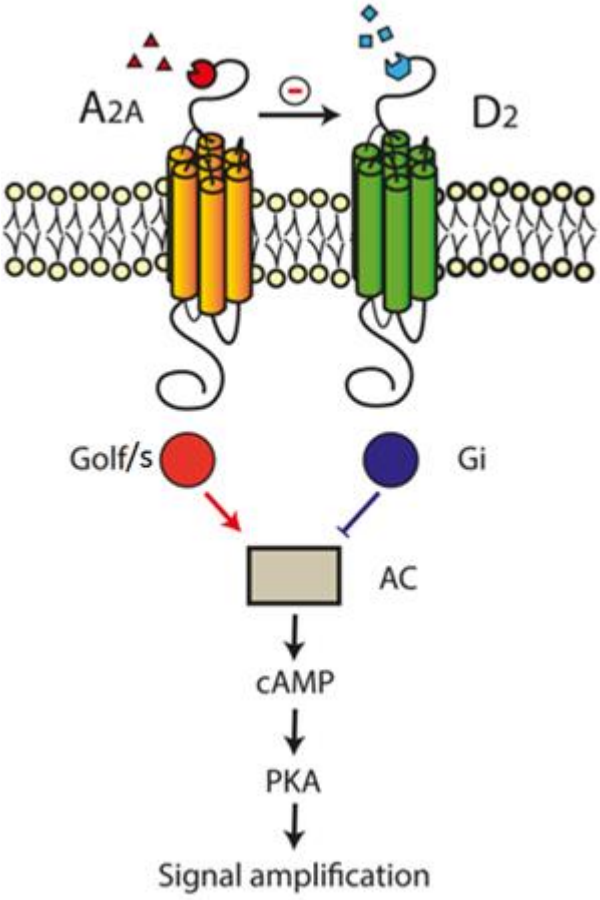

Figure 1.17 Allosteric antagonism of Gi/o mediated D2R signaling in the A2A–D2R heteroreceptor. (Taken from Pinna *et al*., (2018)).

In addition, GPCRs studies indicated that different receptors integrate to form active receptor oligomers during signal transduction. A study, by Navarro and colleagues, on the molecular architecture of A1A-A2A heterotetramer (a heteromer of A1A- and A2A homodimers) suggested the possibility of simultaneous binding of Gi and Gs

proteins to their respective A1A- and A2A homodimer (Figure 1.18) (Navarro et al., 2016).

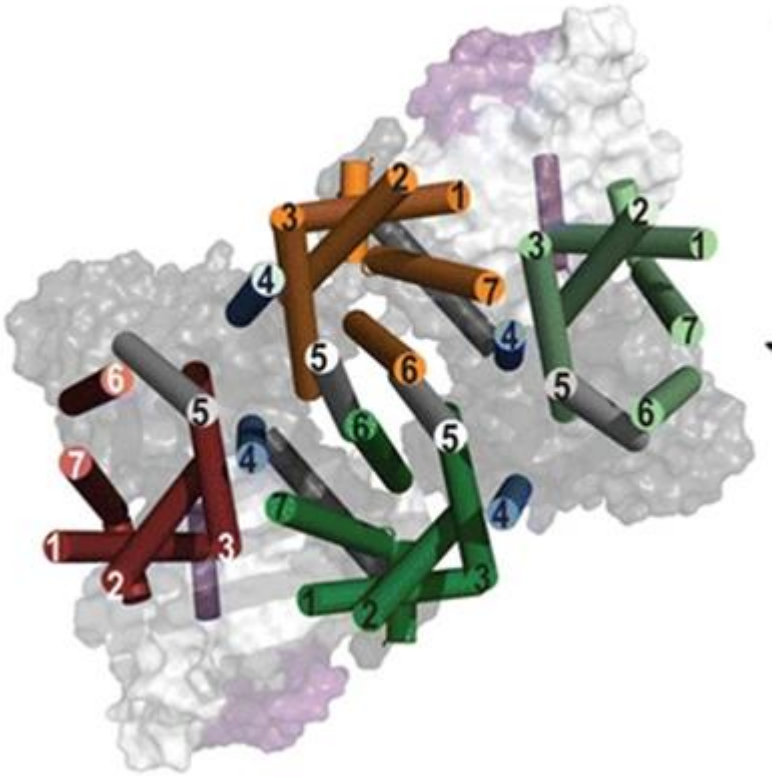

Figure 1.18 Molecular model of the A1AR-A2AR tetramer in complex with Gi and Gs. Gi-bound shown in red, Gi-unbound A1AR shown in orange, Gs-bound A2AR shown in dark green, Gs-unbound A2AR shown in light green, and the α, β-, and γ-subunits of Gi and Gs shown in dark gray, light gray, and purple, respectively (Taken from Navarro *et al*., (2016)).

1.3.1 Ras-dimer formation

Ras proteins, which are structurally related with Gα proteins and are also known as small G proteins, are involved in many different signaling pathways by binding and activating wide range of effectors, such as ERK, Akt, and Raf. Most of these pathways result in cellular responses such as cell proliferation, migration, survival, and differentiation. Various mutations in their active site, the G domain, adversely

affect the protein activity. Among those, the mutations that cause the Ras proteins to remain constitutively active have been detected in ~30% of all human cancers (Schubbert et al., 2007). RAS genes are the first oncogenes detected in human cancer cells and are known as the most mutated oncogenes in all human cancer types (Stephen *et al*. 2014).

The generally accepted signaling mechanism of Ras proteins is the one by which they function as monomers. However, Inouye and colleagues suggested in their study, for the first time, the importance of Ras dimerization and/or oligomerization by showing that Raf1 activation in the liposome is associated with Ras dimerization in *in vitro* conditions (Inouye et al., 2000). Physiological and functional importance of the Ras nanocluster has been demonstrated in studies following this work. For instance, Nan and colleagues showed dimerization of GTP-bound K-Ras4B proteins in the cell membrane by using photo-active localization microscopy method (PALM) (Nan et al., 2015). Most recently, Muratcioglu and colleagues showed that the active K-Ras4B homodimerizes *in silico* and *in vitro* through two major interfaces; α-helix and β-sheet interface (Figure 1.19) (Muratcioglu et al., 2020). According to this study, the β-sheet interface interferes with the region where effectors such as Raf, PI3K, and RalGDS bind, while the α-helix interface coincides with the allosteric region at the C-terminus of the G-domain. The α-helix interface is thought to promote Raf activation. In addition, it is predicted that using drugs targeting the α-helix interface can reduce the oncogenic signal of Raf protein (O'Bryan, 2019).

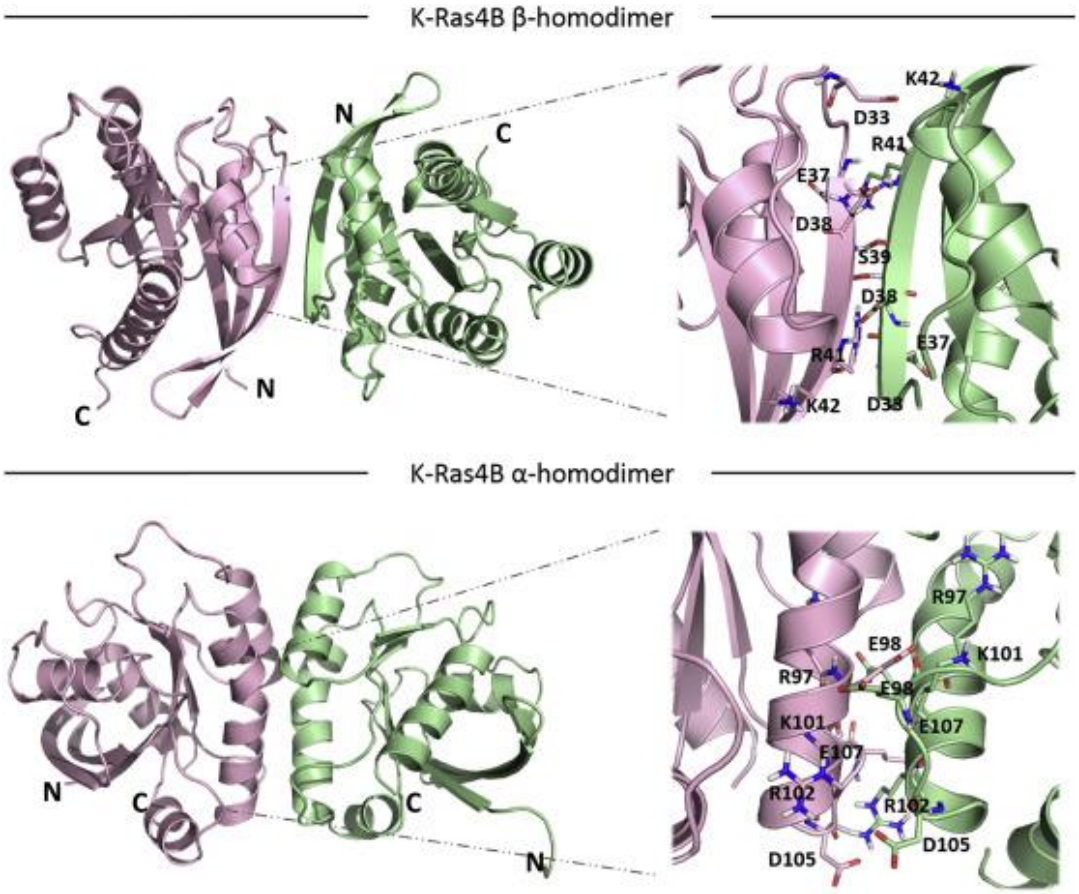

Figure 1.19 K-Ras4B homodimer interaction simulation. H bonds/salt bridges forming residues at the interface shown as sticks (right panels) (Taken from Muratcioglu *et al*., (2020)).

1.4 Protein-Protein interaction detection methods

Proteins are involved in all biological systems in a cell, and while many proteins perform their functions independently, most proteins (>80%) interact with each others for proper biological activity. Besides the fate of the proteins within the cell (synthesis, maturation, vesicle budding, trafficking, and degradation), intracellular processes such as receptor dimerization, signaling cascades, gene regulation, metabolism, and catabolism are all performed by PPIs (Xing et al., 2016). The study of PPIs is important to (1) track down the function of protein within the cell, and (2) predict the drug ability of molecules (Nooren & Thornton, 2003). The detailed study

of PPIs has become one of the major objectives of systems biology. PPIs can be classified in different ways based on their structural and functional characteristics. To illustrate, on the basis of their interaction surface, PPIs may be homo- or hetero-oligomeric; as measured by their stability, they may be transient (in signaling pathways) or permanent (in stable protein complex formation); as examined by their affinity, they may be obligate or non-obligate (Zhang, 2009).

Protein-protein interaction detection methods are generally classified into three types, *in vitro*, *in vivo,* and *in silico* methods. Detection methods such as affinity chromatography, coimmunoprecipitation, and NMR spectroscopy are classiefed under the *in vitro* methods and are performed in a controlled environment outside a living organism. Examples of the *in vivo* detection methods are yeast two-hybrid (Y2H, Y3H), bioluminescence resonance energy transfer (BRET), Förster resonance energy transfers (FRET), and bimolecular fluorescence complementation (BiFC) Llères *et al*., 2007). While experimental approaches are time-consuming and expensive, *in silico* approaches, such as the PRISM web server, are more efficient as fast PPI prediction tools (Baspinar et al., 2014).

1.4.1 Förster Resonance Energy Transfer (FRET)

Fluorescence-based methods are widely used due to their ease of utilization, the broad range of fluorophores, and the possibility of various read-out modes (microscopy and plate reader). Among all fluorescent-based methods, FRET has been extensively used (1) to monitor protein interactions *in vivo* due to high distance sensitivity (Day & Davidson, 2012), and (2) in biological studies to investigate the characteristics, functions, and dynamics of biomolecules, including proteins and nucleic acids (Okamoto & Sako, 2017).

1.4.1.1 Basics of FRET

Förster Resonance energy transfer, which was first described by Theodore Försters in 1948, is an electromagnetic phenomenon whereby energy is non-radiatively transferred from an exited donor fluorophore (FRET donor) to a nearby ground-state acceptor fluorophore (FRET acceptor) via long-range dipole-dipole coupling (Skruzny et al., 2019). The efficiency of energy transfer (E_{FRET}) from FRET donor to FRET acceptor depends on (1) the separation distance (r) between the two fluorophores (Figure 1.20-A). E_{FRET} is inversely proportional to the sixth power of r:

$$Efret = \frac{1}{1 + \left(\frac{r}{Ro}\right)^6}$$

R_o is the Förster radius which is the separation distance leading to 50% of energy transfer from FRET donor to FRET acceptor. The typical R_o is mostly around 5nm, effective energy transfer occurs when FRET donor and acceptor are within ± 3nm of R_o. As a result, FRET can be applied as a 'molecular ruler' for distance calculation in the 1-10nm range Broussard & Green, 2017); (2) dipole-dipole orientation of FRET donor and acceptor (Figure 1.20-B). Efficient energy transfer occurs upon parallel alignment of FRET donor and acceptor dipoles (Ciruela, 2008); (3) degree of spectral overlap between donor emission spectra and acceptor excitation spectra (Figure 1.20-C) (Day & Davidson, 2012); (4) quantum yield of the donor (ϕ_D); and (5) the extinction coefficient of the acceptor (ε_A) (Skruzny et al., 2019).

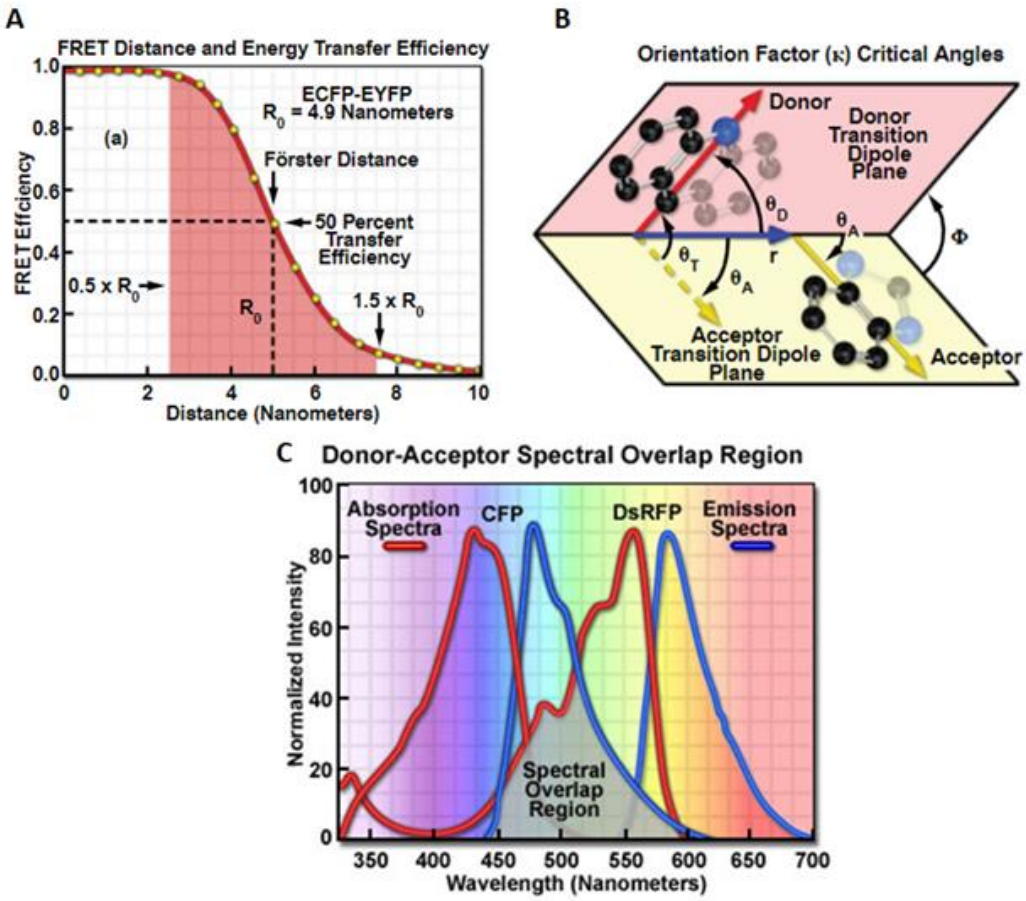

Figure 1.20 **Basic priciples of FRET.** A – The distance dependency of FRET efficiency, B – orientation factor between the two fluorophore dipoles, C – excitation and absorption spectra of a FRET pair, CFP (FRET donor) and DsRFP (FRET acceptor). (Taken from https://www.microscopyu.com/applications/fret/basics-of-fret-microscopy)

1.4.1.2 FRET imaging through Confocal fluorescent microscope

Spinning disc confocal microscope (SDM), in contrast to standard fluorescence microscope, has many advantages: (1) rapid excitation, (2) eliminate out-of-focus light by using pinholes resulting in higher resolution, greater contrast, less noise and, (3) imaging at a faster rate. Consequently, SDM is very useful when imaging live cells. This system includes a rapidly rotating Nipkow-Petran disc (Pinhole array disc) with a spiral pattern of pinholes, as seen in Figure 1.21. The pinholes are positioned

in such way so that when the disc spins around every part with frame rates going up to 1000 frames per second (Stehbens et al., 2012).

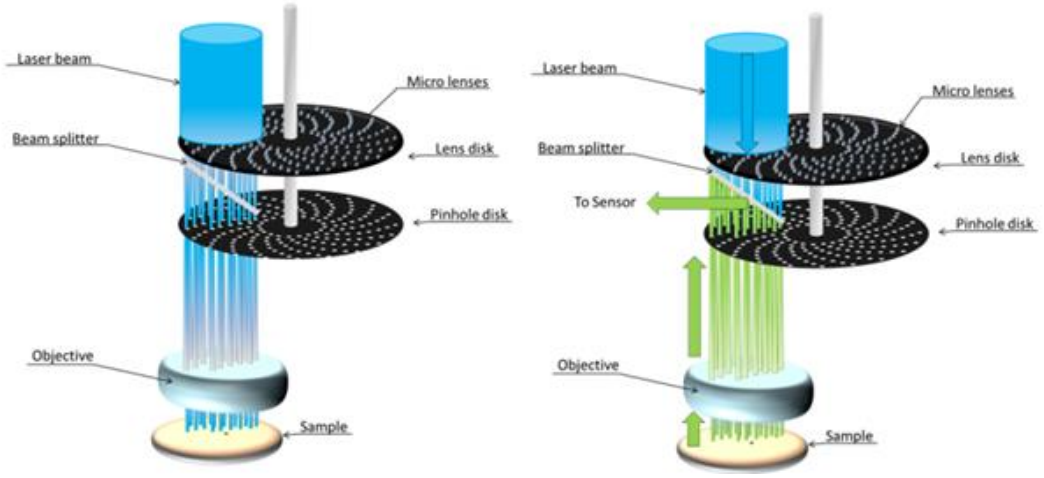

Figure 1.21 Principle of the spinning disk confocal microscope. First, the laser beam passes through a Nipkow-Petran disc called the lens disc, which concentrates the lights at the second disc—eventually, leading the light to the sample by passing the objective (Left panel). The emitted fluorescent light by the sample is filtered y the pinhole disc because pinholes in this pinhole disc reduce the out-of-focus fluorescence (right panel). (Taken from https://www.cherrybiotech.com/scientific-note/microscopy/introduction-to-spinning-disk-confocal-microscopy)

Due to its capacity to produce images eliminated from out-of-focus information, an excellent platform for FRET imaging is formed allowing the investigation of (intra- and/or inter) molecular interactions within with high spatial and temporal resolution *in vivo*. The discovery of the Green Fluorescent Protein (GFP) by Shimomura and colleagues in 1962 has led to the development of novel fluorescent proteins (FPs) with distinct characteristics, such as favorable FPs for FRET technique. Consequently, this has driven the interest in the FRET technique as well as the development of a variety of methods to measure FRET efficiency (E_{FRET}). Some examples of ways to quantify E_{FRET} are Acceptor Emission Sensitized 3-cube, acceptor photobleaching, donor photobleaching (also known as Fluorescence-lifetime imaging microscopy (FLIM) FRET), and Spectral Imaging. (Padilla-Parra & Tramier, 2012).

1.4.1.3 FRET assay using a monochromator plate reader

Multi-mode microplate readers, which are used in most biochemical laboratories, fall into two main categories: (1) filter-based and (2) monochromator-based. While the filter-based readers use filters, one for the excitation wavelength and the other for emission wavelength, to select the desired wavelengths, the monochromator-based readers use multiple diffraction gratings to create the desired excitation and emission wavelengths through the provided software. An advantage of the monochromator-based readers is its spectral sanning ability which is not possible with a filter-based plate reader. This spectral scaninning detection mode allows to measure wavelengths over a broad range following a given excitation wavelength. In this study, a 2x2 monochromator-based microplate reader was used. This type of monochromator allows individual optimization of wavelengths for both excitation and emission in fluorescence readings. While the excitation gratings shape the light into the sample volume, the emisision gratings guide the fluorescence emission to the detector (Figure 1.22). Since fluorescence is the absorption of light and its transformation into emission, the spectral scanning read mode permitted us to record the FRET emission spectrum of our FRET pairs by exciting the donor fluorophore with a selected wavelength and measuring the emission spectrum range of the acceptor fluorophore.

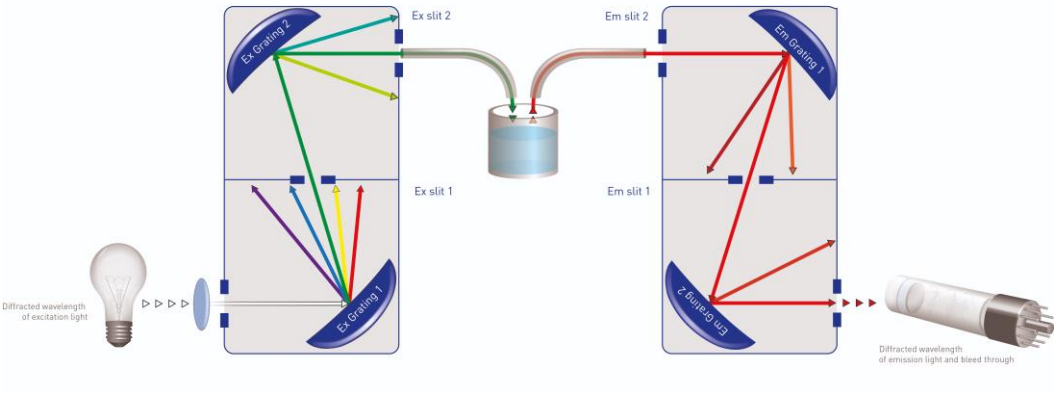

Figure 1.22 schematic illustration of the components of a 2x2 monochromator microplate reader. (Taken from https://www.scientistlive.com/sites/scientistlive/files/Fig1_0.jpg)

1.4.2 Blocking GPCR-Gα protein interaction using Gα-minigene

GPCRs-driven signaling pathways are involved in pretty much every physiological function and in many pathologies. The molecular interactions that occur between the receptors and the G proteins are fundamental to the transduction of extracellular signals into specific cellular responses. The COOH-termini of heterotrimeric G protein α subunits (Gα) (Figure 1.23) are critical for both binding to their associated G protein-coupled receptors (GPCRs) and determining specificity. In this way, by using synthetic peptides (minigenes) corresponding to the COOH-terminus can function as competitive inhibitors of receptor-G protein interactions because these small synthetic peptides will selectively block the site on the receptor-G protein interface (Gilchrist et al., 2002).

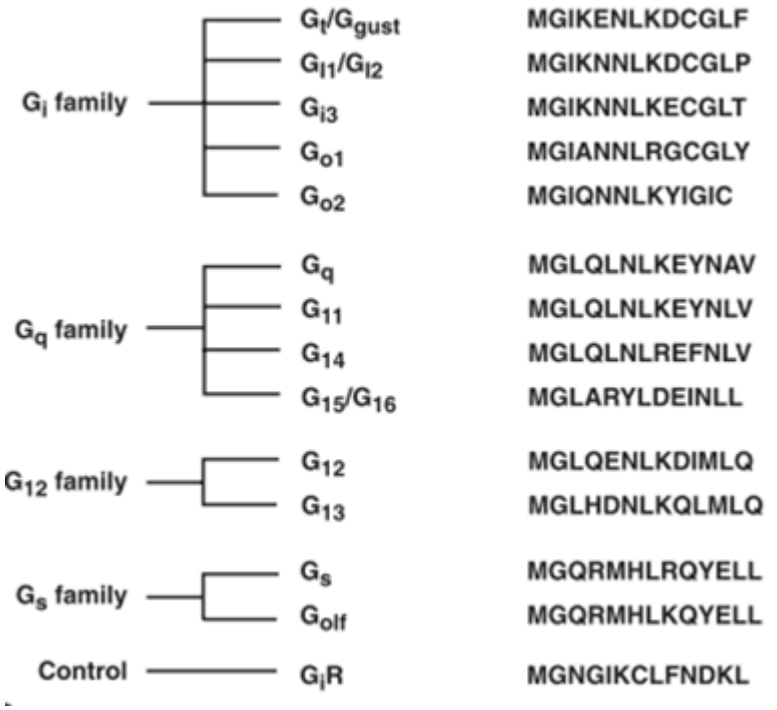

Figure 1.23 **COOH-terminal sequences of heterotrimeric G-proteins.**
Alignment of the expressed 13 amino-acid peptides encoded by the COOH-termini minigenes.

1.5 Aim of Study

In a classical GPCR signal pathway, one GPCR couples with one G-protein to transfer the signal inside the cell to effector proteins. Recent studies, showed that receptor dimerization is common to GPCR-mediated signaling. Moreover, under physiological conditions, the signaling unit is seen as the GPCR dimer- G-protein mode. In addition, studies have revealed that GPCRs having homo- or hetero- dimers interact with a single Gα protein and, therefore a single heterotrimeric G-protein. Experimental and computational studies have demonstrated that receptor tetramer models brought two different G proteins, each interacting with homo-dimers of GPCRs, to close proximity (Navarro et al., 2016).

Furthermore, studies with Ras proteins, which are structural homologs of the α subunit of heterotrimeric G-proteins, have shown that these proteins form dimers

playing important roles in different signaling pathways (M. Chen et al., 2016). Similarly, it has been demonstrated that Dynamin protein, which is not a member of the Ras family, but carries the GTP binding domain (G- domain), also forms dimers, and this dimerization is important in GTPase activity (Chappie et al., 2010). In the light of these studies, G proteins dimerization through G-domain became more pronounced. Previous work carried out in our Lab., by a former graduate student Özge Atay, for the first time demonstrated Gαi1-Gαi1 interaction in live cells (Atay, 2019).

The aim of this study is to quantitively investigate the receptor oligomerization-dependency on the Gαi homodimerization in live cells using FRET. In order to attain this, Gαi1 proteins labeled at various positions with Enhance Green Fluorescent Protein (EGFP) and mCherry fluorescent protein genes were used. The labeled proteins were co-transfected into N2A cells using appropriate controls to assess protein-protein interaction. In addition, the Gαi1 homodimerization have been analysed under two conditions: (1) in presence of Gαi1 minigene, which consists of the last 11 amino acids of the Gαi1 subunit (COOH-terminal), to block the interaction with cognate GPCRs and (2) agonist-induced receptor oligomerization to investigate receptor-dependency on Gαi homodimerization.

CHAPTER 2

MATERIALS AND METHODS

2.1 Preparation of construct plasmids

Gαi1 tagging with fluorescent proteins

Within the scope of 117Z868 numbered TÜBİTAK project titled as "Investigation of Gα protein dimerization mechanisms in live cells", mammalian expression plasmids containing fluorescently tagged human GNAI1 genes (encoding for Gαi1 protein) were prepared. EGFP and mCherry genes were inserted between A121-E122 position in GNAI1 gene (Galés et al., 2006). These constructs were prepared using standard molecular cloning techniques.

Construction of Gαi1-specific minigene

In this study, the dependency of receptors on the homodimerization of Gαi1 proteins was investigated by blocking the receptor-Gαi1 protein interaction using Gαi1 minigene. For the preparation of this construct, the oligonucleotides encoding the last 11 amino acids of the Gα subunits were synthesized with important signals containing 5' and 3' ends.

2.1.1 Primer design

Gαi1 tagging with fluorescent proteins

GNAI1 gene tagged with EGFP and mChery at specific integration site was obtained by the integration PCR method (two PCR reactions back-to-back). The first PCR was performed to amplify the fluorescent proteins, EGFP and mCherry, with 24 bp overlapping regions matching the integration site (A121-E122) on the wild-type

Gαi1 protein and a 18 bp linker (TCTGGAGGAGGAGGATC). The designed primers used for EGFP and mCherry amplification are shown in Table 2.1 below in the 5' to 3' direction.

Table 2.1 Primers used for EGFP/mCherry amplification

Gαi1 (121-122) EGF/mCherry Forward	TAGGGCTATGGGGAGGTTGTCTGGAGGAGGAGGATCTATGGTGAGCAA GGGCGAGG
Gαi1 (121-122) EGF/mCherry Reverse	AGTCACCAAAGTCTATCTTAGATCCTCCTCCT CAGACTTGT ACAGCTCGTCCATG

Construction of Gαi1-specific minigene

The Gαi1 minigene cassette with at the 5' end a human ribosome binding site (indicated in green), a start codon (indicated in red) and a glycine codon (indicated in blue) to protect the ribosome binding site (degradation) and the 3' end a protective glycine codon and a stop codon (indicated in purple) was obtained using PCR amplification. The obtained double-stranded DNA was flanked by restriction sites XhoI-HindIII (indicated in bold) and a *GTTGTTGTT* sequence at both ends for efficient restriction digestion. Primers designed for Gαi1 minigene generation are given in Table 2.2 in the 5' to 3' direction.

Table 2.2 Primers designed for Gαi1-specific minigene construction

Gαi1 minigene Forward	GTTGTTGTT**CTCGAG**GCCGCCACCATGGGAAT AAAAAATAATCTAAAAGA
Gαi1 minigene Reverse	GTTGTTGTT**AAGCTT**TTATCCAAAGAGACCACAA

2.1.2 Polymerase Chain Reaction (PCR) and conditions

Gαi1 tagging with fluorescent proteins

In this thesis, EGFP and mCherry were inserted at the, by literature approved, A121-E122 position in GNAI1 gene sequence using the integration PCR method (two PCR reactions back-to-back). Integration PCR enables to insert DNA at specific sites on a target sequence without using restriction enzymes. However, the only requirement is that the amplified fragments (product of first PCR) should be flanked with DNA sequences complementary to the integration site. A schematic representation of this method is shown in Figure 2.1.

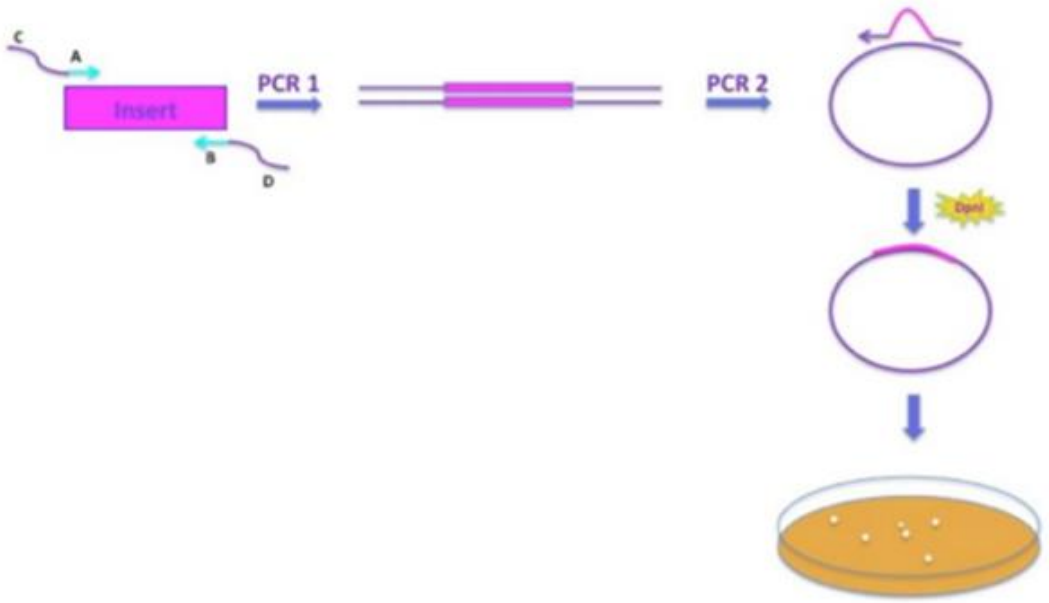

Figure 2.1 Schematic representation of integration PCR method. A and B parts of primers fit with the insert, while C and D parts are the flanking regions that fit the vector in which the integration is planned (Taken from)

In the first PCR, the fluorescent proteins EGFP and mCherry, were amplified together with the linker sequence and flanking region homologues to integration site of the wild- type GNAI1 gene. The PCR reaction components and conditions of the first PCR are given in Table 2.3 and 2.4.

Table 2.3 PCR mixture for amplification of EGFP/mCherry with flanking regions (1st PCR)

Reagent	Amount
5X Phire Reaction Buffer	25 µl
Phire HS II DNA Polymerase	1 µl
EGFP/mCherry in pcDNA3.1(-)	100 ng
10mM dNTPs	1 µl
Forward primer	1.25 µl from 20mM stock
Reverse primer	1.25 µl from 20mM stock
DMSO	11.5 µl
Nuclease free water (nfw)	Up to 50 µl

Table 2.4 Optimal PCR condition for the EGFP/mCherry amplification

Pre-denaturation	98°C	30 sec	
Denaturation	98°C	10 sec	34 cycles
Annealing	55°C	30 sec	
Extension	72°C	1 min	
Final extension	72°C	5 min	

Afterwards, during the second PCR, those amplicons were used as megaprimers, and GNAI1-containing pcDNA3.1 was used as template with a 1:5 template to primer ratio. The reaction components and optimal conditions of the second PCR are given in Table 2.5 and 2.6. At the end of the second PCR, DpnI was added to all PCR products to completely remove non-fluorescently tagged wild-type methylated template.

Table 2.5 PCR mixture for the EGFP/mCherry integration into Gαi1 protein

Reagent	Amount
Phire Green Hot start II PCR MasterMix	25 µl
wt Gαi1 in pcDNA3.1(-)	100 ng
1st PCR products	500 ng
DMSO	1.5 µl
Nuclease free water (nfw)	Up to 50 µl

Table 2.6 Optimal PCR condition for the Integration PCR method

Pre-denaturation	98°C	3 min	
Denaturation	98°C	30 sec	18 cycles
Annealing	55°C	1 min	
Extension	72°C	2 min/kb	
Final extension	72°C	5 min	

Construction of Gαi1-specific minigene

The PCR reaction components and conditions for the construction of the Gαi1 minigene are given in Table 2.7 and Table 2.8, respectively.

Table 2.7 PCR mixture for the construction of Gαi1-specific minigene

	Volume µL
wt Gαi1 in pcDNA3.1(-)	100 ng
Forward primer (Xhol)	0.25 µL from 20µM stock
Reverse primer (Hindlll)	0.25 µL 20µM stock
Phire Green MM	10 µL
nfw	Up to 20µL

Table 2.8 Optimal PCR conditions for construction of Gαi1-specific minigene

Pre-denaturation	98°C	30 sec	
Denaturation	98°C	10 sec	34 cycles
Annealing	55°C	30 sec	
Extension	72°C	10 sec	
Final extension	72°C	1 min	

After the PCR reactions to generate the desired constructs, Gαi1(121-122) EGFP/mCh and Gαi1 minigenes, all PCR products were loaded in agarose gel for size control and extraction. While for the visualization of Gαi1(121-122) EGFP/mCh constructs a 1% agarose gel with TAE buffer and 0.5 µg/mL Ethidium Bromide was prepared, a 2% agarose gel was prepared for Gαi1 minigenes because of the small size of these constructs. A 1 kb DNA ladder (Fisher, Product code:11803983) was loaded into one well to verify the sizes of the PCR products. The gels ran at 90-110 V for 35-40 min in the 1X TAE buffer. Then, the bands having the desired size were excised from the gel and extracted according to the protocol of QIAGEN Gel Extraction Kit (Cat# 28704). Important to mention is that to increase DNA yield, 30 µl preheated nuclease-free water was used, in the last elution step, instead of the 50 µl Elution Buffer provided by the kit.

2.1.3 Restriction digestion

After the PCR products were generated, the restriction digestion step was performed. By using appropriate restriction digestion enzymes, sticky ends of the amplified products and vector were obtained. The restriction digestion enzymes were purchased from New England Biolabs Inc. (NEB) (MA, USA). The reaction mixture contained at least 1000 ng DNA, 1 µl enzyme, 1.5 µl CutSmart® NEB buffer, and water to a final volume of 20 µl. Subsequently, the mixture was subjected to digestion for 4 hours at 37 ºC. After the restriction digestion process, the desired products were detected by running in 1% agarose gel for Gαi1 (121-122) EGFP/mCherry constructs and 2% agarose gel for Gαi1-

specific minigene at 100V for 30 minutes. The bands were visualized under UV and isolated by using the Qiagen Gel extraction kit.

2.1.4 Ligation and Ligation control PCR

During the ligation process, the generated sticky ends of the amplified products, Gαi1 (121-122) EGFP/mCherry constructs and Gαi1-specific minigene, and vector, pcDNA3.1(-) are compatible and therefore will bind to each other. In this study, the ligation vector:insert ratio 1:3, 1:5, 1:10, and 1:15 were performed. The ligation reaction mixture with a final volume of 20 µl contained at least 150 ng restricted vector pcDNA3.1(-), the amplified products, 1 µl T4 DNA ligase enzyme (NEB, Cat#0202T), 2 µl 1X T4 DNA ligase buffer, and nuclease-free water for completing to final volume. As a negative control, a ligation reaction without the amplified products was included to check for self-ligation of plasmids. The ligation reactions were incubated for 16 hours at room temperature.

2.1.5 Transformation of competent *E. coli* cells and Colony PCR

In this study, the Escherichia coli XL1 strain was utilized for bacterial transformation. Hereby, the successfully ligated products and negative control were transformed into competent *E. coli* cells. To start the procedure, the RbCl competent *E. coli* XL1 strain cells were taken from the -80°C freezer and kept for 15 minutes on ice. After that, 7 µl ligation products and 1 µl negative control were added to the cells and incubated for 30 minutes on ice. After the incubation, the cells were heat-shocked by placing the mixture first for 45 seconds on a heat block at a temperature of 42°C and then incubated it again for 3 minutes on ice. To help to recover the bacterial cells after heat-shock, the volume of the mixture was completed to 1 mL by adding SOC media. The mixture was incubated at 37°C for 1 hour on a shaker at 180 rpm and subsequently centrifuged for a few minutes at 4000 rpm. The supernatant, a volume of approximately 600 µl was discarded. The pellet of cells was resuspended in the remaining 400 µl SOC. For inoculation, the resuspended pellet of

cells was disseminated on with ampicillin prepared LB agar plate. For bacterial colony growth, the agar plates were incubated for overnight (14-16 hours) at 37°C.

2.1.6 Plasmid isolation

The Thermo Scientific's GeneJET plasmid miniprep kit (#K0503) was used for the isolation of plasmid. Single colonies from the agar plates were chosen and inoculated into mixture of 5 mL LB with 5 µL ampicillin. Subsequently, this mixture was first incubated at 37°C for overnight (16 hours) in the shaker at 180 rpm and then centrifuged at 4000 rpm for 5 minutes. The supernatant was removed. The isolation of plasmid from the pellet was carried out as described in the manufacturer's instructions. The quantity of the plasmid was increased by using nuclease-free water instead of distilled water.

2.2 Mammalian Cell Culture

2.2.1 Subculture and Cell maintenance of neuroblastoma cell line, Neuro-2a (N2a)

The neuro-2a (N2a) neuroblastoma cells were supplied from ATCC and cultured in a T25 flask containing Dulbecco's Midified Eagle Medium (DMEM, Gibco) supplemented with reduced serum medium (OptiMEM, Gibco), 10% Fetal Bovine Serum (FBS, Gibco), and 1% Penicilin/Streptomycin as antibiotic. The flasks with the cells were maintained in a humidified incubator at 37°C and 5% CO_2. The N2a cells generally needed approximately 70 hours for reaching confluency of 80%-90%, so the N2a cells were passaged twice a week. All the N2a cell culture procedures were performed in sterile conditions at the laminar flow hood. For passaging the N2a cells, first the cell medium was gently aspirated, and the N2a cells were washed with pre-warmed 1X PBS. After the washing step, the cells were dissociated from the flask area by adding 500 µL Trypl-E to the side wall of the flask and incubating for

5 minutes in the humidified incubator at 37°C and 5% CO_2. Meanwhile, a new T25 flasks was labeled with a new passage number and 8 mL new medium was added. The flask with N2A cells was taken out from the humidified incubator, and the trypsinization was stopped by adding 8 mL new medium. After mixing gently, 400 µL of this cell suspension was transferred to the new flask. The N2a cells were subcultured until the passage number had reached 45. To know the approximate number of N2a cells in 1 mL cell suspension, 10 µL of N2a cell suspension was transferred on a hemocytometer and counted in all 4x4 squares under the microscope (10X). After counting, the average over the four areas was calculated and multiplied by 10.000, as shown in the equation below:

$$\text{Number of cells/mL} = \frac{total\ number\ of\ counted\ N2a\ cells}{4} \times 10^4$$

For microscope imaging experiments, 35 mm glass bottom dishes seeded with 60.000 N2a cells were used. For plate reader experiments, first 35 mm plastic bottom dishes seeded with 120.000 N2a cells were used and after transfection procedure 10.000 N2a cells were transferred and seeded in each well into 96 well plate.

2.2.2 Transfection of N2a cells with construct plasmids

Transient transfection, namely introducing constructed plasmids into mammalian cells, was performed by using LipofectamineTM LTX and Plus™ Reagent according to the manufacturer's protocol. Both chemicals were purchased from Invitrogen (MA, USA). After the seeding N2a cells in glass bottom and plastic bottom dishes, they were incubated in humidified incubator for 24 hours. This step was needed for increasing the cell attachment. Subsequently, for microscope imaging 100-300 ng of plasmid DNA, while for plate reader experiments 100-500 ng of DNA was diluted and mixed with 100 µL OptiMEM, 4 µL Plus™ reagent was added, and the solution was incubated for 15 minutes at room temperature. Next, 4 µL Lipofectamine™ LTX was added into other 100 µL OptiMEM™ containing tubes. Afterwards, the Lipofectamine™ LTX - OptiMEM™ mixture was added into

the Plus reagent - plasmid DNA- OptiMEM^{TM} mixture. this final mixture was incubated for 30 minutes for Lipofectamine LTX-DNA complex formation. During the incubation, the N2s cells were gently washed with 1X PBS. After the washing step, 680 µL OptiMEM^{TM} was added to each dish, and lastly 200 µL of transfection mixture was added on the N2a cells. Then the dishes were put in the humidified incubator for 3 hours at 37° and 5% CO2. After the incubation, 2 mL media was added to the N2A cells and incubated for 24 more hours in humidified incubator at 37°C and 5% CO_2.

2.3 Imaging and Analysis

2.3.1 Imaging with Spinning Disc Confocal Microscope

For all live cell imaging experiments, the Leica DMI4000B automated inverted epifluorescence microscope equipped with confocal attachment (Andor AMH200 Metal Halide lamp, Zyla 5.5 sCMOS and DSD2 Differential spinning disc) was used. The Andor DSD2 confocal microscope has (1) maximum frame rate of 22 frames per second, (2) excitation range of 370 – 700 nm and, (3) emission range of 410-750. The spinning disc in this system allows the elimination of out-of-focus light leading to detailed images. All images were taken with 63X oil NA 1.4 objective.

The method used for the FRET microscopy experiments is called, the 3-cube method. For this method three 35mm glass bottom dishes were prepared: (1) N2a cells transfected with Gαi1 (121-122) EGFP, (2) N2a cells transfected with Gαi1 (121-122) mCherry and, (3) N2a cells co-transfected with Gαi1 (121-122) EGFP and with Gαi1 (121-122) mCherry. The first and second dishes were necessary to bleed-through corrections. These bleed-though contaminations from the donor and acceptor fluorophores are a results of the overlap of the donor and acceptor emission spectra (donor spectral bleed-through DSBT) and overlap of the excitation spectrum of donor and acceptor fluorophores (acceptor spectral bleed-through ASBT) respectively. This method, also, required the use of three different filter channels in

order to perform the experiments; (1) Donor channel, which directly excites and collects emission from EGFP, with excitation wavelengths of 470-500 nm and emission wavelengths of 500-550 nm, (2) Acceptor channel, which selectively excites and collect fluorescence from mCherry, with excitation wavelength of 560-600 nm and emission wavelengths of 600-650 nm and, (3) FRET channel with excitation wavelength of 470-500 nm to directly excite donor fluorophore, Gαi1 (121-122) EGFP, and emission wavelengths of 600-650 nm to collect fluorescence emission from acceptor fluorophore, Gαi1 (121-122) mCherry. Both the acceptor and donor fluorophores contribute to the bleed-through contaminations that can be detected in the FRET channel. The donor bleed-through was detected by imaging the dish containing N2a cells transfected with Gαi1 (121-122) EGFP in the FRET channel and Donor channel, while the contribution of acceptor bleed-though was detected by imaging N2a cells transfected with Gαi1 (121-122) mCherry in the FRET channel and Acceptor channel. For the FRET dish, which contains N2a cells co-transfected with Gαi1 (121-122) EGFP and with Gαi1 (121-122) mCherry, images were taken from the FRET channel, EGFP channel, and mCherry channel. All images were taken as stacks containing two images or three images, for bleed-through dishes and FRET dishes respectively.

2.3.2 Image and Data analysis with Pix-FRET program

FRET method has been extensively used to monitor protein interactions in live-cell experiments. However, the high spectral overlap between donor emission and acceptor excitation spectra, which is required in FRET, commonly results in a typical degree of background noise that interferes with FRET signals, and therefore, these spectral bleed-through contaminations (DSBT and ASBT) should be separated from the actual FRET signal. To overcome these artifacts, PixFRET algorithm was used. The bleed-through images, resulting from the only donor and only acceptor expressing dishes (two image stack), were analyzed, and normalized separately using the PixFRET plug-in of ImageJ program. Afterward, the FRET images (three image

stack) were analyzed accordingly resulting in determination of actual FRET efficiencies.

2.4 FRET assay using Monochromator plate reader

After the FRET imaging, Gαi1 protein homodimerization was also studied using the microplate reader, SpectraMax ID3. In comparison to the FRET imaging procedure, FRET assay using the microplate reader had several differences: (1) the collected signal was derived from approximately 10.000 cells while during the imaging only 50-100 cells were collected, (2) by using Fluorescence Spectrum tool, FRET emission spectrum was recorded by exciting the donor fluorophore with 450 nm and collecting spectral emission signal from a given range, 490-750 nm, including the donor and FRET emission spectra. For FRET experiments, three experimental sets were prepared: (1) N2a cells transfected with only Gαi1 (121-122) EGFP, (2) N2a cells transfected with only Gαi1 (121-122) mCherry and, (3) N2a cells co-transfected with Gαi1 (121-122) EGFP and with Gαi1 (121-122) mCherry. After transfection and respected incubation time, 10.000 cells were transferred into each well of SPL black 96-well plate. After normalization, the recorded FRET emission spectra would allow us to see a decrease in EGFP peak and an increase in mCherry peak if any energy transfer occurs.

CHAPTER 3

RESULTS AND DISCUSSION

3.1.1 Localization of EGFP and mCherry labeled Gαi1 proteins at A121-E122 position using membrane-targeted organelle marker

In this thesis, the effect of GPCRs on the Gαi1-Gαi1 dimerization was studied using the FRET method. The selected FRET pair consisted of EGFP and mCherry as the donor and acceptor fluorophore, respectively. It has been shown that these two fluorescent proteins have a good spectral overlap according to the donor emission and acceptor and relatively low crosstalk due to the large Stokes shift of EGFP (Albertazzi *et al.*, 2009).

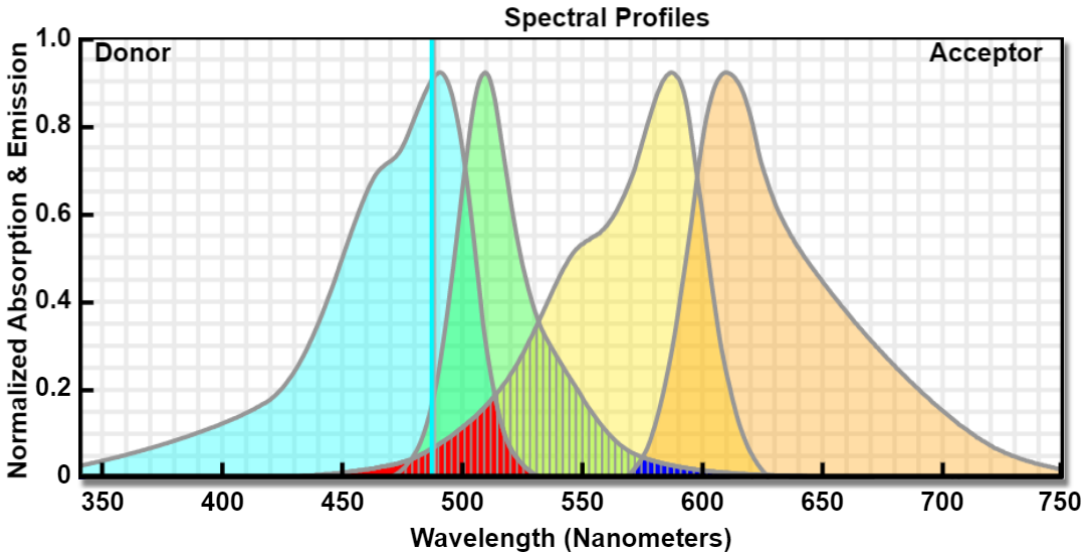

Figure 3.1 Spectral properties of the selected FRET pair, EGFP, and mCherry. (Taken from Deci *et al.*, 2016)

The EGFP and mCherry tagged Gαi1 containing plasmid constructs were transiently transfected separately into Neuro2a cells (N2a) which is a fast-growing mouse neuroblastoma cell line. Confocal images of the transfected N2a were taken using

Leica DMI 4000 equipped with Andor DSD2 spinning disk confocal microscope using 63X oil NA1.4 objective. A membrane-targeting signal sequence of the neuronal protein, Gap-43, labelled with EGFP or mCherry was used to confirm the membrane localization of the fluorescently tagged Gαi1 proteins.

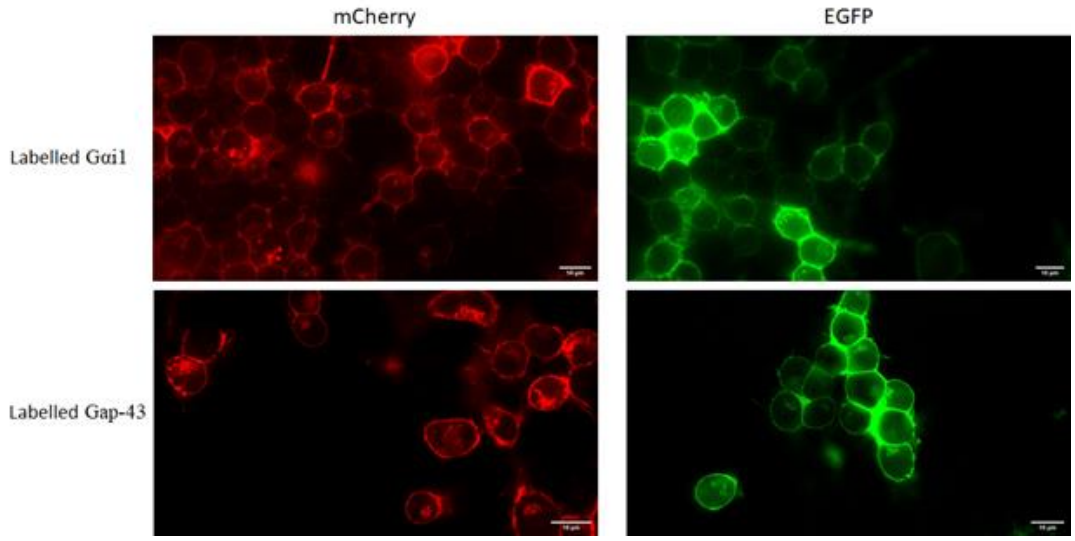

Figure 3.2 Confocal images of mCherry and EGFP labelled Gαi1 and Gap-43 proteins. mCherry images were taken from the mCherry channel (100% light intensity and 1000ms excitation time), EGFP images were taken using EGFP channel (50% light intensity and 1000ms excitation time).

Besides their primary role as a molecular switch on the cell membrane, heterotrimeric G proteins together with their regulators, are also suggested to localize and function in intracellular organelles of the cell (Cho & Kehrl, 2007). As expected, labeled Gαi1 proteins gave a fluorescent signal on the cell membrane as well as in the intracellular compartments of the cell (Figure 3.2).

3.2 Effect of blocking the GPCR-Gα protein interaction on the Gαi1 homodimerization by using Gαi1-specific minigenes

As mentioned in Chapter 1, several studies suggest that heterotrimeric G proteins get close in proximity when two receptor homodimers, each coupled to one G-protein, interact with each other forming a heterotetrametric structure (Navarro et al., 2016).

Besides that, Ras proteins, which are structurally like Gα subunit, are generally known for their ability to form dimers (Muratcioglu et al., 2020). In the light of these studies, this thesis aimed to investigate the effect of blocking the GPCR-G protein coupling on the Gαi1-Gαi1 interaction.

3.2.1 Preparation of Gαi1-specific minigene

As mentioned in Chapter 1, to block the GPCR-Gαi1 protein interaction, Gα-specific minigene was used. This minigene, which consists of the last 11 amino acids of the Gα protein, binds with a much higher affinity to the appropriate receptor and block the receptor binding of the Gα proteins. In this study, Gαi1 specific minigene was constructed to investigate receptor dependency of the Gαi1 homodimerization. This minigene was ligated between XhoI-HindIII restriction sites on the mammalian expression vector, pcDNA3.1(-).

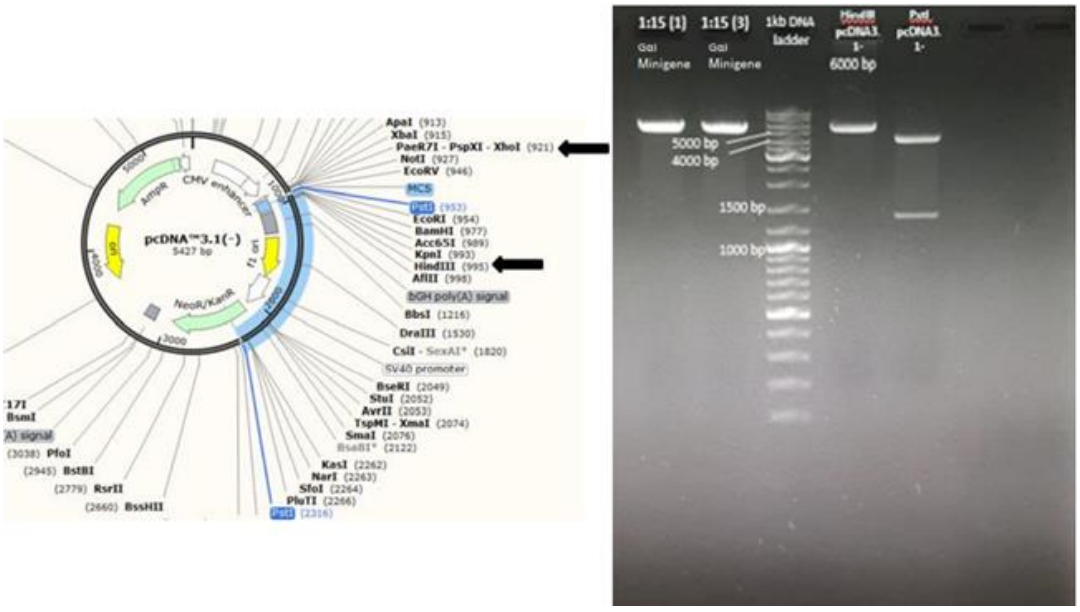

Figure 3.3 Strategy to insert small Gαi1 specific minigene into pcDNA3.1.

By selecting XhoI-HindIII cut sites for insertion, double cutter pstI became a unique cutter in pcDNA3.1(-) vector (Figure 3.3, left panel). After PstI digestion of Gαi1-specific minigene inserted plasmids and empty pcDNA3.1(-), Gαi1 specific

minigene inserted plasmids linearized whereas empty pcDNA3.1 showed a drop-out (figure 3.3, right panel). Following size and restriction control, during sequencing analysis, no mutation was detected.

3.2.2 Visualization of the Gαi1 homodimerization in the presence of Gαi1-specific minigene

To analyse the effect of the GPCRs on the homodimerization of the Gαi1 proteins, the experimental setup included two sets of FRET studies. In the first set, Gαi1(121) EGFP and Gαi1 (121) mCherry construct samples were co-transfected into N2a cells to determine the homodimerization. In the second set, Gαi1(121) EGFP, Gαi1 (121) mCherry construct samples were co-transfected together with Gαi1-specific minigene construct samples. An increase in FRET efficiency of the Gαi1-Gαi1 interaction in the presence of minigenes would suggest a GPCR-independent Gαi1 homodimerization.

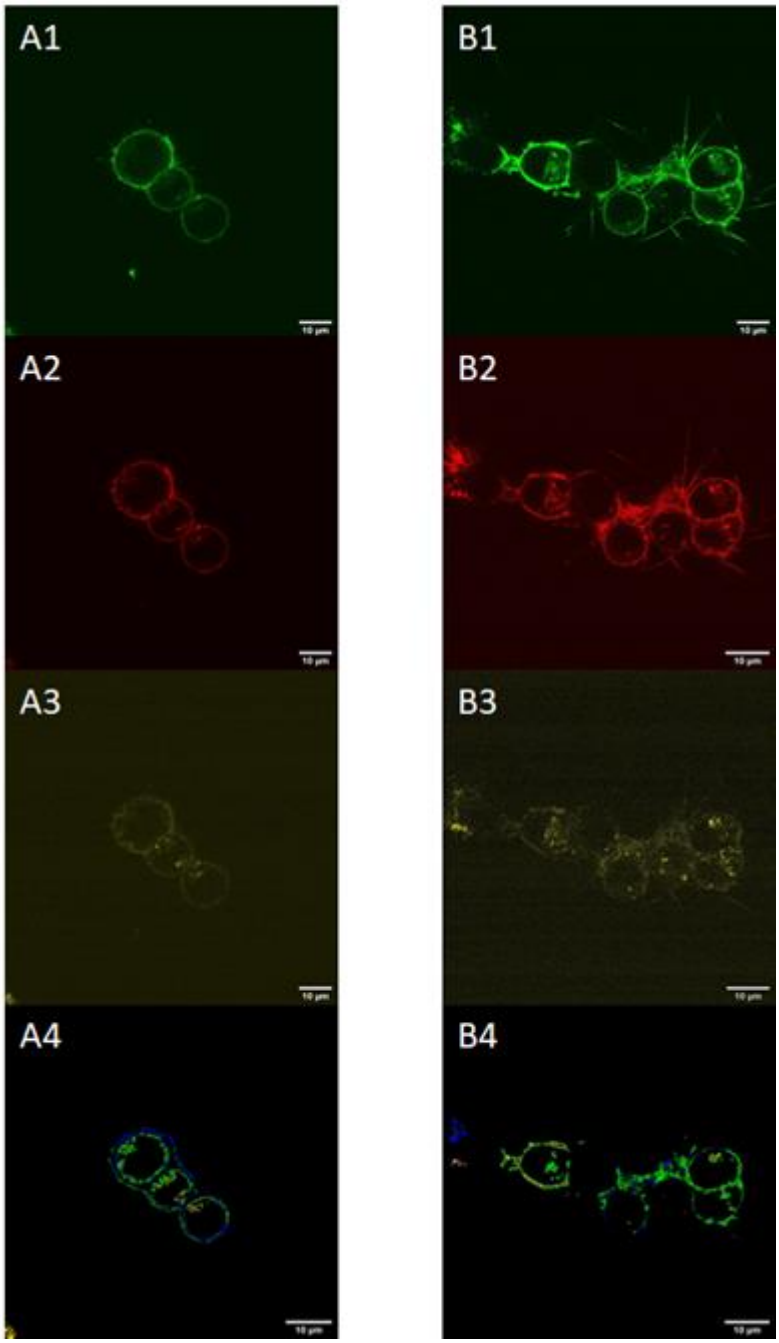

Figure 3.4 Confocal FRET imaging studies of Gαi1 homodimerization in the presence of Gαi1-specific minigene. A1-A4 - 500ng of Gαi1(121) EGFP and Gαi1(121) mCherry, B1-B4 - 500ng of Gαi1(121) EGFP, Gαi1(121) mCherry and Gαi1-specific minigene. **A1 and B1** were taken with EGFP channel with excitation at 488 nm, 490 nm – 575 nm emission region and 800V master gain; **A2 and B2** were taken with mCherry channel with excitation at 561nm, 620 nm – 670 nm emission region; **A3 and B3** were taken with FRET channel with excitation at 488 nm, 620 nm – 670 nm emission region. **A4 and B4** show the FRET efficiencies

(Color blue represents 0-10%, green 11-20%, yellow 21-30%, red 31-40%, and white 41-50% FRET Efficiency)

After the imaging process, pixFRET plugin of imageJ was used for FRET efficiency analysis. The calculated FRET efficiencies of labeled Gαi1 homodimerization without and with minigene are represented as line graphs in Figure 3.5 and show a distinct peak at 11% and 18%, respectively. However, the FRET signal between Gαi1 (121) EGFP and Gαi1 (121) mCherry in addition to Gαi1-specific minigene has less total pixel counts compared to solely Gαi1 homodimerization. This can be interpreted by the low transfection efficiency of 3 plasmids (Gαi1 EGFP, Gαi1 mCherry and Gαi1-specific minigene) into the same cell to observe homodimerization. Despite the less pixels, FRET efficiency shown in the graph suggests an GPCR-independent Gαi1 homodimerization since the Gαi1-specific minigene blocks the GPCR- Gαi1 coupling by binding to the receptor.

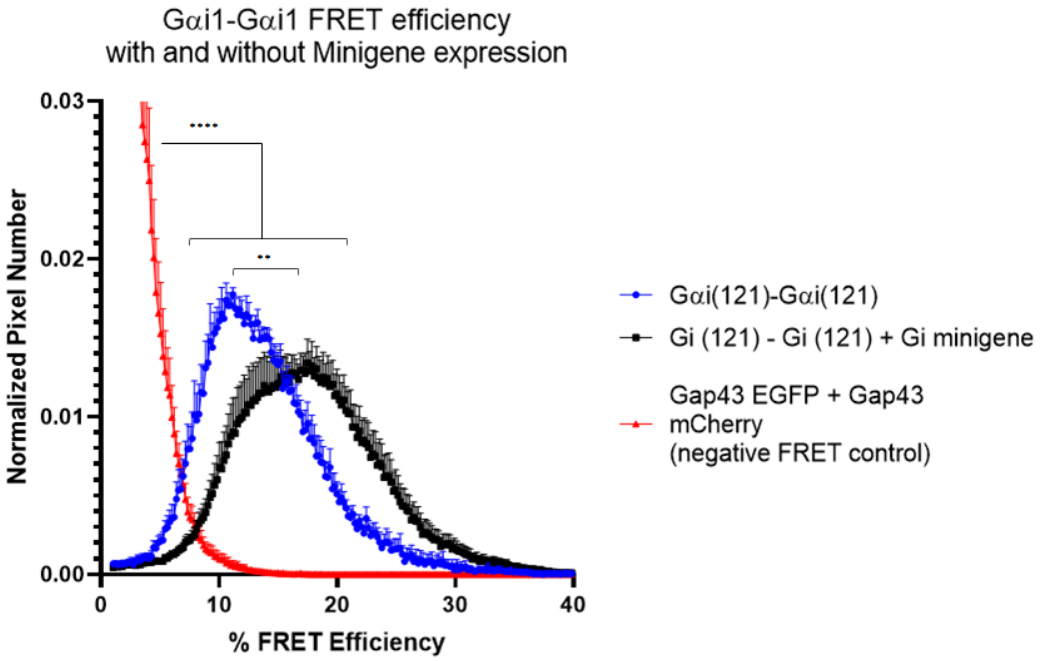

Figure 3.5 Graphical representation of the FRET efficiency of the Gαi1 homodimerization with and without minigene expression, represented in black and blue respectively, compared to negative FRET control represented in red (Gap43-EGFP and Gap43-mCherry). This graphic was created using Graphpad prism 8.0.2,

and statistical analysis was performed by One Way ANOVA. (Gαi1 (121-122) EGFP- Gαi1 (121-122) mCherry/(Gαi1 (121-122) EGFP- Gαi1 (121-122) mCherry + Gαi1-specific minigene vs negative FRET (Gap43-EGFP and Gap43-mCherry $p<0.0001$; Gαi1 (121-122) EGFP- Gαi1 (121-122) mCherry vs (Gαi1 (121-122) EGFP- Gαi1 (121-122) mCherry + Gαi1-specific minigene $p<0.01$).

3.2.3 FRET-based microplate reader assay to monitor GPCR-independent Gαi1 homodimerization

The effect of blocking the GPCR-G protein coupling site on the Gαi1-Gαi1 interaction was also quantitively studied using SpectraMax ID3 microplate reader. Again, two sets of FRET studies were set up: (1) solely Gαi1 homodimerization in which Gαi1(121) EGFP and Gαi1 (121) mCherry construct samples were co-transfected into N2a cells, (2) Gαi1 homodimerization in presence of Gαi1-specific minigenes overexpression in which Gαi1(121) EGFP, Gαi1 (121) mCherry and Gαi1-specific minigene construct samples were co-transfected. In addition, non-interacting membrane-targeted proteins, Gap43-EGFP and Gap43-mCherry, were co-transfected into N2a cells as negative control to previous FRET samples. 500 ng of Gαi1(121) EGFP and Gαi1 (121) mCherry construct and 100 ng of Gap43-EGFP and Gap43-mCherry were used for transfection into 100.000 cells.

The emission spectrum of the FRET constructs, Gαi1- Gαi1 in presence and absence of Gαi1-specific minigene was obtained by exciting the donor fluorophores, Gαi1-EGFP and/or Gap43-EGFP, with 450 nm wavelength and measuring emission spectrum ranging from 470 nm to 750 nm. The complete area under the raw FRET emission spectra was calculated and normalized (Figure 3.6-A). Since, in its simplest way FRET can be seen as the decrease in donor emission (donor quenching), the donor region (500-525 nm) was considered and compared to the negative FRET control, Gap43-EGFP and Gap43-mCherry (Figure 3.6-B). However, the increase in Acceptor sensitivity also a way to quantify FRET signal (Figure 3.6-C). In order to clearly investigate the FRET signal from the FRET emission spectra, the ratio of FRET region (acceptor peak emission) to donor peak region was calculated (Figure 3.7).

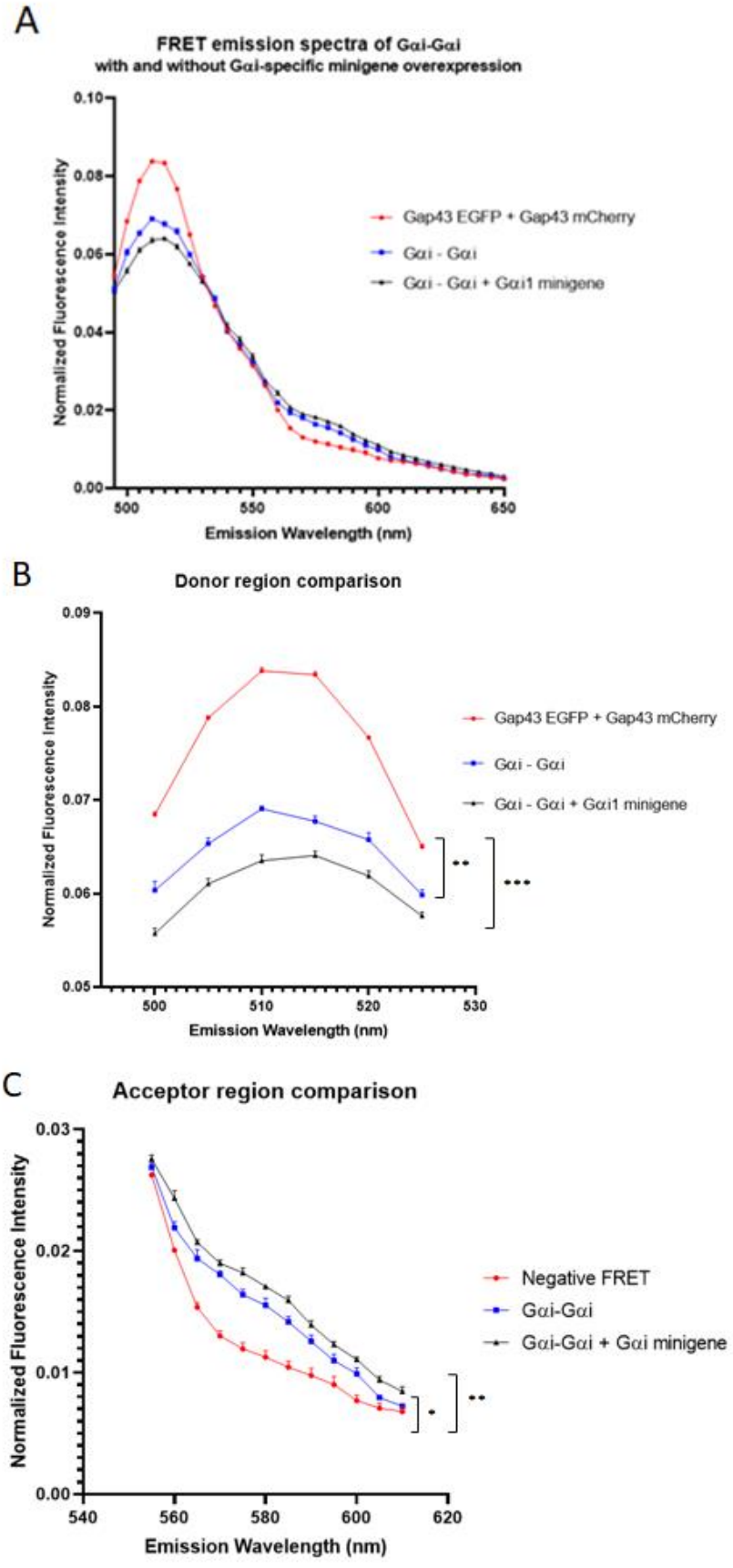
A
FRET emission spectra of Gαi-Gαi
with and without Gαi-specific minigene overexpression
Normalized Fluorescence Intensity
0.10
0.08
0.06
0.04
0.02
0.00
500
550
600
650
Emission Wavelength (nm)
Gap43 EGFP + Gap43 mCherry
Gαi - Gαi
Gαi - Gαi + Gαi1 minigene
B
Donor region comparison
Normalized Fluorescence Intensity
0.09
0.08
0.07
0.06
0.05
500
510
520
530
Emission Wavelength (nm)
Gap43 EGFP + Gap43 mCherry
Gαi - Gαi
Gαi - Gαi + Gαi1 minigene
**
***
C
Acceptor region comparison
Normalized Fluorescence Intensity
0.03
0.02
0.01
0.00
540
560
580
600
620
Emission Wavelength (nm)
Negative FRET
Gαi-Gαi
Gαi-Gαi + Gαi minigene
*
**

Figure 3.6 FRET emission spectra of FRET samples, Gαi1- Gαi1 with and without minigene overexpression. **A)** the overall spectral area, **B)** donor (EGFP) region comparison and **C)** Acceptor region of Gαi1- Gαi1 +/- Gαi1-specific minigene and negative FRET control were given by the emission wavelength in function of the normalized fluorescence intensity. These graphics were created using Graphpad prism 8.0.2 and statistical analysis was performed by One Way ANOVA (B – Gαi1 (121-122) EGFP- Gαi1 (121-122) mCherry vs negative FRET (Gap43-EGFP and Gap43-mCherry $p<0.0001$, Gαi1 (121-122) EGFP- Gαi1 (121-122) mCherry + Gαi1-specific minigene vs negative FRET $p< 0.0001$; C - Gαi1 (121-122) EGFP- Gαi1 (121-122) mCherry vs negative FRET $p<0.01$, Gαi1 (121-122) EGFP- Gαi1 (121-122) mCherry + Gαi1-specific minigene vs negative FRET $p<0.001$))

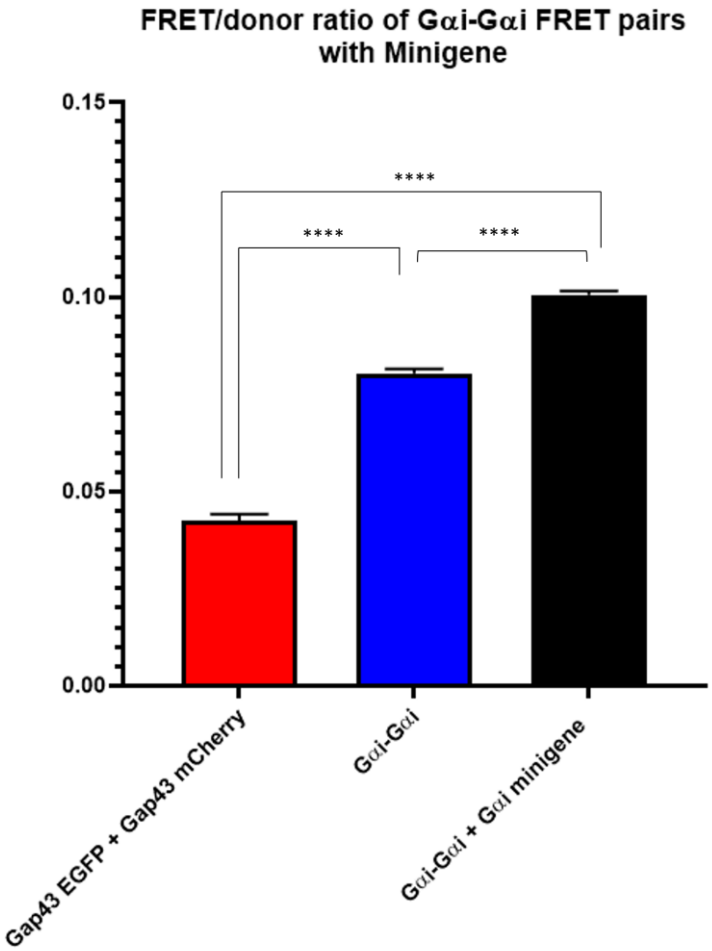

Figure 3.7 FRET/Donor ratio of normalized spectrum of Gαi-Gαi +/- Gαi-specific minigene oversxpression and negative FRET control group(Gap43 EGFP + Gap43 mCerry). These graphics were created using Graphpad prism 8.0.2 and statistical analysis was performed by One Way ANOVA (Gαi1 (121-122) EGFP- Gαi1 (121-

122) mCherry vs negative FRET (Gap43-EGFP and Gap43-mCherry) p<0.0001, Gαi1 (121-122) EGFP- Gαi1 (121-122) mCherry + Gαi1-specific minigene vs negative FRET p< 0.0001 and Gαi1 (121-122) EGFP - Gαi1 (121-122) mCherry vs Gαi1 (121-122) EGFP - Gαi1 (121-122) mCherry + Gαi1-specific minigene p<0.0001))

Determination of the amount of donor quenching in the presence and absence of acceptor is one of the most common methods to quantify transfer efficiency (Cardullo, 2007). In Figure 3.8-A, the donor emission of Gαi1-EGFP (in absence of acceptor) is shown compared to FRET pair Gαi1-Gαi1 with and without minigene overexpression, while in Figure 3.8-B, the amount of donor quenching due to FRET is calculated using the following equation:

$$1 - \frac{F\ d, a}{\mathrm{F\ d}}$$

Equation 1 Where $F_{d,a}$ is the fluorescence intensity in the presence of acceptor (the transfer condition), and F_d is the fluorescence intensity in the absence of acceptor.

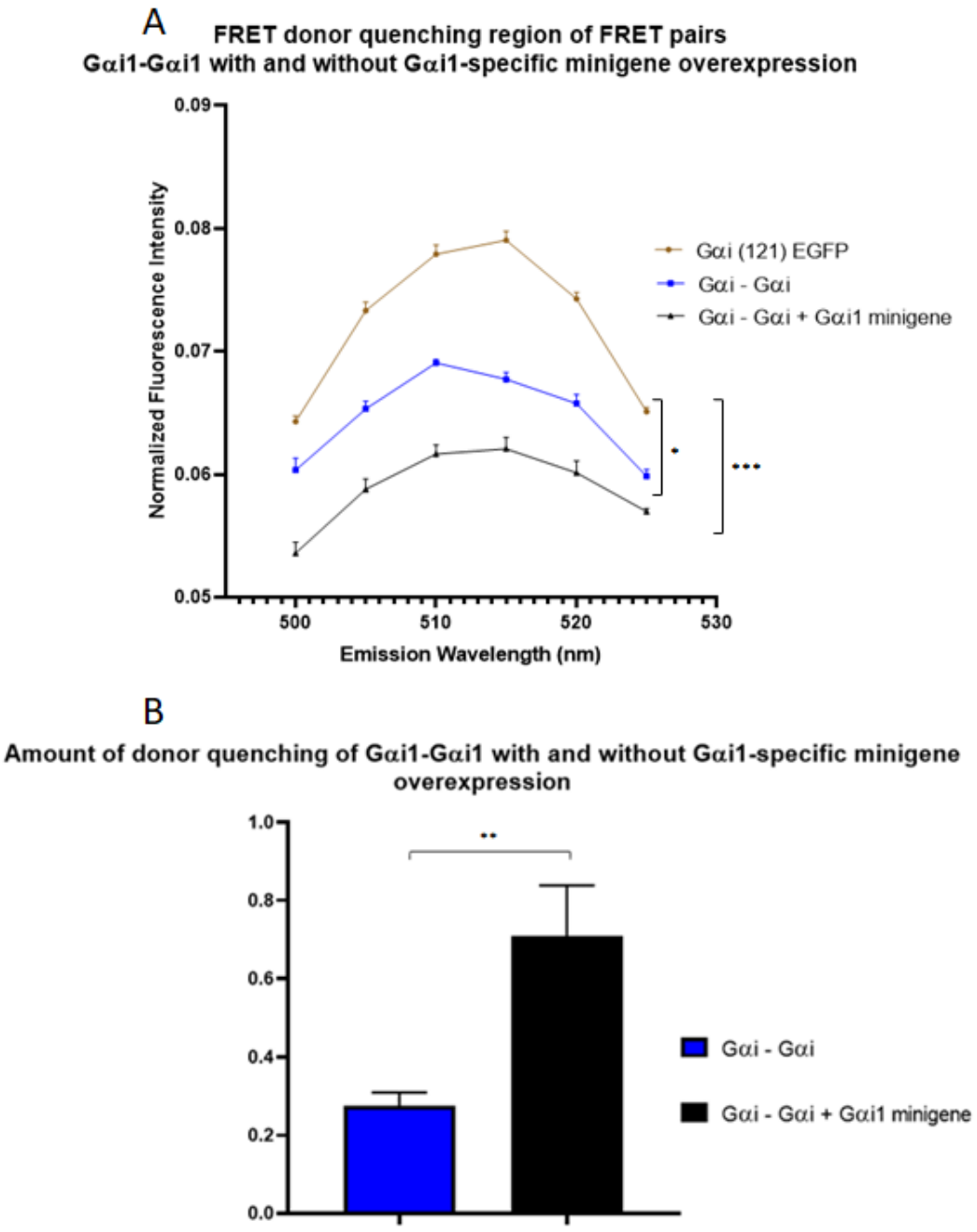

Figure 3.8 Donor quenching characterisation due to FRET. A – Comparison of the Donor quenching region of FRET pairs, Gαi1- Gαi1 +/- Gαi1-specific minigene, to the donor emission of the donor, Gαi1-EGFP, in absence of acceptor. B – the amount of donor emission quenching in Gαi1- Gαi1 versus Gαi1- Gαi1 + Gαi1-specific minigene overexpression. These graphics were created using Graphpad prism 8.0.2 and statistical analysis was performed by A) One Way ANOVA and B) unpaired t-test (A- Gαi1 (121-122) EGFP vs Gαi1 (121-122) EGFP- Gαi1 (121-122) mCherry $p<0.05$, Gαi1 (121-122) EGFP vs Gαi1 (121-122) EGFP- Gαi1

(121-122) mCherry + Gαi1-specific minigene p<0.001; B- Gαi1 (121-122) EGFP- Gαi1 (121-122) mCherry vs Gαi1 (121-122) EGFP- Gαi1 (121-122) mCherry; B) Gαi1 (121-122) EGFP- Gαi1 (121-122) mCherry vs Gαi1 (121-122) EGFP- Gαi1 (121-122) mCherry + Gαi1-specific minigene p<0.01)

3.3 Effect of GPCR signaling activation via ligand treatment on the Gαi1 homodimerization

After the determination of Gαi1 homodimerization when GPCR-Gαi1 protein interface was blocked, the effect of ligand activated GPCR signaling on the Gαi1-Gαi1 interaction was investigated as well. For this, solely Gαi1- Gαi1 interaction and Gαi1- Gαi1 interaction in addition to agonist ligand, quinpirole, were both quantitatively monitored using SpectraMax ID3. In the first FRET sample, 500 ng of Gαi1 (121) EGFP and Gαi1 (121) mCherry were co-transfected into 100.000 N2a cells, while in the second FRET sample, 500ng of Gαi1-specific minigene was also co-transfected together with Gαi1 (121) EGFP and Gαi1 (121) mCherry. For the ligand treatment, 20 µL 20 µM Quinpirole was added to the appropriate sample wells and incubated at 37 ºC and 5 % CO_2 for 20 minutes before measurement.

As depicted in section 3.2.3, the FRET emission spectra of both FRET samples were monitored upon donor excitation. The donor fluorophores, Gαi1-EGFP and/or Gap43-EGFP were excited with 450 nm wavelength, and FRET emission spectra from 470-650 nm were recorded. In Figure 3.9-A, the area normalized FRET emission spectra represented, while in figure 3.9-B the donor peak region of the FRET pairs were compared to the negative FRET control, in Figure 3.9-C the FRET region of the FRET pairs were compared to the negative FRET control and were found significantly different from the negative FRET control, consisting of Gap43-EGFP and Gap43-mCherry and . In Figure 3.10, the ratio of FRET region (acceptor peak emission) to donor peak region was calculated of the FRET pairs, Gαi1- Gαi1 and Gαi1- Gαi1 + Quinpirole, and compared to that of the negative FRET control.

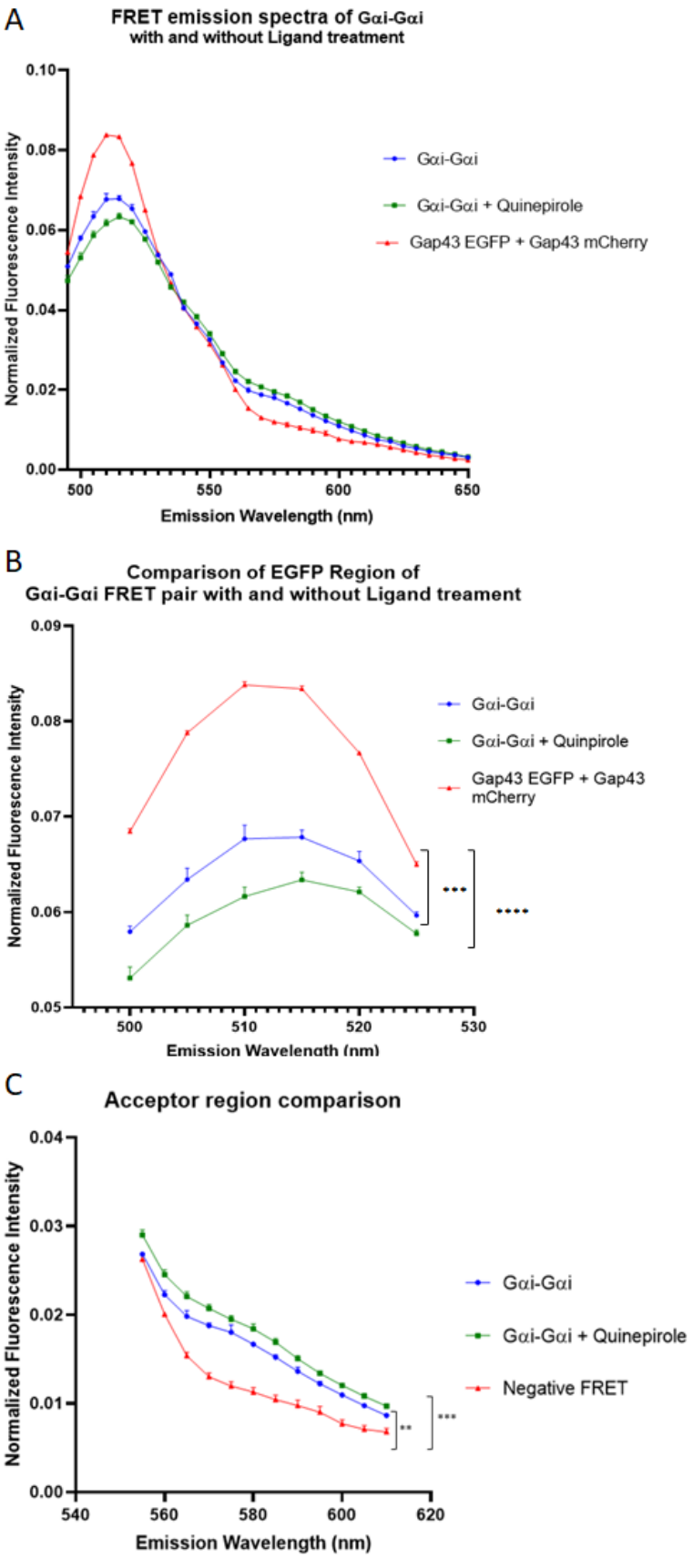
A
FRET emission spectra of Gαi-Gαi
with and without Ligand treatment
Normalized Fluorescence Intensity
Emission Wavelength (nm)
Gαi-Gαi
Gαi-Gαi + Quinepirole
Gap43 EGFP + Gap43 mCherry
B
Comparison of EGFP Region of
Gαi-Gαi FRET pair with and without Ligand treament
Normalized Fluorescence Intensity
Emission Wavelength (nm)
Gαi-Gαi
Gαi-Gαi + Quinpirole
Gap43 EGFP + Gap43 mCherry
***
****
C
Acceptor region comparison
Normalized Fluorescence Intensity
Emission Wavelength (nm)
Gαi-Gαi
Gαi-Gαi + Quinepirole
Negative FRET
**
***

Figure 3.9 characteristics of the FRET emission spectra of Gαi1- Gαi1 with and without Quinpirole treatment. A) the overall spectral area, B) donor (EGFP) region comparison and C) FRET region comparison of Gαi1- Gαi1 +/- ligand addition and negative FRET control were given by the emission wavelength in function of the normalized fluorescence intensity. These graphics were created using Graphpad prism 8.0.2 and statistical analysis was performed by One Way ANOVA (B – Gαi1 (121-122) EGFP- Gαi1 (121-122) mCherry vs negative FRET (Gap43-EGFP and Gap43-mCherry $p<0.001$, Gαi1 (121-122) EGFP- Gαi1 (121-122) mCherry + Quinpirole vs negative FRET $p< 0.0001$; C - Gαi1 (121-122) EGFP- Gαi1 (121-122) mCherry vs negative FRET $p<0.01$, Gαi1 (121-122) EGFP- Gαi1 (121-122) mCherry + Quinpirole vs negative FRET $p<0.001$))

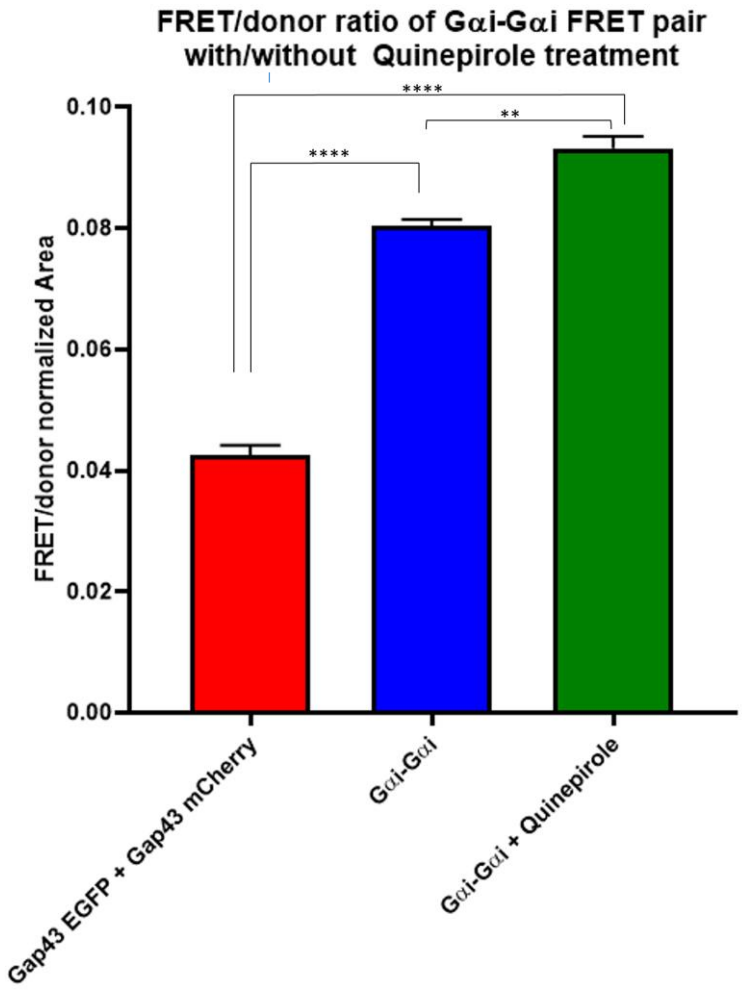

Figure 3.10 FRET/Donor ratio of normalized spectrum of Gαi-Gαi with/without Quinpirole treatment and negative FRET control group (Gap43 EGFP + Gap43 mCerry). These graphics were created using Graphpad prism 8.0.2 and statistical analysis was performed by One Way ANOVA (Gαi1 (121-122) EGFP- Gαi1 (121-

122) mCherry vs negative FRET (Gap43-EGFP and Gap43-mCherry) p<0.0001, Gαi1 (121-122) EGFP- Gαi1 (121-122) mCherry + Quinepirole addition vs negative FRET p< 0.0001 and Gαi1 (121-122) EGFP - Gαi1 (121-122) mCherry vs Gαi1 (121-122) EGFP - Gαi1 (121-122) mCherry + Quinpirole addition p<0.01))

The same equation, as mentioned in section 3.2.3, was used to calculate the amount of donor quenching by taking the ratio of donor intensity in presence ($F\ d, a$) and absence of acceptor ($\mathrm{F\ d}$) fluorophore. In this way, FRET group treated with agonist, quinpirole, was compared to the non-treated group. In Figure 3.11-A, the donor emission of Gαi1-EGFP (in the absence of acceptor) is shown compared to FRET pair Gαi1-Gαi1 with and without agonist-treatment, while in figure 3.11-B, the amount of donor quenching due to FRET is calculated using the previous equation (equation 1).

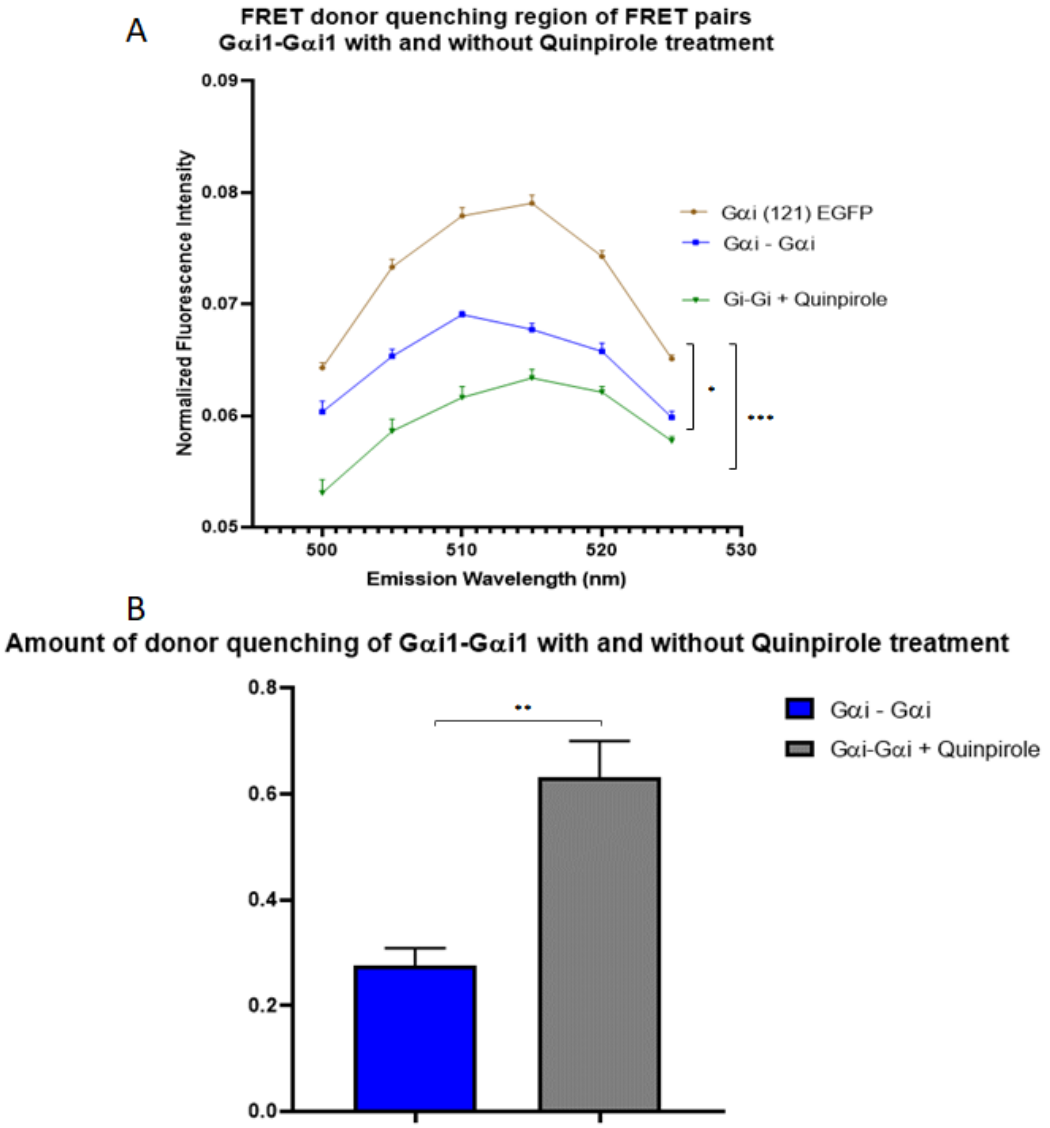

Figure 3.11 **Donor quenching characterisation due to FRET.** A – Comparison of the Donor quenching region of FRET pairs, Gαi1- Gαi1 +/- Quinpirole treatment, to the donor emission of the donor-only, Gαi1-EGFP, in absence of acceptor. B – the amount of donor emission quenching in Gαi1- Gαi1 versus Gαi1- Gαi1 + Quinpirole. These graphics were created using Graphpad prism 8.0.2 and statistical analysis was performed by A) One Way ANOVA and B) unpaired t-test (A – Gαi1 (121-122) EGFP vs Gαi1 (121-122) EGFP- Gαi1 (121-122) mCherry $p<0.05$, Gαi1 (121-122) EGFP vs Gαi1 (121-122) EGFP- Gαi1 (121-122) mCherry + Quinpirole $p<0.001$, Gαi1 (121-122) EGFP- Gαi1 (121-122) mCherry vs Gαi1 (121-122) EGFP- Gαi1 (121-122) mCherry + Quinpirole $p<0.05$; B) Gαi1 (121-122) EGFP- Gαi1 (121-122) mCherry vs Gαi1 (121-122) EGFP- Gαi1 (121-122) mCherry + Quinpirole $p<0.01$)

3.4 Discussion

In this study, by using FRET method, it has been shown that Gαi1 homodimerization occurs on the cell membrane when the receptor interaction was prevented with minigenes. Furthermore, the interaction of Gαi1 proteins under the minigene condition was found significantly higher than the interaction when the receptor interaction was not blocked. These results suggest that when the occurrence of GPCR-Gαi1 protein coupling during basal GPCR signaling (no ligand stimulation) inside the cells where GPCR-G-protein interactions were prevented using specific minigenes, Gαi1 proteins are more prone to interact with each other at the cell membrane. These results are in agrement with accumulating evidence from the Ras proteins, the structural homologs of Gα proteins which form membrane-bound dimers in order to activate downstream pathways, supporting the hypothesis of "***Receptor Independent Dimerization of G-proteins***" (Muratcioglu et al., 2015) (Rudack et al., 2021). Furthermore, the discovery of non-receptor Guanine Exchange Factors (GEFs) which activate Gα proteins by accelerating the GDP to GTP exchange, as well as the increasing evidence that nucleoside diphosphate kinases (NDPKs) can directly activate G proteins both suggest a similar GTP-dependent homodimerization as Ras proteins for the receptor-independent activated Gα proteins. In addition, several studies suggest that Gi proteins may have an intrinsic receptor-independent effect on adenyl cyclase (AC) besides their traditional role in GPCR signaling. While Rau *et al*. have shown this effect by overexpression of Gαi2 proteins (Rau et al., 2003), Melson *et al*. examined this by eliminating constitutively active receptors (Melsom et al., 2014).

Quinpirole acts as a selective agonist for several GPCRs such as Dopamine D2 receptor (D2R). Several D2R homodimerization studies suggest that in their resting state D2R form unstable homodimers and quinpirole addition prolonged the dimer formation by a factor of 1.5 (Kasai et al., 2013). Other ligand-binding studies claim that D2R form high-order oligomers, in which at least four dopamine receptors come to molecular proximity, has functional relevance (PG, 2005) (Guo et al., 2008).

By using the same protein-protein detection method, FRET, it has been shown that agonist addition significantly increased the FRET signal compared to non-agonist stimulated Gαi1- Gαi1 interaction. These results can be interpreted in multiple ways: (1) it can be possible that two Gαi1 proteins come to binding proximity due to the dimerization of two D2R dimers. In a recent study, Navarro *et al*. showed via BRET assays that adenosine A1-A2A heteroteramers are bound to Gi and Gs proteins respectively, and that these two G proteins are interacting within the rhombus-shaped heterotetramer (Navarro et al., 2018). However, another interpretation (2) could be in the inverse direction namely that non-receptor activated Gαi1 proteins form active homodimers at the cell membrane and that these homodimers bind and stabilize ligand bound receptor homo- or heteroreceptor complex formation.

The findings in this study should be interpreted very carefully because our study was not able the capture the whole picture. During analysis of our results, we felt the urge to further examine the two conditions of Gαi1 homodimerization; (1) blocking GPCR-Gαi1 interaction and (2) ligand-induced receptor oligomerization; in overexpression of dopamine D2 receptors together with Gαi1-specific minigenes, as well as investigate Gαi1 homodimerization in the absence of basal GPCR signaling by using selective antagonist (comparing it to Gαi1 homodimerization with minigenes) or in the presence of accessory proteins that receptor-independently activate the Gαi proteins. The results of these experiments should have given more decisive conclusions regarding the receptor dependency on the Gαi1 homodimerization.

CHAPTER 4

CONCLUSION AND FUTURE STUDIES

4.1 Conclusion

Previous to this thesis, our, former Lab. member and graduate Özge Atay had shown the Gαi1 homodimerization on the cell membrane (Atay, 2019). However, whether this interaction was due to GPCR oligomerization or independent of GPCRs has not been concluded. In this study, the impact of homo- or heteroreceptor formation on the Gαi1 homodimerization have been analysed under two conditions: (1) blocking GPCR-Gαi1 interaction and (2) ligand-induced receptor oligomerization (Figure 4.1). The major findings of this work were presented in Chapter 3 and discussed in section 3.4.

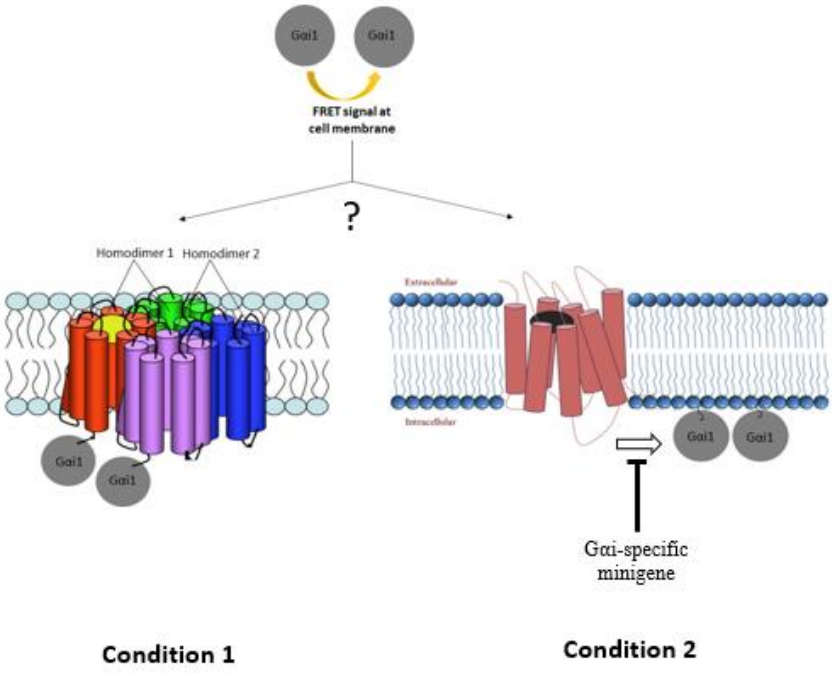

Figure 4.1 Representatin of the two conditions to investigate of the effect GPCR oligomerization on Gαi1 homodimerization.

In section 3.2, the Gαi1 homodimerization, at which the GPCR-Gαi1 protein interaction was blocked using Gαi1-specific minigenes, have been studied and found that in the presence of minigene expression, the Gαi1 homodimerization gave a stronger FRET signal compared to Gαi1- Gαi1 interaction when the receptor-Gαi1 binding interface was not blocked with Gαi1-specific minigenes.

The effect of ligand-induced receptor oligomerization on the Gαi1 homodimerization was investigated in section 3.3. The results of these experiments showed that upon ligand addition, the homodimerization of Gαi1 proteins was significantly increased in comparison to the non-ligand treated Gαi1 homodimerization.

Heterotrimeric G proteins are key mediators of cellular signal transduction in eukaryotic cells, and evidence shows that abnormal G-protein signaling plays an important role in numerous diseases. Therefore, we strongly believe that new perspective, presented in this thesis, concerning the dimerization characteristic of Gαi1 proteins will open a completely new research area. Up to now, Gαi-overexpression studies focussed on their effect on the cAMP pathway and its role in heart failure (Rau *et al*., 2003). However, in this study, the dimerization ability of Gαi1 proteins under several occasions has been studied and shown. We strongly believe that Gαi1 homodimers are involved in yet unraveled pathways.

4.2 Future studies

Besides the fact that Gα protein signaling have multiple starting points other than the active GPCRs, our study strongly suggests the homo- or heterodimerization of Gα proteins. In this work, we experimentally showed the homodimerization of Gαi1 proteins using FRET method. As mentioned in Chapter 1, the structure of Gα subunits consist of 2 domains: (1) the highly conserved Ras-like G-domain, and (2) the variable α-helical domain. In Figure 4.3, the structural similarity of GTP-bound K-Ras (represented in green) and GTP-bound Gαi1 protein (represented in pink) is shown by using UCSF Chimera, which is a program to visualize and analyze molecular structures.

Figure 4.2 **Structural alignment of K-Ras and Gαi1 protein structures.** UCSF Chimera program was used to visualize the structural similarity of the G-domains of both proteins. (K-Ras PDB ID: 3GFT, GNAI1 PDB ID: 1GFI).

Muratcioglu *et al*. showed in a recent study that Ras proteins possess a GTP-dependent dimerization. Furthermore, they showed that GTP-bound K-Ras4B has two dimer interfaces. While the β-sheet interface coincides with effector binding regions such as Raf, PI3K, and RalGDS, the α-helix interface interferes with the allosteric region at the C-terminus of the G-domain. However, the α-helix interface was thought to be of physiological importance.

Our preliminary bioinformatic studies regarding the Gαi1- Gαi1 dimerization were based on the α-interface of the K-Ras dimerization simulation shared by Prof. Özlem Keskin and shown in Figure 4.4. By using the Surface/Binding Analysis tool, two inter-model hydrogen bounds were found between D251-C254 on the α3-helix (Figure 4.5). The α3-helix is also involved in the Ras dimerization as well. In our future studies, we plan to investigate this predicted promising Gαi1-Gαi1

homodimerization interface. Substitution of the H-bond forming residues to Alanine on one of the Gαi1 sequences via site-directed mutagenesis or blocking the complete α3-helix interface by specific interfering sequences would allow us to confirm the predicted promising interface.

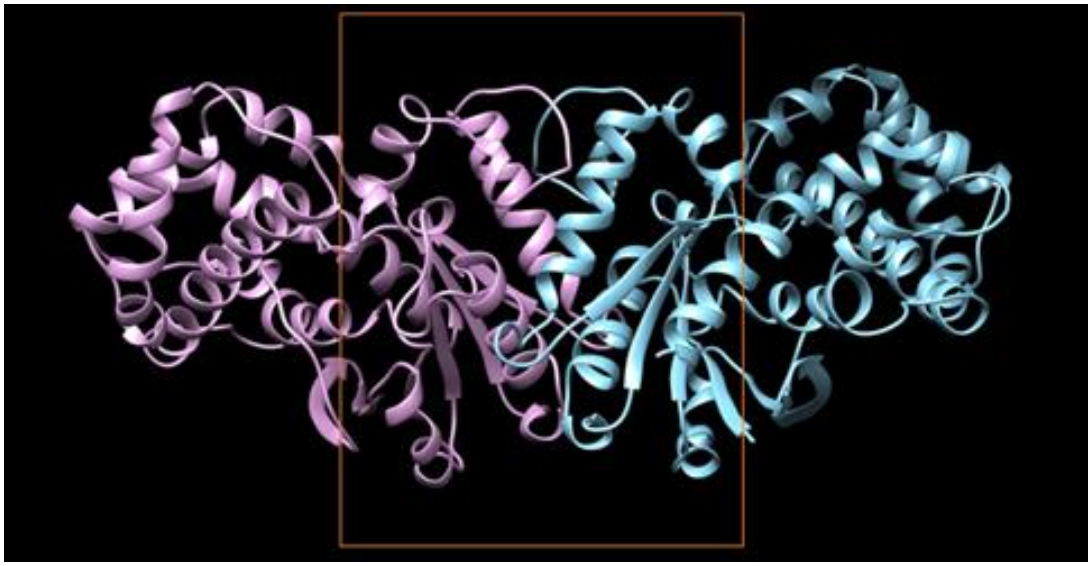

Figure 4.3 **Predicted homodimer structure of Gαi1 proteins. (**Pink GNAI1 PDB ID: 1GFI, Blue GNAI1 PDB ID: 1GIL).

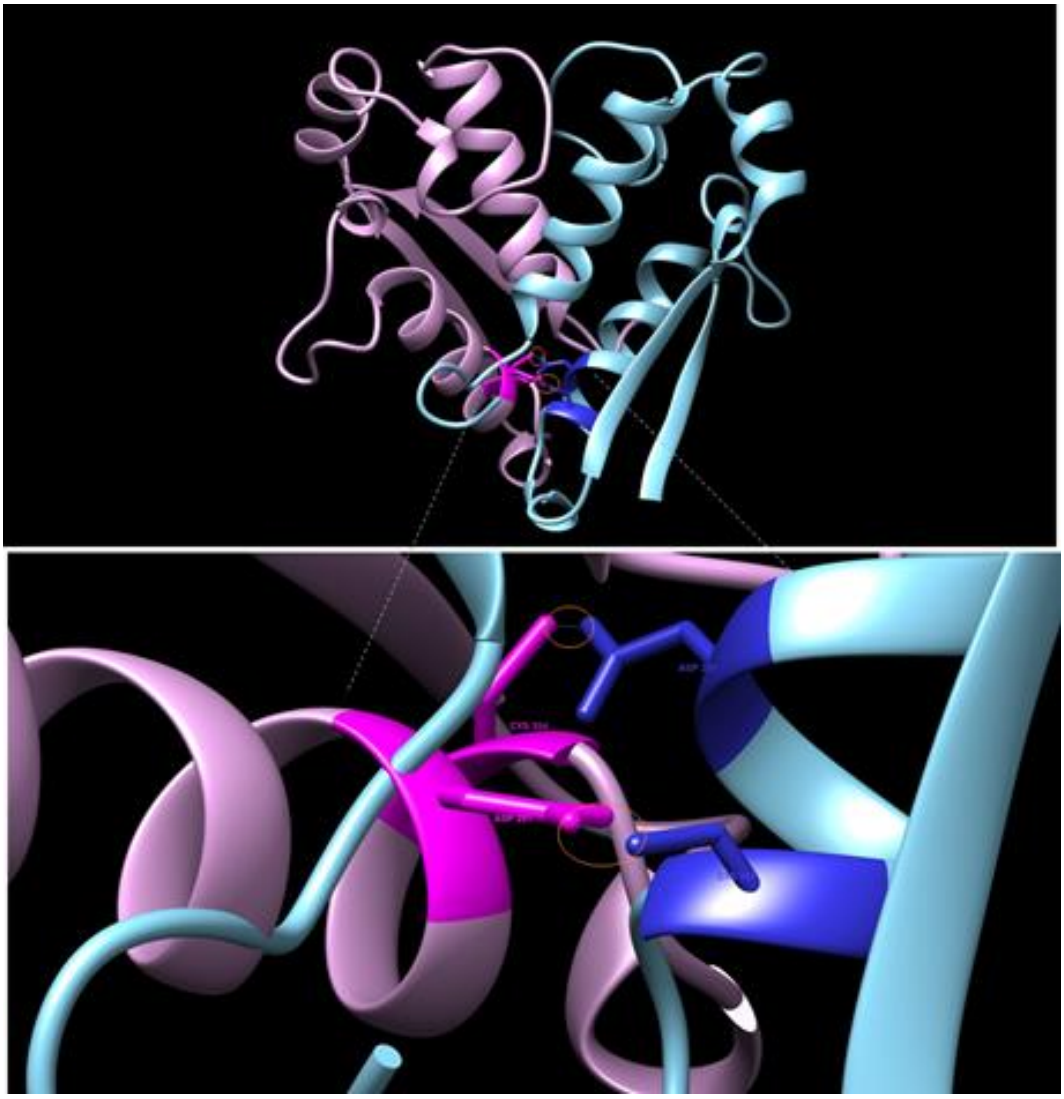

Figure 4.4 **Residues at the interface forming H-bonds are D251 (on pink structure) – C254 (on blue structure) and vice versa.**

REFERENCES

Ali Khan Pathan, A., Panthi, B., Khan, Z., Reddy Koppula, P., saud alanazi, M., Reddy Parine, N., & chourasia, M. (2016). *OncoTargets and Therapy Dovepress Lead identification for the K-Ras protein: virtual screening and combinatorial fragment-based approaches*. https://doi.org/10.2147/OTT.S99671

Baspinar, A., Cukuroglu, E., Nussinov, R., Keskin, O., & Gursoy, A. (2014). PRISM: a web server and repository for prediction of protein-protein interactions and modeling their 3D complexes. *Nucleic Acids Research*, *42*, 285–289. https://doi.org/10.1093/nar/gku397

Blumer, J. B., Cismowski, M. J., Sato, M., & Lanier, S. M. (2005). AGS proteins: Receptor-independent activators of G-protein signaling. *Trends in Pharmacological Sciences*, *26*(9), 470–476. https://doi.org/10.1016/j.tips.2005.07.003

Blumer, J. B., Smrcka, A. v., & Lanier, S. M. (2007). Mechanistic pathways and biological roles for receptor-independent activators of G-protein signaling. *Pharmacology & Therapeutics*, *113*(3), 488–506. https://doi.org/10.1016/J.PHARMTHERA.2006.11.001

Bos, J. L., Rehmann, H., & Wittinghofer, A. (2007). GEFs and GAPs: Critical Elements in the Control of Small G Proteins. *Cell*, *129*(5), 865–877. https://doi.org/10.1016/J.CELL.2007.05.018

Broussard, J. A., & Green, K. J. (2017). Research Techniques Made Simple: Methodology and Applications of Förster Resonance Energy Transfer (FRET) Microscopy. *Journal of Investigative Dermatology*, *137*(11), e185–e191. https://doi.org/10.1016/J.JID.2017.09.006

C, D.-J., & SGB, F. (2019). Conformational Transitions and the Activation of Heterotrimeric G Proteins by G Protein-Coupled Receptors. *ACS Pharmacology & Translational Science*, *2*(4), 285–290. https://doi.org/10.1021/ACSPTSCI.9B00054

Cabrera-Vera, T. M., Vanhauwe, J., Thomas, T. O., Medkova, M., Preininger, A., Mazzoni, M. R., & Hamm, H. E. (2003). Insights into G Protein Structure, Function, and Regulation. *Endocrine Reviews*, *24*(6), 765–781. https://doi.org/10.1210/er.2000-0026

Cardullo, R. A. (2007). Theoretical Principles and Practical Considerations for Fluorescence Resonance Energy Transfer Microscopy. *Methods in Cell Biology*, *81*, 479–494. https://doi.org/10.1016/S0091-679X(06)81023-X

Chappie, J. S., Acharya, S., Leonard, M., Schmid, S. L., & Dyda, F. (2010). G domain dimerization controls dynamin's assembly-stimulated GTPase activity. *Nature 2010 465:7297*, *465*(7297), 435–440. https://doi.org/10.1038/nature09032

Chen, C. A., & Manning, D. R. (2001). Regulation of G proteins by covalent modification. *Oncogene 2001 20:13*, *20*(13), 1643–1652. https://doi.org/10.1038/sj.onc.1204185

Chen, M., Peters, A., Huang, T., & Nan, X. (2016). Ras Dimer Formation as a New Signaling Mechanism and Potential Cancer Therapeutic Target. *Mini Reviews in Medicinal Chemistry*, *16*(5), 391. https://doi.org/10.2174/1389557515666151001152212

Ciruela, F. (2008). Fluorescence-based methods in the study of protein-protein interactions in living cells. In *Current Opinion in Biotechnology* (Vol. 19, Issue 4, pp. 338–343). https://doi.org/10.1016/j.copbio.2008.06.003

Cismowski, M. J. (2006). Non-receptor activators of heterotrimeric G-protein signaling (AGS proteins). *Seminars in Cell and Developmental Biology*, *17*(3), 334–344. https://doi.org/10.1016/j.semcdb.2006.03.003

Colicelli, J. (2004). Human RAS superfamily proteins and related GTPases. *Science's STKE : Signal Transduction Knowledge Environment*, *2004*(250). https://doi.org/10.1126/stke.2502004re13

CR, M., FS, W., RJ, K., CA, J., MD, H., MB, J., & DP, S. (2005). G alpha selectivity and inhibitor function of the multiple GoLoco motif protein GPSM2/LGN. *Biochimica et Biophysica Acta*, *1745*(2), 254–264. https://doi.org/10.1016/J.BBAMCR.2005.05.002

Day, R. N., & Davidson, M. W. (2012). Fluorescent proteins for FRET microscopy: Monitoring protein interactions in living cells. *BioEssays*, *34*(5), 341–350. https://doi.org/10.1002/bies.201100098

Derouiche, L., & Massotte, D. (2019). G protein-coupled receptor heteromers are key players in substance use disorder. *Neuroscience and Biobehavioral Reviews*, *106*, 73–90. https://doi.org/10.1016/J.NEUBIOREV.2018.09.026

Dessauer, C. W., Chen-Goodspeed, M., & Chen, J. (2002). Mechanism of Galpha i-mediated inhibition of type V adenylyl cyclase. *The Journal of Biological Chemistry*, *277*(32), 28823–28829. https://doi.org/10.1074/jbc.M203962200

Downes, G. B., & Gautam, N. (1999). The G protein subunit gene families. *Genomics*, *62*(3), 544–552. https://doi.org/10.1006/geno.1999.5992

Ferré, S., Bonaventura, J., Tomasi, D., Navarro, G., Moreno, E., Cortés, A., Lluís, C., Casadó, V., & Volkow, N. D. (2016). Allosteric mechanisms within the adenosine A2A-dopamine D2 receptor heterotetramer. In *Neuropharmacology* (Vol. 104, pp. 154–160). Elsevier Ltd. https://doi.org/10.1016/j.neuropharm.2015.05.028

Gilchrist, A., Li, A., & Hamm, H. E. (2002). G alpha COOH-terminal minigene vectors dissect heterotrimeric G protein signaling. *Science's STKE : Signal Transduction Knowledge Environment*, *2002*(118), 1–19. https://doi.org/10.1126/scisignal.1182002pl1

Guo, W., Urizar, E., Kralikova, M., Mobarec, J. C., Shi, L., Filizola, M., & Javitch, J. A. (2008). Dopamine D2 receptors form higher order oligomers at physiological expression levels. *The EMBO Journal*, *27*(17), 2293. https://doi.org/10.1038/EMBOJ.2008.153

Hauser, A. S., Attwood, M. M., Rask-Andersen, M., Schiöth, H. B., & Gloriam, D. E. (2017). Trends in GPCR drug discovery: New agents, targets and indications. *Nature Reviews Drug Discovery*, *16*(12), 829–842. https://doi.org/10.1038/nrd.2017.178

Inouye, K., Mizutani, S., Koide, H., & Kaziro, Y. (2000). Formation of the Ras dimer is essential for Raf-1 activation. *Journal of Biological Chemistry*, *275*(6), 3737–3740. https://doi.org/10.1074/jbc.275.6.3737

JB, B., & SM, L. (2014). Activators of G protein signaling exhibit broad functionality and define a distinct core signaling triad. *Molecular Pharmacology*, *85*(3), 388–396. https://doi.org/10.1124/MOL.113.090068

Johnston, C. A., & Siderovski, D. P. (2007). Structural basis for nucleotide exchange on Gαi subunits and receptor coupling specificity. *Proceedings of the National Academy of Sciences*, *104*(6), 2001–2006. https://doi.org/10.1073/PNAS.0608599104

Kamato, D., Thach, L., Bernard, R., Chan, V., Zheng, W., Kaur, H., Brimble, M., Osman, N., Little, P. J., & Xu, S. (2015). *Structure, function, pharmacology, and therapeutic potential of the G protein, Gα /q,11*. 24. https://doi.org/10.3389/fcvm.2015.00014

Kasai, R. S., Shuichi, •, Ito, V., Awane, R. M., Fujiwara, T. K., & Kusumi, • Akihiro. (2013). The Class-A GPCR Dopamine D2 Receptor Forms Transient Dimers Stabilized by Agonists: Detection by Single-Molecule Tracking. *Cell Biochemistry and Biophysics*, *76*, 29–37. https://doi.org/10.1007/s12013-017-0829-y

Lagerström, M. C., & Schiöth, H. B. (2008). Structural diversity of G protein-coupled receptors and significance for drug discovery. *Nature Reviews Drug Discovery 2008 7:4*, *7*(4), 339–357. https://doi.org/10.1038/nrd2518

Lambright, D. G., Noel, J. P., Hamm, H. E., & Sigler, P. B. (1994). Structural determinants for activation of the α-subunit of a heterotrimeric G protein. *Nature*, *369*(6482), 621–628. https://doi.org/10.1038/369621a0

Lania, A., Mantovani, G., & Spada, A. (2012). CAMP pathway and pituitary tumorigenesis. *Annales d'Endocrinologie*, *73*(2), 73–75. https://doi.org/10.1016/J.ANDO.2012.03.027

Latorraca, N. R., Venkatakrishnan, ‖ A J, & Dror, R. O. (2016). *GPCR Dynamics: Structures in Motion*. https://doi.org/10.1021/acs.chemrev.6b00177

Leurs, R., Bakker, R. A., Timmerman, H., & de Esch, I. J. P. (2005). The histamine H3 receptor: from gene cloning to H3 receptor drugs. *Nature Reviews Drug Discovery 2005 4:2*, *4*(2), 107–120. https://doi.org/10.1038/nrd1631

Llères, D., Swift, S., & Lamond, A. I. (2007). Detecting protein-protein interactions in vivo with FRET using multiphoton fluorescence lifetime imaging microscopy (FLIM). *Current Protocols in Cytometry / Editorial Board, J. Paul Robinson, Managing Editor ... [et Al.]*, *Chapter 12*. https://doi.org/10.1002/0471142956.cy1210s42

Lyons, J., Landis, C. A., Harsh, G., Vallar, L., Grünewald, K., Feichtinger, H., Duh, Q.-Y., Clark, O. H., Kawasaki, E., Bourne, H. R., & McCormick, F. (1990). Two G Protein Oncogenes in Human Endocrine Tumors. *Science*, *249*(4969), 655–658. https://doi.org/10.1126/SCIENCE.2116665

Melsom, C. B., Ørstavik, Ø., Osnes, J. B., Skomedal, T., Levy, F. O., & Krobert, K. A. (2014). Gi proteins regulate adenylyl cyclase activity independent of receptor activation. *PLoS ONE*, *9*(9). https://doi.org/10.1371/journal.pone.0106608

Muratcioglu, S., Aydin, C., Odabasi, E., Ozdemir, E. S., Firat-Karalar, E. N., Jang, H., Tsai, C. J., Nussinov, R., Kavakli, I. H., Gursoy, A., & Keskin, O. (2020). Oncogenic K-Ras4B Dimerization Enhances Downstream Mitogen-activated Protein Kinase Signaling. *Journal of Molecular Biology*, *432*(4), 1199–1215. https://doi.org/10.1016/J.JMB.2020.01.002

Muratcioglu, S., Chavan, T. S., Freed, B. C., Tarasova, N. I., Gaponenko, V., & Nussinov Correspondence, R. (2015). GTP-Dependent K-Ras Dimerization. *Structure*, *23*, 1325–1335. https://doi.org/10.1016/j.str.2015.04.019

Nan, X., Tamgüney, T. M., Collisson, E. A., Lin, L. J., Pitt, C., Galeas, J., Lewis, S., Gray, J. W., McCormick, F., & Chu, S. (2015). Ras-GTP dimers activate the Mitogen-Activated Protein Kinase (MAPK) pathway. *Proceedings of the National Academy of Sciences of the United States of America*, *112*(26), 7996–8001. https://doi.org/10.1073/pnas.1509123112

Navarro, G., Cordomí, A., Brugarolas, M., Moreno, E., Aguinaga, D., Pérez-Benito, L., Ferre, S., Cortés, A., Casadó, V., Mallol, J., Canela, E. I., Lluís, C., Pardo, L., McCormick, P. J., & Franco, R. (2018). Cross-communication between Gi and Gs in a G-protein-coupled receptor heterotetramer guided by a receptor C-terminal domain. *BMC Biology*, *16*(1). https://doi.org/10.1186/S12915-018-0491-X

Navarro, G., Cordomí, A., Zelman-Femiak, M., Brugarolas, M., Moreno, E., Aguinaga, D., Perez-Benito, L., Cortés, A., Casadó, V., Mallol, J., Canela, E. I., Lluís, C., Pardo, L., García-Sáez, A. J., McCormick, P. J., & Franco, R. (2016). *Quaternary structure of a G-protein-coupled receptor heterotetramer in complex with G i and G s*. https://doi.org/10.1186/s12915-016-0247-4

Ng, S. Y. L., Lee, L. T. O., & Chow, B. K. C. (2013). Receptor oligomerization: From early evidence to current understanding in class B GPCRs. In *Frontiers in Endocrinology* (Vol. 3, Issue JAN, p. 175). Frontiers. https://doi.org/10.3389/fendo.2012.00175

Nooren, I. M. A., & Thornton, J. M. (2003). Diversity of protein-protein interactions. In *EMBO Journal* (Vol. 22, Issue 14, pp. 3486–3492). EMBO J. https://doi.org/10.1093/emboj/cdg359

O'Bryan, J. P. (2019). Pharmacological targeting of RAS: Recent success with direct inhibitors. In *Pharmacological Research* (Vol. 139, pp. 503–511). Academic Press. https://doi.org/10.1016/j.phrs.2018.10.021

Okamoto, K., & Sako, Y. (2017). Recent advances in FRET for the study of protein interactions and dynamics. In *Current Opinion in Structural Biology* (Vol. 46, pp. 16–23). Elsevier Ltd. https://doi.org/10.1016/j.sbi.2017.03.010

Oldham, W. M., & Hamm, H. E. (2008). Heterotrimeric G protein activation by G-protein-coupled receptors. *Nature Reviews Molecular Cell Biology*, *9*(1), 60–71. https://doi.org/10.1038/nrm2299

Padilla-Parra, S., & Tramier, M. (2012). FRET microscopy in the living cell: Different approaches, strengths and weaknesses. *BioEssays*, *34*(5), 369–376. https://doi.org/10.1002/bies.201100086

Paduch, M., Jeleń, F., & Otlewski, J. (2001). Structure of small G proteins and their regulators. *Acta Biochimica Polonica*, *48*(4), 829–850. https://doi.org/10.18388/abp.2001_3850

PG, S. (2005). Oligomers of D2 dopamine receptors: evidence from ligand binding. *Journal of Molecular Neuroscience : MN*, *26*(2–3), 155–160. https://doi.org/10.1385/JMN:26:2-3:155

Qu, L., Pan, C., He, S. M., Lang, B., Gao, G. D., Wang, X. L., & Wang, Y. (2019). The ras superfamily of small gtpases in non-neoplastic cerebral diseases. In *Frontiers in Molecular Neuroscience* (Vol. 12). Frontiers Media S.A. https://doi.org/10.3389/fnmol.2019.00121

Radhika, V., & Dhanasekaran, N. (2001). Transforming G proteins. *Oncogene 2001 20:13*, *20*(13), 1607–1614. https://doi.org/10.1038/sj.onc.1204274

Rau, T., Nose, M., Remmers, U., Weil, J., Weiβmüller, A., Davia, K., Harding, S., Peppel, K., Koch, W. J., & Eschenhagen, T. (2003). Overexpression of wild-type Gαi-2 suppresses β-adrenergic signaling in cardiac myocytes. *The FASEB Journal*, *17*(3), 1–23. https://doi.org/10.1096/FJ.02-0660FJE

Rondard, P., Huang, S., Monnier, C., Tu, H., Blanchard, B., Oueslati, N., Malhaire, F., Li, Y., Trinquet, E., Labesse, G., Pin, J. P., & Liu, J. (2008). Functioning of the dimeric GABAB receptor extracellular domain revealed by glycan wedge scanning. *EMBO Journal*, *27*(9), 1321–1332. https://doi.org/10.1038/emboj.2008.64

RT, D., & JS, G. (2007). G-protein-coupled receptors and cancer. *Nature Reviews. Cancer*, *7*(2), 79–94. https://doi.org/10.1038/NRC2069

Rudack, T., Teuber, C., Scherlo, M., Güldenhaupt, J., Schartner, J., Lübben, M., Klare, J., Gerwert, K., & Kötting, C. (2021). The Ras dimer structure. *Chemical Science*, *12*(23), 8178–8189. https://doi.org/10.1039/D1SC00957E

S, S., H, P., L, M., & T, W. (2012). Imaging intracellular protein dynamics by spinning disk confocal microscopy. *Methods in Enzymology*, *504*, 293–313. https://doi.org/10.1016/B978-0-12-391857-4.00015-X

Schmidt, A., & Hall, A. (2002). Guanine nucleotide exchange factors for Rho GTPases: Turning on the switch. In *Genes and Development* (Vol. 16, Issue 13, pp. 1587–1609). Cold Spring Harbor Laboratory Press. https://doi.org/10.1101/gad.1003302

Schubbert, S., Shannon, K., & Bollag, G. (2007). Hyperactive Ras in developmental disorders and cancer. *Nature Reviews Cancer*, *7*(4), 295–308. https://doi.org/10.1038/nrc2109

Siderovski, D. P., & Willard, F. S. (2005). The GAPs, GEFs, and GDIs of heterotrimeric G-protein alpha subunits Review. *International Journal of Biological Sciences*, *1*, 51–66. www.biolsci.org

Siehler, S. (2009). Regulation of RhoGEF proteins by G12/13-coupled receptors. *British Journal of Pharmacology*, *158*(1), 41. https://doi.org/10.1111/J.1476-5381.2009.00121.X

Skruzny, M., Pohl, E., & Abella, M. (2019). FRET microscopy in yeast. In *Biosensors* (Vol. 9, Issue 4). MDPI AG. https://doi.org/10.3390/bios9040122

Song, S., Cong, W., Zhou, S., Shi, Y., Dai, W., Zhang, H., Wang, X., He, B., & Zhang, Q. (2019). Small GTPases: Structure, biological function and its interaction with nanoparticles. In *Asian Journal of Pharmaceutical Sciences* (Vol. 14, Issue 1, pp. 30–39). Shenyang Pharmaceutical University. https://doi.org/10.1016/j.ajps.2018.06.004

Syrovatkina, V., Alegre, K. O., Dey, R., & Huang, X. Y. (2016). Regulation, Signaling, and Physiological Functions of G-Proteins. In *Journal of Molecular Biology* (Vol. 428, Issue 19, pp. 3850–3868). Academic Press. https://doi.org/10.1016/j.jmb.2016.08.002

T, F., CNJ, R., D, S., AJ, V., M, K., CG, T., DB, V., & MM, B. (2015). Universal allosteric mechanism for Gα activation by GPCRs. *Nature*, *524*(7564), 173–179. https://doi.org/10.1038/NATURE14663

Takesono, A., Cismowski, M. J., Ribas, C., Bernard, M., Chung, P., Hazard, S., Duzic, E., & Lanier, S. M. (1999). Receptor-independent Activators of Heterotrimeric G-protein Signaling Pathways *. *Journal of Biological Chemistry*, *274*(47), 33202–33205. https://doi.org/10.1074/JBC.274.47.33202

Wang, W., Qiao, Y., & Li, Z. (2018). *New Insights into Modes of GPCR Activation*. https://doi.org/10.1016/j.tips.2018.01.001

Wennerberg, K., Rossman, K. L., & Der, C. J. (2005). The Ras superfamily at a glance. *Journal of Cell Science*, *118*(5), 843–846. https://doi.org/10.1242/jcs.01660

Wettschureck, N., & Offermanns, S. (2005). Mammalian G proteins and their cell type specific functions. *Physiological Reviews*, *85*(4), 1159–1204. https://doi.org/10.1152/physrev.00003.2005

Wong, S. K. F. (2003). G protein selectivity is regulated by multiple intracellular regions of GPCRs. *NeuroSignals*, *12*(1), 1–12. https://doi.org/10.1159/000068914

Xing, S., Wallmeroth, N., Berendzen, K. W., & Grefen, C. (2016). Topical Review on Protein-Protein Interaction Techniques Techniques for the Analysis of Protein-Protein Interactions in Vivo 1[OPEN] Critical discussion of technological limitations and advantages of the most prominent in vivo protein-protein interaction techniques emphasizing their application to plant research. *Plant Physiology Ò*, *171*, 727–758. https://doi.org/10.1104/pp.16.00470

Y, T., T, S., & T, M. (2001). Small GTP-binding proteins. *Physiological Reviews*, *81*(1), 153–208. https://doi.org/10.1152/PHYSREV.2001.81.1.153

Yang, D., Zhou, Q., Labroska, V., Qin, S., Darbalaei, S., Wu, Y., Yuliantie, E., Xie, L., Tao, H., Cheng, J., Liu, Q., Zhao, S., Shui, W., Jiang, Y., & Wang, M.-W. (2021). G protein-coupled receptors: structure- and function-based drug discovery. *Signal Transduction and Targeted Therapy 2020 6:1*, *6*(1), 1–27. https://doi.org/10.1038/s41392-020-00435-w

Zhang, A. (2009). Protein interaction networks: Computational analysis. In *Protein Interaction Networks Computational Analysis* (Vol. 9780521888950). Cambridge University Press. https://doi.org/10.1017/CBO9780511626593

APPENDICES

A. COMPOSITION OF CELL CULTURE SOLUTIONS

Table A. 1 Composition of D-MEM with high glucose

COMPONENT	CONCENTRATION (mg/L)
Amino Acids	
Glycine	30
L-Arginine hydrochloride	84
L-Cysteine 2HCl	63
L-Glutamine	580
L-Histidine hydrochloride-H_2O	42
L-Isoleucine	105
L-Leucine	105
L-Lysine hydrochloride	146
L-Methionine	30
L-Phenylalanine	66
L-Serine	42
L-Threonine	95
L-Tryptophan	16
L-Tyrosine	72
L-Valine	94
Vitamins	
Choline chloride	4
D-Calcium pantothenate	4
Niacinamide	4
Pyridoxine hydrochloride	4
Riboflavin	0.4
Thiamine hydrochloride	4

i-Inositol	7.2
Inorganic Salts	
Calcium chloride	264
Ferric nitrate	0.1
Magnesium sulfate	200
Potassium chloride	400
Sodium bicarbonate	3700
Sodium chloride	6400
Sodium phosphate monobasic	141
Other components	
D-Glucose (Dextrose)	4500
Phenol Red	15
Sodium pyruvate	110

Table A. 2 Composition of 1X Phosphate Buffered Saline (PBS) solution

NaCl	8 g/L
KCl	0.2 g/L
Na_2HPO_4	1.44 g/L
KH_2PO_4	0.24 g/L

Components were dissolved into 1L deionized sterile water and pH adjusted to 7.4.

B. COMPOSITION OF BACTERIAL CULTURE MEDIA AND BUFFERS

Table B. 1 Composition of Luria Bertani (LB) Medium

10 g/L	Tryptone
5 g/L	Yeast Extract
5 g/L	NaCl

All components are dissolved in distilled H_2O, 20g/L is added for solid medium preparation. The pH of the medium is adjusted to 7.0.

Table B. 2 Composition of SOC

Sormam lazim

Table B. 3 Composition of 1X Tris Base, Acetic acid, EDTA (TAE) Buffer

40mM	Tris
20mM	Acetic Acid
1mM	EDTA

Dissolve in 1 liter dH_2O.

Table B. 4 Composition of TFBI and TFBII

TFB I	Solution Concentration	Prepared Stock	For 100 mL Solution take from prepared stock
KOAc	30 mM	300 mM	10 mL
RbCl	100 mM	1000 mM	10 mL
$CaCl_2$	10 mM	1000 mM	1 mL
$MnCl_2$	50 mM	1000 mM	5 mL
Glycerol	15 %	87 %	17.2 mL

Complete the solution to 100 mL with distilled water and adjust pH to 5.8. After adjusting the pH, autoclave the solution or filter the solution using 0.45 mm filter.

TFB II	Solution Concentration	Prepared Stock	For 10 mL Solution take from prepared stock
MOPS/PIPES	10 mM	1000 mM	0.1 mL
$CaCl_2$	75 mM	1000 mM	0.75 mL
RbCl	10 mM	1000 mM	0.1 mL
Glycerol	15 %	87 %	1.7 mL

Complete the solution to 100 mL with distilled water and adjust pH to 5.8. After adjusting the pH, autoclave the solution or filter the solution using 0.45 mm filter.

C. MAP OF THE MAMMALIAN EXPRESSION VECTOR

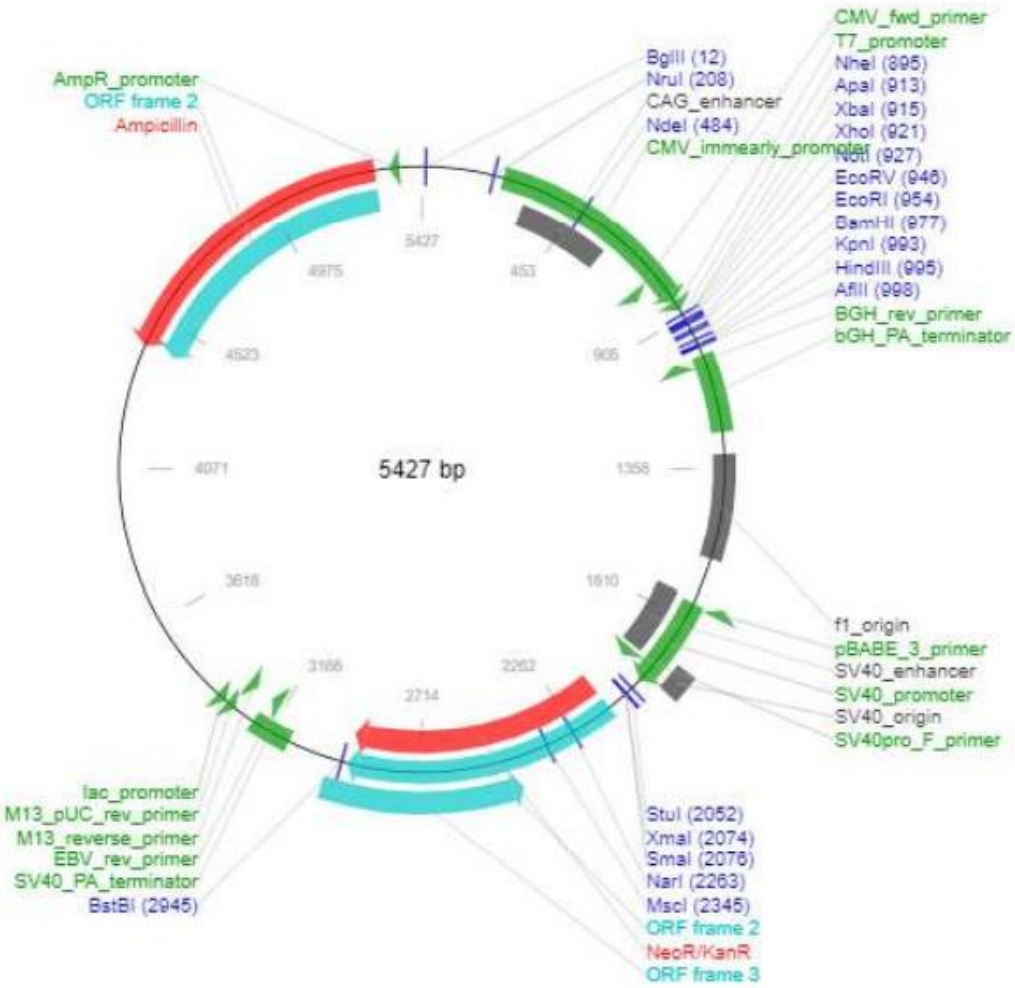

Figure C. 1 Map of mammalian expresion vector pcDNA 3.1 (-) with the CMV promoter (www.addgene.org).

D. CODING SEQUENCE OF FUSION PROTEINS

Coding sequence of Gαi1(121-122) EGFP

ATGGGCTGCACGCTGAGCGCCGAGGACAAGGCGGCGGTGGAGCGGAGTAAGATGA
TCGACCGCAACCTCCGTGAGGACGGCGAGAAGGCGGCGCGCGAGGTCAAGCTGCT
GCTGCTCGGTGCTGGTGAATCTGGTAAAAGTACAATTGTGAAGCAGATGAAAATT
ATCCATGAAGCTGGTTATTCAGAAGAGGAGTGTAAACAATACAAAGCAGTGGTCT

ACAGTAACACCATCCAGTCAATTATTGCTATCATTAGGGCTATGGGGAGGTTGAA
GATAGACTTTGGTGACTCAGCCCGGGCGGATGATGCACGCCAACTCTTTGTGCTA
GCTGGATCTGGAGGAGGAGGATCTATGGTGAGCAAGGGCGAGGAGCTGTTCACCG
GGGTGGTGCCCATCCTGGTCGAGCTGGACGGCGACGTAAACGGCCACAAGTTCAG
CGTGTCCGGCGAGGGCGAGGGCGATGCCACCTACGGCAAGCTGACCCTGAAGTTC
ATCTGCACCACCGGCAAGCTGCCCGTGCCCTGGCCCACCCTCGTGACCACCCTGA
CCTACGGCGTGCAGTGCTTCAGCCGCTACCCCGACCACATGAAGCAGCACGACTT
CTTCAAGTCCGCCATGCCCGAAGGCTACGTCCAGGAGCGCACCATCTTCTTCAAG
GACGACGGCAACTACAAGACCCGCGCCGAGGTGAAGTTCGAGGGCGACACCCTGG
TGAACCGCATCGAGCTGAAGGGCATCGACTTCAAGGAGGACGGCAACATCCTGGG
GCACAAGCTGGAGTACAACTACAACAGCCACAACGTCTATATCATGGCCGACAAG
CAGAAGAACGGCATCAAGGTGAACTTCAAGATCCGCCACAACATCGAGGACGGCA
GCGTGCAGCTCGCCGACCACTACCAGCAGAACACCCCCATCGGCGACGGCCCCGT
GCTGCTGCCCGACAACCACTACCTGAGCACCCAGTCCAAGCTTAGCAAAGACCCC
AACGAGAAGCGCGATCACATGGTCCTGCTGGAGTTCGTGACCGCCGCCGGGATCA
CTCTCGGCATGGACGAGCTGTACAAGTCTGGAGGAGGAGGATCTGCTGCTGAAGA
AGGCTTTATGACTGCAGAACTTGCTGGAGTTATAAAGAGATTGTGGAAAGATAGT
GGTGTACAAGCCTGTTTCAACAGATCCCGAGAGTACCAGCTTAATGATTCTGCAG
CATACTATTTGAATGACTTGGACAGAATAGCTCAACCAAATTACATCCCGACTCA
ACAAGATGTTCTCAGAACTAGAGTGAAAACTACAGGAATTGTTGAAACCCATTTT
ACTTTCAAAGATCTTCATTTTAAAATGTTTGATGTGGGAGGTCAGAGATCTGAGC
GGAAGAAGTGGATTCATTGCTTCGAAGGAGTGGCGGCGATCATCTTCTGTGTAGC
ACTGAGTGACTACGACCTGGTTCTAGCTGAAGATGAAGAAATGAACCGAATGCAT
GAAAGCATGAAATTGTTTGACAGCATATGTAACAACAAGTGGTTTACAGATACAT
CCATTATACTTTTTCTAAACAAGAAGGATCTTTTTGAAGAAAAAATCAAAAAGAG
CCCTCTCACTATATGCTATCAAGAATATGCAGGATCAAACACATATGAAGAGGCA
GCTGCATATATTCAATGTCAGTTTGAAGACCTCAATAAAAGAAAGGACACAAAGG
AAATATACACCCACTTCACATGTGCCACAGATACTAAGAATGTGCAGTTTGTTTT
TGATGCTGTAACAGATGTCATCATAAAAAATAATCTAAAAGATTGTGGTCTCTTT
TAG

Coding sequence of G*α*i1(121-122) EGFP

ATGGGCTGCACGCTGAGCGCCGAGGACAAGGCGGCGGTGGAGCGGAGTAAGATGA
TCGACCGCAACCTCCGTGAGGACGGCGAGAAGGCGGCGCGCGAGGTCAAGCTGCT
GCTGCTCGGTGCTGGTGAATCTGGTAAAAGTACAATTGTGAAGCAGATGAAAATT
ATCCATGAAGCTGGTTATTCAGAAGAGGAGTGTAAACAATACAAAGCAGTGGTCT
ACAGTAACACCATCCAGTCAATTATTGCTATCATTAGGGCTATGGGGAGGTTGAA
GATAGACTTTGGTGACTCAGCCCGGGCGGATGATGCACGCCAACTCTTTGTGCTA
GCTGGATCTGGAGGAGGAGGATCTATGGTGAGCAAGGGCGAGGAGGATAACATGG
CCATCATCAAGGAGTTCATGCGCTTCAAGGTGCACATGGAGGGCTCCGTGAACGG
CCACGAGTTCGAGATCGAGGGCGAGGGCGAGGGCCGCCCCTACGAGGGCACCCAG
ACCGCCAAGCTGAAGGTGACCAAGGGTGGCCCCCTGCCCTTCGCCTGGGACATCC
TGTCCCCTCAGTTCATGTACGGCTCCAAGGCCTACGTGAAGCACCCCGCCGACAT
CCCCGACTACTTGAAGCTGTCCTTCCCCGAGGGCTTCAAGTGGGAGCGCGTGATG
AACTTCGAGGACGGCGGCGTGGTGACCGTGACCCAGGACTCCTCCCTGCAGGACG

GCGAGTTCATCTACAAGGTGAAGCTGCGCGGCACCAACTTCCCCTCCGACGGCCC
CGTAATGCAGAAGAAGACCATGGGCTGGGAGGCCTCCTCCGAGCGGATGTACCCC
GAGGACGGCGCCCTGAAGGGCGAGATCAAGCAGAGGCTGAAGCTGAAGGACGGCG
GCCACTACGACGCTGAGGTCAAGACCACCTACAAGGCCAAGAAGCCCGTGCAGCT
GCCCGGCGCCTACAACGTCAACATCAAGTTGGACATCACCTCCCACAACGAGGAC
TACACCATCGTGGAACAGTACGAACGCGCCGAGGGCCGCCACTCCACCGGCGGCA
TGGACGAGCTGTACAAGTCTGGAGGAGGAGGATCTGCTGCTGAAGAAGGCTTTAT
GACTGCAGAACTTGCTGGAGTTATAAAGAGATTGTGGAAAGATAGTGGTGTACAA
GCCTGTTTCAACAGATCCCGAGAGTACCAGCTTAATGATTCTGCAGCATACTATT
TGAATGACTTGGACAGAATAGCTCAACCAAATTACATCCCGACTCAACAAGATGT
TCTCAGAACTAGAGTGAAAACTACAGGAATTGTTGAAACCCATTTTACTTTCAAA
GATCTTCATTTTAAAATGTTTGATGTGGGAGGTCAGAGATCTGAGCGGAAGAAGT
GGATTCATTGCTTCGAAGGAGTGGCGGCGATCATCTTCTGTGTAGCACTGAGTGA
CTACGACCTGGTTCTAGCTGAAGATGAAGAAATGAACCGAATGCATGAAAGCATG
AAATTGTTTGACAGCATATGTAACAACAAGTGGTTTACAGATACATCCATTATAC
TTTTTCTAAACAAGAAGGATCTTTTTGAAGAAAAAATCAAAAAGAGCCCTCTCAC
TATATGCTATCAAGAATATGCAGGATCAAACACATATGAAGAGGCAGCTGCATAT
ATTCAATGTCAGTTTGAAGACCTCAATAAAAGAAAGGACACAAAGGAAATATACA
CCCACTTCACATGTGCCACAGATACTAAGAATGTGCAGTTTGTTTTTGATGCTGT
AACAGATGTCATCATAAAAAATAATCTAAAAGATTGTGGTCTCTTTTAG

Coding sequence of GAP-43 EGFP

GCTAGCATGCTGTGCTGTATGAGAAGAACCAAACAGGTTGAAAAGAATGATGAGG
ACCAAAAGATTCTCGAGATGGTGAGCAAGGGCGAGGAGCTGTTCACCGGGGTGGT
GCCCATCCTGGTCGAGCTGGACGGCGACGTAAACGGCCACAAGTTCAGCGTGTCC
GGCGAGGGCGAGGGCGATGCCACCTACGGCAAGCTGACCCTGAAGTTCATCTGCA
CCACCGGCAAGCTGCCCGTGCCCTGGCCCACCCTCGTGACCACCCTGACCTACGG
CGTGCAGTGCTTCAGCCGCTACCCCGACCACATGAAGCAGCACGACTTCTTCAAG
TCCGCCATGCCCGAAGGCTACGTCCAGGAGCGCACCATCTTCTTCAAGGACGACG
GCAACTACAAGACCCGCGCCGAGGTGAAGTTCGAGGGCGACACCCTGGTGAACCG
CATCGAGCTGAAGGGCATCGACTTCAAGGAGGACGGCAACATCCTGGGGCACAAG
CTGGAGTACAACTACAACAGCCACAACGTCTATATCATGGCCGACAAGCAGAAGA
ACGGCATCAAGGTGAACTTCAAGATCCGCCACAACATCGAGGACGGCAGCGTGCA
GCTCGCCGACCACTACCAGCAGAACACCCCCATCGGCGACGGCCCCGTGCTGCTG
CCCGACAACCACTACCTGAGCACCCAGTCCGCCCTGAGCAAAGACCCCAACGAGA
AGCGCGATCACATGGTCCTGCTGGAGTTCGTGACCGCCGCCGGGATCACTCTCGG
CATGGACGAGCTGTACAAG

Coding sequence of GAP-43 EGFP

GCTAGCATGCTGTGCTGTATGAGAAGAACCAAACAGGTTGAAAAGAATGATGAGG
ACCAAAAGATTCTCGAGATGGTGAGCAAGGGCGAGGAGGATAACATGGCCATCAT
CAAGGAGTTCATGCGCTTCAAGGTGCACATGGAGGGCTCCGTGAACGGCCACGAG
TTCGAGATCGAGGGCGAGGGCGAGGGCCGCCCCTACGAGGGCACCCAGACCGCCA
AGCTGAAGGTGACCAAGGGTGGCCCCCTGCCCTTCGCCTGGGACATCCTGTCCCC

TCAGTTCATGTACGGCTCCAAGGCCTACGTGAAGCACCCCGCCGACATCCCCGAC
TACTTGAAGCTGTCCTTCCCCGAGGGCTTCAAGTGGGAGCGCGTGATGAACTTCG
AGGACGGCGGCGTGGTGACCGTGACCCAGGACTCCTCCCTGCAGGACGGCGAGTT
CATCTACAAGGTGAAGCTGCGCGGCACCAACTTCCCCTCCGACGGCCCCGTAATG
CAGAAGAAGACCATGGGCTGGGAGGCCTCCTCCGAGCGGATGTACCCCGAGGACG
GCGCCCTGAAGGGCGAGATCAAGCAGAGGCTGAAGCTGAAGGACGGCGGCCACTA
CGACGCTGAGGTCAAGACCACCTACAAGGCCAAGAAGCCCGTGCAGCTGCCCGGC
GCCTACAACGTCAACATCAAGTTGGACATCACCTCCCACAACGAGGACTACACCA
TCGTGGAACAGTACGAACGCGCCGAGGGCCGCCACTCCACCGGCGGCATGGACGA
GCTGTACAAG

Coding sequence of GAP-43 EGFP-RGSLVPR-mCherry

GCTAGCATGCTGTGCTGTATGAGAAGAACCAAACAGGTTGAAAAGAATGATGAGG
ACCAAAAGATTCTCGAGATGGTGAGCAAGGGCGAGGAGGATAACATGGCCATCAT
CAAGGAGTTCATGCGCTTCAAGGTGCACATGGAGGGCTCCGTGAACGGCCACGAG
TTCGAGATCGAGGGCGAGGGCGAGGGCCGCCCCTACGAGGGCACCCAGACCGCCA
AGCTGAAGGTGACCAAGGGTGGCCCCCTGCCCTTCGCCTGGGACATCCTGTCCCC
TCAGTTCATGTACGGCTCCAAGGCCTACGTGAAGCACCCCGCCGACATCCCCGAC
TACTTGAAGCTGTCCTTCCCCGAGGGCTTCAAGTGGGAGCGCGTGATGAACTTCG
AGGACGGCGGCGTGGTGACCGTGACCCAGGACTCCTCCCTGCAGGACGGCGAGTT
CATCTACAAGGTGAAGCTGCGCGGCACCAACTTCCCCTCCGACGGCCCCGTAATG
CAGAAGAAGACCATGGGCTGGGAGGCCTCCTCCGAGCGGATGTACCCCGAGGACG
GCGCCCTGAAGGGCGAGATCAAGCAGAGGCTGAAGCTGAAGGACGGCGGCCACTA
CGACGCTGAGGTCAAGACCACCTACAAGGCCAAGAAGCCCGTGCAGCTGCCCGGC
GCCTACAACGTCAACATCAAGTTGGACATCACCTCCCACAACGAGGACTACACCA
TCGTGGAACAGTACGAACGCGCCGAGGGCCGCCACTCCACCGGCGGCATGGACGA
GCTGTACAAGCGGGGCAGCCTGGTCCCTGGAATGGTGAGCAAGGGCGAGGAGCTG
TTCACCGGGGTGGTGCCCATCCTGGTCGAGCTGGACGGCGACGTAAACGGCCACA
AGTTCAGCGTGTCCGGCGAGGGCGAGGGCGATGCCACCTACGGCAAGCTGACCCT
GAAGTTCATCTGCACCACCGGCAAGCTGCCCGTGCCCTGGCCCACCCTCGTGACC
ACCCTGACCTACGGCGTGCAGTGCTTCAGCCGCTACCCCGACCACATGAAGCAGC
ACGACTTCTTCAAGTCCGCCATGCCCGAAGGCTACGTCCAGGAGCGCACCATCTT
CTTCAAGGACGACGGCAACTACAAGACCCGCGCCGAGGTGAAGTTCGAGGGCGAC
ACCCTGGTGAACCGCATCGAGCTGAAGGGCATCGACTTCAAGGAGGACGGCAACA
TCCTGGGGCACAAGCTGGAGTACAACTACAACAGCCACAACGTCTATATCATGGC
CGACAAGCAGAAGAACGGCATCAAGGTGAACTTCAAGATCCGCCACAACATCGAG
GACGGCAGCGTGCAGCTCGCCGACCACTACCAGCAGAACACCCCCATCGGCGACG
GCCCCGTGCTGCTGCCCGACAACCACTACCTGAGCACCCAGTCCGCCCTGAGCAA
AGACCCCAACGAGAAGCGCGATCACATGGTCCTGCTGGAGTTCGTGACCGCCGCC
GGGATCACTCTCGGCATGGACGAGCTGTACAAG

Gαi Minigene Casette Sequence

GCCGCCACCATGGGAATAAAAAATAATCTAAAGATTGTGGTCTCTTT

E. STATISTICAL ANALYSIS OF THE CONFOCAL MICROSCOPY RESULTS OF Gαi-Gαi FRET PAIR WITH Gαi-PROTEIN SPECIFIC MINIGENES

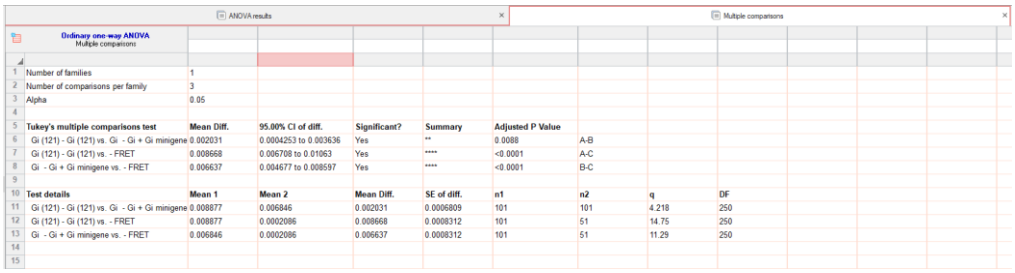

Ordinary one-way ANOVA Multiple comparisons								
Number of families	1							
Number of comparisons per family	3							
Alpha	0.05							
Tukey's multiple comparisons test	**Mean Diff.**	**95.00% CI of diff.**	**Significant?**	**Summary**	**Adjusted P Value**			
Gi (121) - Gi (121) vs. Gi - Gi + Gi minigene	0.002031	0.0004253 to 0.003636	Yes	**	0.0088	A-B		
Gi (121) - Gi (121) vs. - FRET	0.008668	0.006708 to 0.01063	Yes	****	<0.0001	A-C		
Gi - Gi + Gi minigene vs. - FRET	0.006637	0.004677 to 0.008597	Yes	****	<0.0001	B-C		
Test details	**Mean 1**	**Mean 2**	**Mean Diff.**	**SE of diff.**	**n1**	**n2**	**q**	**DF**
Gi (121) - Gi (121) vs. Gi - Gi + Gi minigene	0.008877	0.006846	0.002031	0.0006809	101	101	4.218	250
Gi (121) - Gi (121) vs. - FRET	0.008877	0.0002086	0.008668	0.0008312	101	51	14.75	250
Gi - Gi + Gi minigene vs. - FRET	0.006846	0.0002086	0.006637	0.0008312	101	51	11.29	250

Figure E. 1 LSM Confocal microscope result from Gαi (121) EGFP-Gαi (121) mCherry with minigene FRET groups analyzed with Ordinary One Way Anova analysis.

F. STATISTICAL ANALYSIS OF MONOCHROMATOR PLATE READER RESULT Gαi-Gαi FRET PAIRS WITH Gαi-PROTEIN SPECIFIC MINIGENES

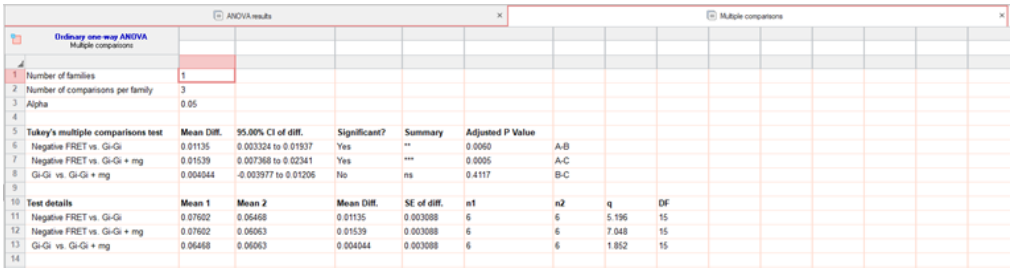

Ordinary one-way ANOVA Multiple comparisons								
Number of families	1							
Number of comparisons per family	3							
Alpha	0.05							
Tukey's multiple comparisons test	**Mean Diff.**	**95.00% CI of diff.**	**Significant?**	**Summary**	**Adjusted P Value**			
Negative FRET vs. Gi-Gi	0.01135	0.003324 to 0.01937	Yes	**	0.0060	A-B		
Negative FRET vs. Gi-Gi + mg	0.01539	0.007368 to 0.02341	Yes	***	0.0005	A-C		
Gi-Gi vs. Gi-Gi + mg	0.004044	-0.003977 to 0.01206	No	ns	0.4117	B-C		
Test details	**Mean 1**	**Mean 2**	**Mean Diff.**	**SE of diff.**	**n1**	**n2**	**q**	**DF**
Negative FRET vs. Gi-Gi	0.07602	0.06468	0.01135	0.003088	6	6	5.196	15
Negative FRET vs. Gi-Gi + mg	0.07602	0.06063	0.01539	0.003088	6	6	7.048	15
Gi-Gi vs. Gi-Gi + mg	0.06468	0.06063	0.004044	0.003088	6	6	1.852	15

Figure F. 1 Gαi (121) EGFP - Gαi (121) mCherry , Gαi (121) EGFP - Gαi (121) mCherry + Gαi-specific minigene and negative FRET control group at Donor (EGFP) spectral peak region result analysis with Ordinary One way ANOVA .

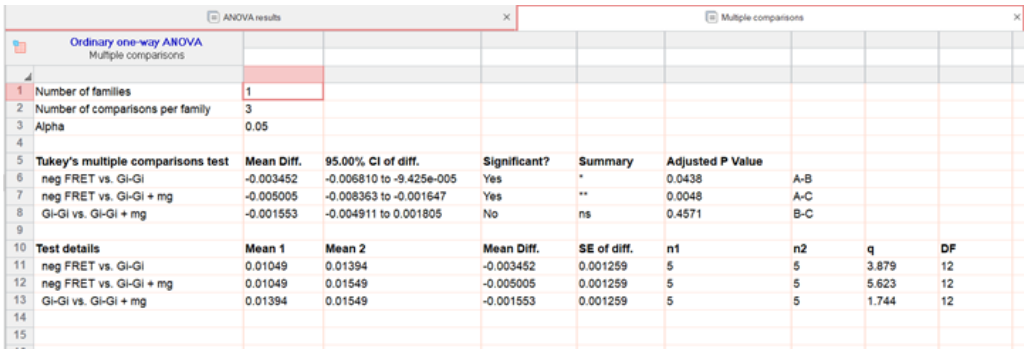

ANOVA results | Multiple comparisons

Ordinary one-way ANOVA
Multiple comparisons

1	Number of families	1							
2	Number of comparisons per family	3							
3	Alpha	0.05							
4									
5	**Tukey's multiple comparisons test**	**Mean Diff.**	**95.00% CI of diff.**	**Significant?**	**Summary**	**Adjusted P Value**			
6	neg FRET vs. Gi-Gi	-0.003452	-0.006810 to -9.425e-005	Yes	*	0.0438	A-B		
7	neg FRET vs. Gi-Gi + mg	-0.005005	-0.008363 to -0.001647	Yes	**	0.0048	A-C		
8	Gi-Gi vs. Gi-Gi + mg	-0.001553	-0.004911 to 0.001805	No	ns	0.4571	B-C		
9									
10	**Test details**	**Mean 1**	**Mean 2**	**Mean Diff.**	**SE of diff.**	**n1**	**n2**	**q**	**DF**
11	neg FRET vs. Gi-Gi	0.01049	0.01394	-0.003452	0.001259	5	5	3.879	12
12	neg FRET vs. Gi-Gi + mg	0.01049	0.01549	-0.005005	0.001259	5	5	5.623	12
13	Gi-Gi vs. Gi-Gi + mg	0.01394	0.01549	-0.001553	0.001259	5	5	1.744	12
14									
15									

Figure F. 2 Gαi (121) EGFP - Gαi (121) mCherry , Gαi (121) EGFP - Gαi (121) mCherry + Gαi-specific minigene and Gap43 FRET control groups at Acceptor (mCherry) spectral peak region result analysis with Ordinary One way ANOVA .

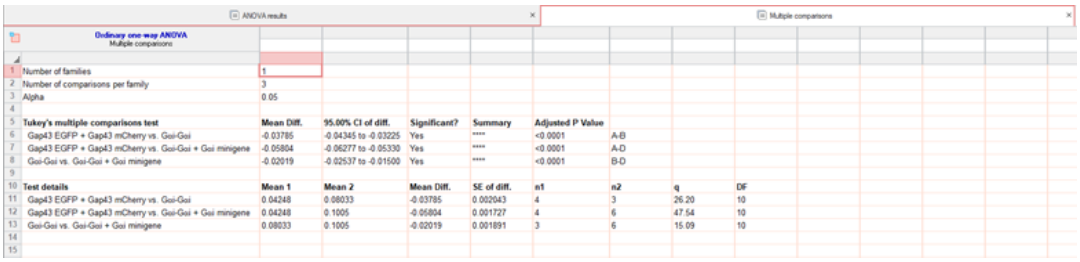

ANOVA results | Multiple comparisons

Ordinary one-way ANOVA
Multiple comparisons

1	Number of families	1							
2	Number of comparisons per family	3							
3	Alpha	0.05							
4									
5	**Tukey's multiple comparisons test**	**Mean Diff.**	**95.00% CI of diff.**	**Significant?**	**Summary**	**Adjusted P Value**			
6	Gap43 EGFP + Gap43 mCherry vs. Gαi-Gαi	-0.03785	-0.04345 to -0.03225	Yes	****	<0.0001	A-B		
7	Gap43 EGFP + Gap43 mCherry vs. Gαi-Gαi + Gαi minigene	-0.05804	-0.06277 to -0.05330	Yes	****	<0.0001	A-D		
8	Gαi-Gαi vs. Gαi-Gαi + Gαi minigene	-0.02019	-0.02537 to -0.01500	Yes	****	<0.0001	B-D		
9									
10	**Test details**	**Mean 1**	**Mean 2**	**Mean Diff.**	**SE of diff.**	**n1**	**n2**	**q**	**DF**
11	Gap43 EGFP + Gap43 mCherry vs. Gαi-Gαi	0.04248	0.08033	-0.03785	0.002043	4	3	26.20	10
12	Gap43 EGFP + Gap43 mCherry vs. Gαi-Gαi + Gαi minigene	0.04248	0.1005	-0.05804	0.001727	4	6	47.54	10
13	Gαi-Gαi vs. Gαi-Gαi + Gαi minigene	0.08033	0.1005	-0.02019	0.001891	3	6	15.09	10
14									
15									

Figure F. 3 Gαi (121) EGFP - Gαi (121) mCherry , Gαi (121) EGFP - Gαi (121) mCherry + Gαi-specific minigene and Gap43 FRET control groups Acceptor/Donor ratio result analysis with Ordinary One way ANOVA.

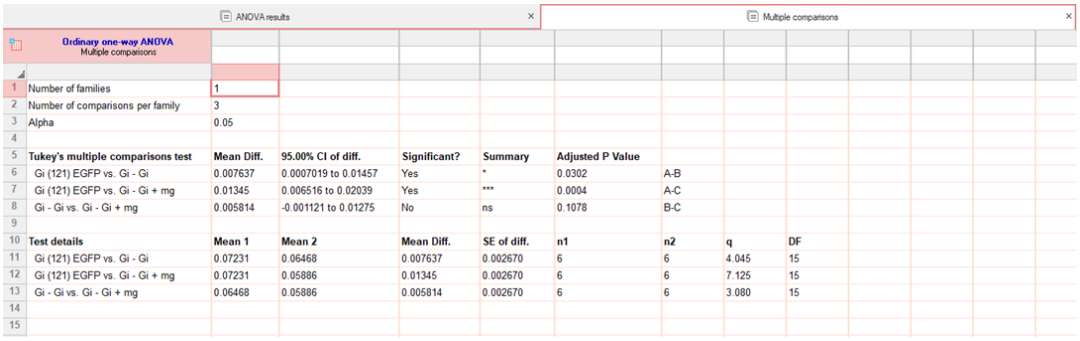

ANOVA results | Multiple comparisons

Ordinary one-way ANOVA
Multiple comparisons

1	Number of families	1							
2	Number of comparisons per family	3							
3	Alpha	0.05							
4									
5	**Tukey's multiple comparisons test**	**Mean Diff.**	**95.00% CI of diff.**	**Significant?**	**Summary**	**Adjusted P Value**			
6	Gi (121) EGFP vs. Gi - Gi	0.007637	0.0007019 to 0.01457	Yes	*	0.0302	A-B		
7	Gi (121) EGFP vs. Gi - Gi + mg	0.01345	0.006516 to 0.02039	Yes	***	0.0004	A-C		
8	Gi - Gi vs. Gi - Gi + mg	0.005814	-0.001121 to 0.01275	No	ns	0.1078	B-C		
9									
10	**Test details**	**Mean 1**	**Mean 2**	**Mean Diff.**	**SE of diff.**	**n1**	**n2**	**q**	**DF**
11	Gi (121) EGFP vs. Gi - Gi	0.07231	0.06468	0.007637	0.002670	6	6	4.045	15
12	Gi (121) EGFP vs. Gi - Gi + mg	0.07231	0.05886	0.01345	0.002670	6	6	7.125	15
13	Gi - Gi vs. Gi - Gi + mg	0.06468	0.05886	0.005814	0.002670	6	6	3.080	15
14									
15									

Figure F. 4 Gαi (121) EGFP, Gαi (121) EGFP - Gαi (121) mCherry , Gαi (121) EGFP - Gαi (121) mCherry + Gαi-specific minigene FRET donor quenching region result analysis with Ordinary One way ANOVA.

	Unpaired t test			
1	Table Analyzed	Data 29		
2				
3	Column B	gigi mg		
4	vs.	vs.		
5	Column A	gigi		
6				
7	**Unpaired t test**			
8	P value	0.0061		
9	P value summary	**		
10	Significantly different (P < 0.05)?	Yes		
11	One- or two-tailed P value?	Two-tailed		
12	t, df	t=4.132, df=6		
13				
14	**How big is the difference?**			
15	Mean of column A	0.2748		
16	Mean of column B	0.7086		
17	Difference between means (B - A) ± SEM	0.4339 ± 0.1050		
18	95% confidence interval	0.1770 to 0.6907		
19	R squared (eta squared)	0.7400		
20				
21	**F test to compare variances**			
22	F, DFn, Dfd	8.804, 2, 4		
23	P value	0.0685		
24	P value summary	ns		
25	Significantly different (P < 0.05)?	No		
26				
27	**Data analyzed**			
28	Sample size, column A	5		
29	Sample size, column B	3		

Figure F. 5 Gαi (121) EGFP - Gαi (121) mCherry , Gαi (121) EGFP - Gαi (121) mCherry + Gαi-specific minigene Amount of Donor quenching result analysis with unpaired t-test.

G. STATISTICAL ANALYSIS OF MONOCHROMATOR PLATE READER RESULT Gαi-Gαi FRET PAIRS WITH/WITHOUT QUINPIROLE TREATMENT

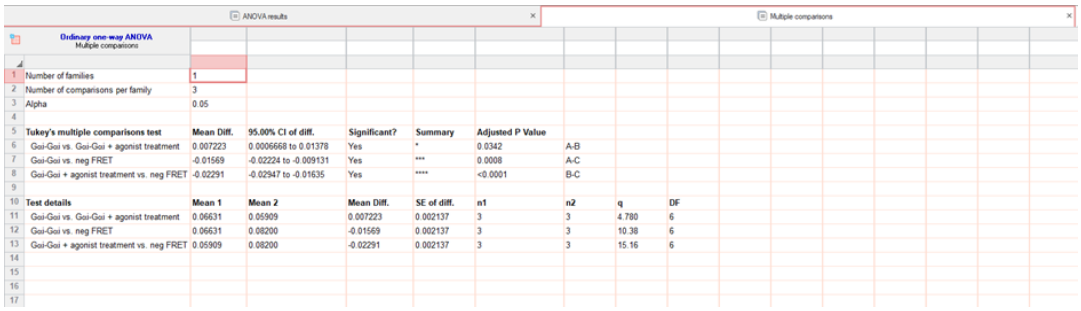

Ordinary one-way ANOVA Multiple comparisons								
Number of families	1							
Number of comparisons per family	3							
Alpha	0.05							
Tukey's multiple comparisons test	**Mean Diff.**	**95.00% CI of diff.**	**Significant?**	**Summary**	**Adjusted P Value**			
Gαi-Gαi vs. Gαi-Gαi + agonist treatment	0.007223	0.0006668 to 0.01378	Yes	*	0.0342	A-B		
Gαi-Gαi vs. neg FRET	-0.01569	-0.02224 to -0.009131	Yes	***	0.0008	A-C		
Gαi-Gαi + agonist treatment vs. neg FRET	-0.02291	-0.02947 to -0.01635	Yes	****	<0.0001	B-C		
Test details	**Mean 1**	**Mean 2**	**Mean Diff.**	**SE of diff.**	**n1**	**n2**	**q**	**DF**
Gαi-Gαi vs. Gαi-Gαi + agonist treatment	0.06631	0.05909	0.007223	0.002137	3	3	4.780	6
Gαi-Gαi vs. neg FRET	0.06631	0.08200	-0.01569	0.002137	3	3	10.38	6
Gαi-Gαi + agonist treatment vs. neg FRET	0.05909	0.08200	-0.02291	0.002137	3	3	15.16	6

Figure G. 1 Ordinary One Way ANOVA analysis of Donor (EGFP) spectrum peak normalized area comparison of Gαi-Gαi FRET pair and negative FRET control group with and without Quinpirole addition.

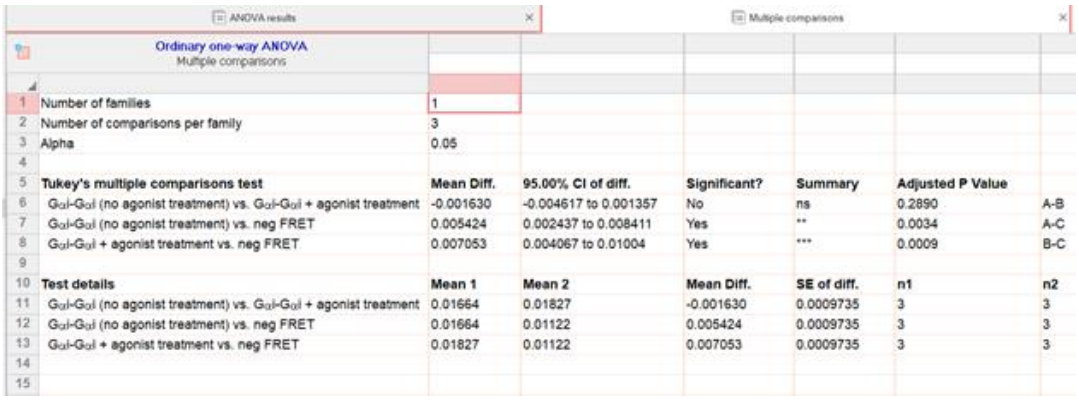

Ordinary one-way ANOVA Multiple comparisons						
Number of families	1					
Number of comparisons per family	3					
Alpha	0.05					
Tukey's multiple comparisons test	**Mean Diff.**	**95.00% CI of diff.**	**Significant?**	**Summary**	**Adjusted P Value**	
Gαi-Gαi (no agonist treatment) vs. Gαi-Gαi + agonist treatment	-0.001630	-0.004617 to 0.001357	No	ns	0.2890	A-B
Gαi-Gαi (no agonist treatment) vs. neg FRET	0.005424	0.002437 to 0.008411	Yes	**	0.0034	A-C
Gαi-Gαi + agonist treatment vs. neg FRET	0.007053	0.004067 to 0.01004	Yes	***	0.0009	B-C
Test details	**Mean 1**	**Mean 2**	**Mean Diff.**	**SE of diff.**	**n1**	**n2**
Gαi-Gαi (no agonist treatment) vs. Gαi-Gαi + agonist treatment	0.01664	0.01827	-0.001630	0.0009735	3	3
Gαi-Gαi (no agonist treatment) vs. neg FRET	0.01664	0.01122	0.005424	0.0009735	3	3
Gαi-Gαi + agonist treatment vs. neg FRET	0.01827	0.01122	0.007053	0.0009735	3	3

Figure G. 2 Ordinary One Way ANOVA analysis of Acceptor (mCherry) spectrum peak normalized area comparison of Gαi-Gαi FRET pair and negative FRET control group with and without Quinpirole addition.

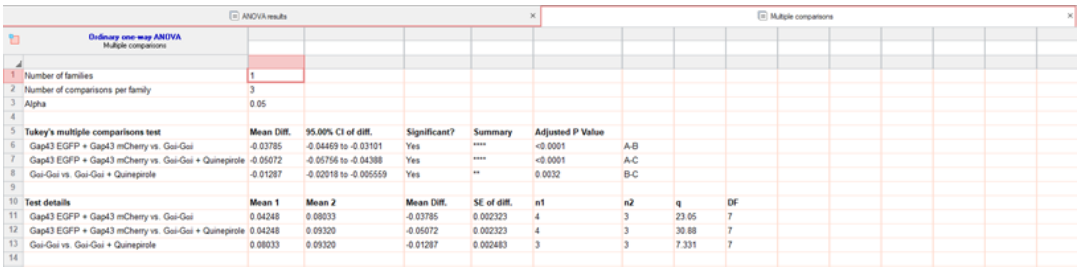

Ordinary one-way ANOVA
Multiple comparisons

1	Number of families	1							
2	Number of comparisons per family	3							
3	Alpha	0.05							
4									
5	**Tukey's multiple comparisons test**	**Mean Diff.**	**95.00% CI of diff.**	**Significant?**	**Summary**	**Adjusted P Value**			
6	Gap43 EGFP + Gap43 mCherry vs. Gαi-Gαi	-0.03785	-0.04469 to -0.03101	Yes	****	<0.0001	A-B		
7	Gap43 EGFP + Gap43 mCherry vs. Gαi-Gαi + Quinepirole	-0.05072	-0.05756 to -0.04388	Yes	****	<0.0001	A-C		
8	Gαi-Gαi vs. Gαi-Gαi + Quinepirole	-0.01287	-0.02018 to -0.005559	Yes	**	0.0032	B-C		
9									
10	**Test details**	**Mean 1**	**Mean 2**	**Mean Diff.**	**SE of diff.**	**n1**	**n2**	**q**	**DF**
11	Gap43 EGFP + Gap43 mCherry vs. Gαi-Gαi	0.04248	0.08033	-0.03785	0.002323	4	3	23.05	7
12	Gap43 EGFP + Gap43 mCherry vs. Gαi-Gαi + Quinepirole	0.04248	0.09320	-0.05072	0.002323	4	3	30.88	7
13	Gαi-Gαi vs. Gαi-Gαi + Quinepirole	0.08033	0.09320	-0.01287	0.002483	3	3	7.331	7
14									

Figure G. 3 Ordinary One Way ANOVA analysis of Acceptor/Donor peak ratio comparison of Gαi-Gαi FRET pair and negative FRET control group with and without Quinpirole addition.

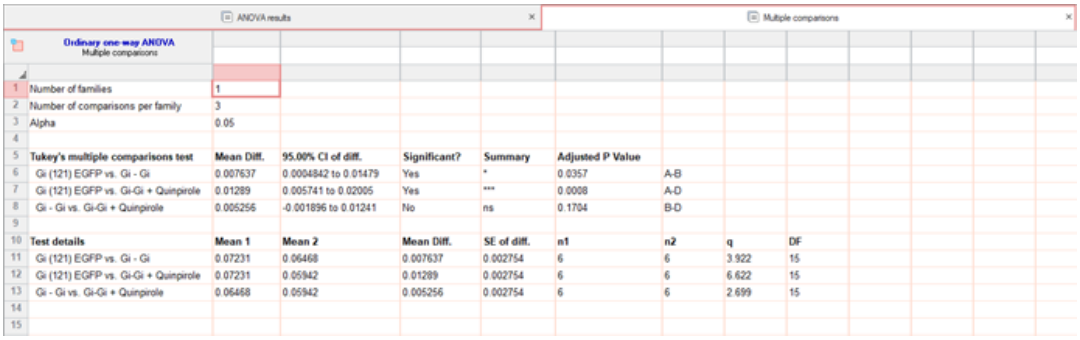

Ordinary one-way ANOVA
Multiple comparisons

1	Number of families	1							
2	Number of comparisons per family	3							
3	Alpha	0.05							
4									
5	**Tukey's multiple comparisons test**	**Mean Diff.**	**95.00% CI of diff.**	**Significant?**	**Summary**	**Adjusted P Value**			
6	Gi (121) EGFP vs. Gi - Gi	0.007637	0.0004842 to 0.01479	Yes	*	0.0357	A-B		
7	Gi (121) EGFP vs. Gi-Gi + Quinpirole	0.01289	0.005741 to 0.02005	Yes	***	0.0008	A-D		
8	Gi - Gi vs. Gi-Gi + Quinpirole	0.005256	-0.001896 to 0.01241	No	ns	0.1704	B-D		
9									
10	**Test details**	**Mean 1**	**Mean 2**	**Mean Diff.**	**SE of diff.**	**n1**	**n2**	**q**	**DF**
11	Gi (121) EGFP vs. Gi - Gi	0.07231	0.06468	0.007637	0.002754	6	6	3.922	15
12	Gi (121) EGFP vs. Gi-Gi + Quinpirole	0.07231	0.05942	0.01289	0.002754	6	6	6.622	15
13	Gi - Gi vs. Gi-Gi + Quinpirole	0.06468	0.05942	0.005256	0.002754	6	6	2.699	15
14									
15									

Figure G. 4 Ordinary One Way ANOVA analysis of FRET donor quenching region of Gαi-Gαi FRET pair with and without Quinpirole addition compared to only donor (Gαi (121) EGFP).

	Unpaired t test	
1	Table Analyzed	Data 29
2		
3	Column C	gigi + Q
4	vs.	vs.
5	Column A	gigi
6		
7	**Unpaired t test**	
8	P value	0.0015
9	P value summary	**
10	Significantly different (P < 0.05)?	Yes
11	One- or two-tailed P value?	Two-tailed
12	t, df	t=4.706, df=8
13		
14	**How big is the difference?**	
15	Mean of column A	0.2748
16	Mean of column C	0.6318
17	Difference between means (C - A) ± SEM	0.3570 ± 0.07587
18	95% confidence interval	0.1821 to 0.5320
19	R squared (eta squared)	0.7346
20		
21	**F test to compare variances**	
22	F, DFn, Dfd	4.016, 4, 4
23	P value	0.2068
24	P value summary	ns
25	Significantly different (P < 0.05)?	No
26		
27	**Data analyzed**	
28	Sample size, column A	5
29	Sample size, column C	5
30		

Figure G. 5 Unpaired t-test analysis of Amount of Donor Quenching of Gαi-Gαi FRET pair with and without Quinpirole addition.